Quaternary Science Reviews 147 (2016) 91–121

Contents lists available at ScienceDirect

Quaternary Science Reviews

journal homepage: www.elsevier.com/locate/quascirev

Deglaciation of Fennoscandia

Arjen P. Stroeven [a, b, *], Clas Hättestrand [a, b], Johan Kleman [a, b], Jakob Heyman [a, b], Derek Fabel [c], Ola Fredin [d, e], Bradley W. Goodfellow [b, f, g], Jonathan M. Harbor [a, b, h], John D. Jansen [a, b, i], Lars Olsen [d], Marc W. Caffee [h, j], David Fink [k], Jan Lundqvist [a, b], Gunhild C. Rosqvist [a, b, l], Bo Strömberg [a, b], Krister N. Jansson [a, b]

[a] *Geomorphology and Glaciology, Department of Physical Geography, Stockholm University, Sweden*
[b] *Bolin Centre for Climate Research, Stockholm University, Sweden*
[c] *SUERC-AMS, Scottish Universities Environmental Research Centre, East Kilbride Scotland, UK*
[d] *Geological Survey of Norway, Trondheim, Norway*
[e] *Department of Geography, Norwegian University of Science and Technology, Trondheim, Norway*
[f] *Department of Geological Sciences, Stockholm University, Sweden*
[g] *Department of Geology, Lund University, Sweden*
[h] *Department of Earth, Atmospheric, and Planetary Sciences, Purdue University, West Lafayette, USA*
[i] *Institute of Earth and Environmental Science, University of Potsdam, Germany*
[j] *Department of Physics and Astronomy/Purdue Rare Isotope Measurement Laboratory, Purdue University, West Lafayette, USA*
[k] *Australian Nuclear Science and Technology Organization, PMB1, Menai, Australia*
[l] *Department of Earth Science, University of Bergen, Norway*

A R T I C L E I N F O

Article history:
Received 1 May 2015
Received in revised form
28 August 2015
Accepted 14 September 2015
Available online 21 October 2015

Keywords:
Fennoscandian Ice Sheet
Deglaciation
Glacial geomorphology
Geochronology
Ice sheet dynamics

A B S T R A C T

To provide a new reconstruction of the deglaciation of the Fennoscandian Ice Sheet, in the form of calendar-year time-slices, which are particularly useful for ice sheet modelling, we have compiled and synthesized published geomorphological data for eskers, ice-marginal formations, lineations, marginal meltwater channels, striae, ice-dammed lakes, and geochronological data from radiocarbon, varve, optically-stimulated luminescence, and cosmogenic nuclide dating. This is summarized as a deglaciation map of the Fennoscandian Ice Sheet with isochrons marking every 1000 years between 22 and 13 cal kyr BP and every hundred years between 11.6 and final ice decay after 9.7 cal kyr BP.

Deglaciation patterns vary across the Fennoscandian Ice Sheet domain, reflecting differences in climatic and geomorphic settings as well as ice sheet basal thermal conditions and terrestrial versus marine margins. For example, the ice sheet margin in the high-precipitation coastal setting of the western sector responded sensitively to climatic variations leaving a detailed record of prominent moraines and other ice-marginal deposits in many fjords and coastal valleys. Retreat rates across the southern sector differed between slow retreat of the terrestrial margin in western and southern Sweden and rapid retreat of the calving ice margin in the Baltic Basin. Our reconstruction is consistent with much of the published research. However, the synthesis of a large amount of existing and new data support refined reconstructions in some areas. For example, the LGM extent of the ice sheet in northwestern Russia was located far east and it occurred at a later time than the rest of the ice sheet, at around 17–15 cal kyr BP. We also propose a slightly different chronology of moraine formation over southern Sweden based on improved correlations of moraine segments using new LiDAR data and tying the timing of moraine formation to Greenland ice core cold stages.

Retreat rates vary by as much as an order of magnitude in different sectors of the ice sheet, with the lowest rates on the high-elevation and maritime Norwegian margin. Retreat rates compared to the climatic information provided by the Greenland ice core record show a general correspondence between retreat rate and climatic forcing, although a close match between retreat rate and climate is unlikely because of other controls, such as topography and marine versus terrestrial margins. Overall, the time slice reconstructions of Fennoscandian Ice Sheet deglaciation from 22 to 9.7 cal kyr BP provide an

* Corresponding author.
E-mail address: arjen.stroeven@natgeo.su.se (A.P. Stroeven).

http://dx.doi.org/10.1016/j.quascirev.2015.09.016

important dataset for understanding the contexts that underpin spatial and temporal patterns in retreat of the Fennoscandian Ice Sheet, and are an important resource for testing and refining ice sheet models.

1. Introduction

Melting of the Greenland and Antarctic ice sheets, and the threat of accelerated melt in response to future climate warming, has firmly positioned ice sheet deglaciation processes and rates on the global research agenda (Warrick and Oerlemans, 1990; Briner et al., 2009; Church et al., 2013; Stokes et al., 2014). This is because an important implication of accelerated ice sheet melt, in addition to ice sheet mass loss through calving, is an expected rise in global mean sea level, with spatial variations around that mean (Milne et al., 2009; Kopp et al., 2010; Slangen et al., 2014) and resulting challenges for coastal land use. The current condition of the Greenland and Antarctic ice sheets, grown out of highlands but also covering extensive lowlands and subglacial basins below sea level, is similar to the situation of the former Laurentide and Fennoscandian ice sheets at their last maximum positions, and implies ice sheet retreat with margins extending offshore. Future retreat patterns, if recent trends persist, will likely differ starkly for margins that are predominantly terrestrial and those that are terminating in a marine environment. The latter are prone to destabilization and run-away effects through sea level rise and margin thinning (Hughes, 1975; Favier et al., 2014). This insight has been gained from the dynamics and deglaciation histories of the former Northern Hemisphere ice sheets (Kleman and Applegate, 2014) and from measurements and modelling pertaining to the Greenland and Antarctic ice sheets (Joughin et al., 2014; Rignot et al., 2014).

At the height of glaciation, during the global Last Glacial Maximum (LGM, 26.5-20 thousand years ago [cal kyr BP]; Clark et al., 2009b), a considerable portion of the Northern Hemisphere landmass above 60 °N was ice-covered (Denton and Hughes, 1981). Reconstructions of the maximum extent and the timing of initial retreat of these Northern Hemisphere ice sheets has been a research focus for the last 175 years (Agassiz, 1840; Torell, 1872, 1873; Jackson and Clague, 1991). The first deglaciation reconstructions were entirely based on geomorphological and sedimentological/stratigraphical evidence for glaciation. In the absence of a reliable dating technique, the pace of deglaciation was initially inferred from the correlation between sequences of silty light- and clayey dark-coloured sediment couplets. These ‘varves’ formed during summer and winter seasons, respectively, through ice sheet melt, runoff, and proglacial sedimentation. Extensive varve deposits are typically exposed between highest shore lines and the present coasts, and can be used for dating of the ice recession. This is because the age of the first varve overlying the formerly subglacial terrain (typically bedrock or till), denotes the age of deglaciation and therefore the former position of the ice sheet margin (De Geer, 1884, 1912, 1940; Sauramo, 1918, 1923). In a series of seminal studies on the deglaciation of the Fennoscandian Ice Sheet, De Geer (1884, 1896, 1912, 1940) developed the Swedish Time Scale (STS) varve chronology (Lidén, 1938; Wohlfarth et al., 1995). In the past three decades many studies have refined the STS (Strömberg, 1985a, b, 1989, 1990; 1994; Kristiansson, 1986; Cato, 1987; Andrén, 1990; Brunnberg, 1995; Wohlfarth et al., 1995, 1998; Hang, 1997; Lindeberg, 2002), eventually resulting in a correlation of the STS with the Greenland GRIP and NGRIP ice core record layer-counting chronology (Andrén et al., 1999, 2002; Stroeven et al., 2015). These attempts to correlate varve- and ice core chronologies have, however, revealed that hundreds of varves are missing in the STS, thus exposing a key shortcoming of this indirect dating technique (Andrén et al., 2002).

With the advent of radiometric dating techniques (Bard and Broecker, 1992), in particular radiocarbon (Anderson et al., 1947; Arnold and Libby, 1949), the timing of maximum glacier extent, has typically been constrained by the first occurrence of living matter in proglacial lakes dammed by the ice margin (yielding ages older than the maximum ice extent) and in lakes dammed by the end moraine once the ice margin had retreated from its maximum extent (yielding ages younger than the maximum ice extent). Dating the initiation of ice-free conditions using radiocarbon has been the dominant dating-driven ice sheet reconstruction method, and an abundance of minimum age constraints has permitted detailed ice-sheet wide retreat reconstructions (e.g., Dyke et al., 2003; Gyllencreutz et al., 2007).

There are a number of limitations associated with radiocarbon dating in formerly glaciated regions (Hajdas, 2008). Critically, there is dearth of datable organic material in many locations because deglaciation occurred in polar deserts. Given the inevitable delay in organic growth following deglaciation, ^{14}C dates provide minimum limiting ages on deglaciation. In addition, the precision of radiocarbon dating is compromised by the potential incorporation of young carbon contaminants, incorporation of old carbon in the depositional environment (marine reservoir or hard water effects; Snyder et al., 1994), and variations in the atmospheric radiocarbon concentration over time. These combined effects produce similar radiocarbon ages for samples that were deposited hundreds of years apart (radiocarbon dating plateaux). Because of these potential pitfalls, considerable effort has been devoted to the improvement of sample preparation methods and calibration of the radiocarbon chronology (Bard et al., 1990, 1997; Wohlfarth et al., 1995; Reimer et al., 2009, 2013). The best radiocarbon age determinations come from environments where terrestrial macrofossils have been used to constrain the age model (Barnekow et al., 1998).

During recent decades two new dating techniques have emerged, based on the burial of sand through optically-stimulated luminescence (OSL) and the exposure of quartz-bearing clasts and bedrock through measuring concentrations of cosmogenic nuclides. In each case, datable material is abundant in pro-glacial and glacial environments.

The OSL method is based on the build-up of a luminescence signal in quartz grains that are shielded from sunlight through burial (Rhodes, 2011). Exposure to sunlight deletes any previous luminescence dose (bleaches the quartz grain). Hence, OSL can be applied to date the burial of quartz grains (feldspar is also routinely measured) given that two crucial conditions are met: 1) during transport the grains are exposed to sunlight for a duration sufficient to become bleached and; 2) the sample has not been re-exposed (Huntley et al., 1985; Aitken, 1998). Whereas the latter condition can usually be verified in stratified sediments, partial-bleaching is a major obstacle when dating glacial sediments, commonly resulting in an over-estimation of the depositional age of the landform (Fuchs and Owen, 2008; Alexanderson and Murray, 2012b). OSL is therefore typically applied in settings where these conditions are more easily met, such as where aeolian, fluvial, or lacustrine sedimentation has occurred. Single-grain approaches account for partial bleaching through evaluating the suitability of individual grains in a sample, which strongly improves the reliability of OSL (Murray and Wintle, 2000).

Cosmogenic nuclide surface exposure dating is applied to samples taken from bedrock or boulders chosen for the information they provide on deglaciation (Gosse and Phillips, 2001). Again, the preferred mineral is quartz, in which four nuclides are produced through exposure to cosmic rays; one stable (^{21}Ne) and three radioactive (^{10}Be, ^{26}Al, and ^{14}C) nuclides. Beryllium-10 has been by far the most reliable nuclide (Portenga and Bierman, 2011) and has been extensively used in recent decades to construct glacial chronologies around the globe (Stone et al., 2003; Balco and Schaefer, 2006; Ivy-Ochs et al., 2006; Rinterknecht et al., 2006; Hein et al., 2010; Heyman, 2014; Rother et al., 2014; Stroeven et al., 2014). Typically, samples are extracted from boulders on end moraine crests, although samples from other landforms (Stroeven et al., 2011) and of bedrock (Fabel et al., 2004; Li et al., 2005) have been shown to also yield useful deglaciation ages. The reliability of cosmogenic nuclide exposure dating for yielding accurate ages of deposition and deglaciation is based on the assumption that the sampled boulder/bedrock surface has been: 1) shielded from cosmic rays prior to the last deglaciation and therefore contains no inherited nuclides; and 2) continuously exposed to the full flux of cosmic rays since deglaciation with no shielding from sediment, snow or vegetation. A breach of assumption 1 would cause erroneously old ages, whereas a breach of assumption 2 would cause erroneously young ages. An evaluation of these assumptions has shown that for sample groups with large age scatter, prior exposure/inheritance is typically less common than incomplete exposure/post-glacial shielding (Heyman et al., 2011). Suites of samples from individual landforms can be statistically analysed to potentially identify anomalous dates and thereby determine accurate landform ages (Applegate et al., 2010, 2012; Heyman, 2014).

An ever increasing availability and handling efficiency of remotely sensed data (aerial photographs, satellite imagery, and LiDAR; Smith et al., 2006) has heralded a resurgence of ice sheet maximum and retreat reconstructions from landforms (Andersen, 1979, 1980, 1981; Lundqvist, 1986, 1994; Boulton and Clark, 1990a, c; Lundqvist and Saarnisto, 1995; Kleman et al., 1997, 2010; Andersen and Pedersen, 1998; Lindström et al., 2000; Ehlers and Gibbard, 2004; Margold et al., 2013). This has led to regional compilations of flow traces (striations, eskers, till lineations, bedrock lineations, basal till fabrics, meltwater channels; e.g., Hättestrand, 1998; Hättestrand and Clark, 2006a) and their inclusion in ice sheet-wide analyses (Kleman et al., 1997; Boulton et al., 2001). Kleman et al. (1997, 2006) grouped coherent patterns of ice flow traces of the same age into flow trace fans (map representations of glacial landform swarms) and combined the undated stacked record of subglacial ice flow traces with dated ice marginal successions to produce a reconstruction of Fennoscandian Ice Sheet evolution over a glacial cycle. LiDAR scanning has produced recent orders-of-magnitude increases in the resolution of elevation data over landscape scales (Dowling et al., 2013). In this compilation we take advantage of LiDAR data to advance our understanding of ice sheet marginal retreat, particularly over southern Sweden (see 5.2.).

Geophysical- and ice sheet-modelling are increasingly used to derive ice sheet reconstructions. These are independent methodologies, the results of which can be evaluated against field evidence (Davis et al., 1999; Lambeck, 1999; Napieralski et al., 2007). As an ice sheet grows and decays, it transfers a shifting load onto Earth's crust which responds through elastic and visco-plastic deformation. As the crust rebounds following maximum glaciation (termed glacial isostatic adjustment: GIA), its effect is recorded, by shifting relative sea levels. Hence, from large sets of shoreline displacement curves it is possible to separate the effects of eustatic sea level rise (through ice sheet melting) and isostatic rebound, which can then be used to inversely deduce the history of the ice load (Lambeck et al., 1998). Because far-field effects of deglaciation, for example in Antarctica, will have direct, predictable, but uneven influence on regional sea level, such as around Scandinavia, Earth-response models need to be global (Slangen et al., 2014).

Ice sheet models are the most holistic way of addressing the temporal evolution of glaciation for a particular ice sheet (Denton and Hughes, 1981, 2002; Budd and Smith, 1982; Payne et al., 1989; Huybrechts, 1993; Marsiat, 1994; Boulton et al., 1995; Holmlund and Fastook, 1995; Hubbard, 1999; Siegert et al., 2001; Kleman et al., 2002; Marshall et al., 2002; Boulton and Hagdorn, 2006; Clason et al., 2014; Seguinot et al., 2015). This is because the extents and thicknesses of ice sheets are calculated over small time increments and over large spatial scales in response to changes in climate (mass balance) forcing. The choice of climate forcing and the conversion of climate to mass balance remains the largest limitation in ice sheet modelling, which necessitates calibration of ice sheet models against field evidence (Li et al., 2007; Napieralski et al., 2007; Seguinot et al., 2014). It is with the aim of providing targets for the evaluation of ice sheet modelling output that we present a new reconstruction of the deglaciation of the Fennoscandian Ice Sheet. Using the new reconstruction we revisit important questions concerning the influence of ice sheet dynamics and paleoclimate forcing on the ice sheet margin history, the pace of retreat for different ice sheet sectors, and the influence of topography on deglaciation patterns and rates. Ice sheet models will ultimately yield the most comprehensive answers to these questions, when properly tuned against the presented deglaciation reconstruction, and provide a framework with which to query the future behaviour of contemporary ice sheets.

At the time of the global LGM a contiguous ice mass covered northern Europe from off-shore western Ireland to onshore northwestern Taimyr Peninsula, on the eastern fringes of the Kara Sea (Svendsen et al., 2004, Fig. 1). From a dynamic perspective, this ice mass consisted of three ice sheets, each of which responded individually to external forcing (geothermal heat, climate, sea level, GIA), and which were amalgamated for a relatively brief period of the total ice sheet duration. Following the global LGM the British-Irish Ice Sheet separated from the Fennoscandian Ice Sheet offshore of southern Norway (Clark et al., 2012) and the Barents Sea Ice Sheet unzipped from the Fennoscandian Ice Sheet offshore northern Norway (Bjarnadóttir et al., 2014). The focus of our study is the retreat of the Fennoscandian Ice Sheet following its isolation from these other ice masses (Fig. 1). Several attempts to establish the deglaciation chronology of the Fennoscandian Ice Sheet precede our efforts (Fig. 2). We present a new reconstruction, which incorporates an abundance of publications during the past 15 years that contain new geomorphological and geochronological data. This is specifically aimed at delivering calendar-year time-slice representations of ice sheet extents for use by ice sheet modellers.

2. Data

2.1. Geomorphology

We begin with a description of the key indicative ice-marginal and subglacial landforms on which the deglaciation reconstruction is primarily based. These include, in a progression from proglacial/ice marginal to subglacial, ice-dammed lakes, marginal meltwater channels, ice-marginal formations (moraines and glacifluvial deposits), eskers, lineations, and striae. We then review the geochronological tools available for deglaciation reconstructions

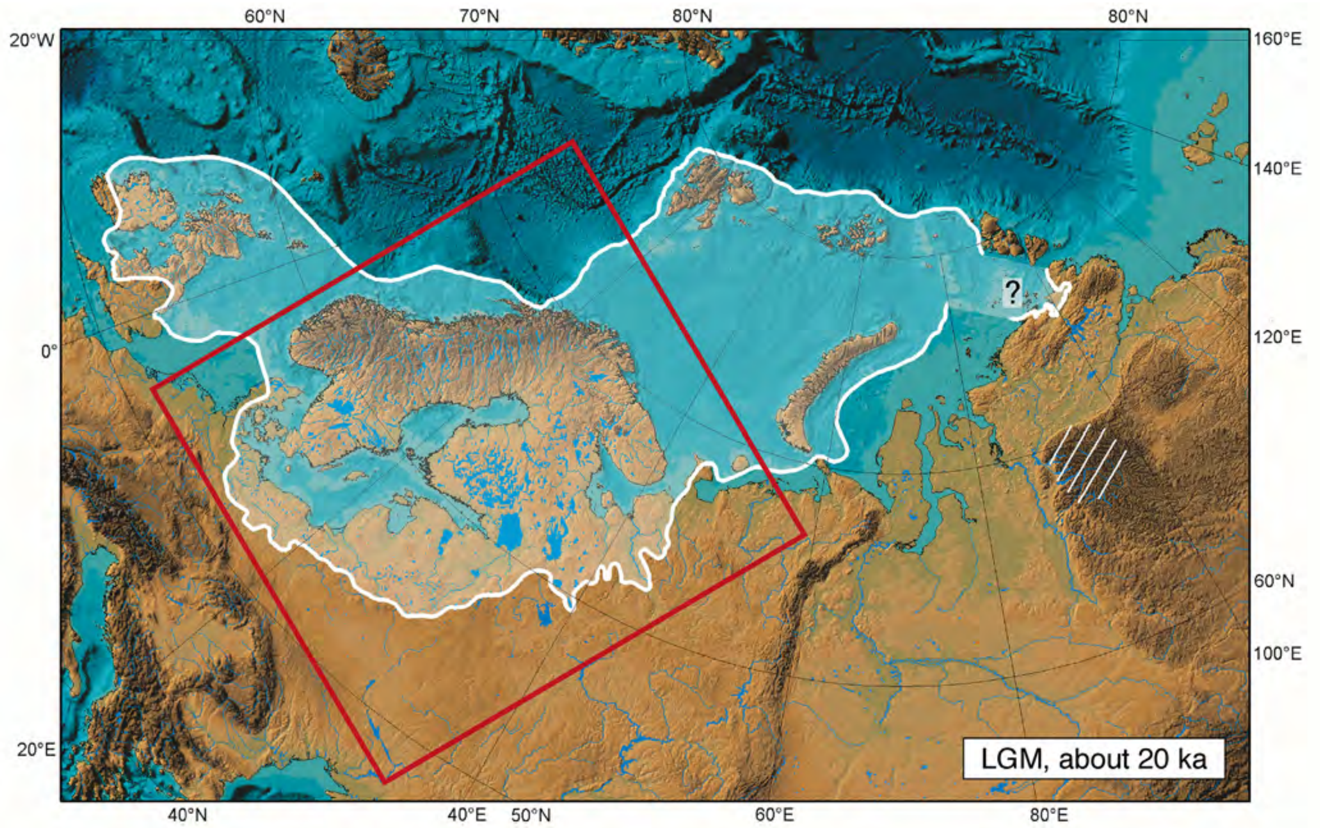

Fig. 1. The Eurasian ice sheet at the Last Glacial Maximum (LGM) as portrayed by Svendsen et al. (2004). This ice sheet complex consisted of the amalgamation of three separate ice sheet centers, the British-Irish Ice Sheet in the west, the Barents Sea Ice Sheet in the east, and the Fennoscandian Ice Sheet, the object of our study, in the center (red box; Figs. 4–7, 9, 10, 12a). (For interpretation of the references to colour in this figure legend, the reader is referred to the web version of this article.)

(e.g., Hughes et al., 2011), shortly review their strengths and pitfalls, and present the data included in our deglaciation reconstruction.

2.1.1. Ice-dammed lakes

Where ice margins block the natural drainage of ice-free catchments, water ponding may lead to the formation of ice-dammed lakes. Such lakes are inherently unstable and drain catastrophically when the ice dam fails. This occurs when the lake hydrostatic pressure exceeds the ice overburden pressure at the lake outlet, when a retreating ice margin exposes lower terrain, or through overtopping. Glacial lakes have formed with dimensions over many orders of magnitude, from the Baltic Ice Lake (349,000 km^2; Jakobsson et al., 2007) to the numerous intermediate- and small-scale ice-dammed lakes impounded between the Scandinavian Mountains and the retreating western margin of the decaying ice sheet (Lundqvist, 1972; Kleman, 1992, Fig. 3). Evidence of former ice-dammed lakes such as shorelines (erosional/depositional), perched deltas, and spillway (overflow) channels are useful tools for reconstructing the ice marginal retreat pattern in areas formerly covered by cold-based ice (Frödin, 1913; Lundqvist, 1973; Jansson, 2003). Fig. 3 shows the post-Younger Dryas extent of ice-dammed lakes in Fennoscandia, compiled from available sources (Lundqvist, 1972, 1973; Melander, 1977; Ulfstedt, 1981; Borgström, 1989; Longva and Thoresen, 1991).

2.1.2. Marginal meltwater channels

Water produced during ice sheet surface melting predominantly runs off the surface and along the ice sheet margin where it abuts higher ground. While flowing along the ice margin, streams erode the ground surface at the junction with the ice and form marginal meltwater channels (Borgström, 1989; Mannerfelt, 1945, 1949; Syverson and Mickelson, 2009). Marginal meltwater channels are typically tens of meters deep, meters wide, and hundreds of meters long, and usually form in subparallel down-slope sequences. Importantly, the slope and orientation of marginal channels occur at oblique angles to the hillslope topography into which they are eroded, and they provide a record of retreating ice margins that is independent of other deglacial landforms (Mannerfelt, 1945; Lundqvist, 1973; Borgström, 1989; Kleman, 1994; Greenwood et al., 2007; Margold et al., 2011). This is because, in contrast to eskers and lineations, marginal meltwater channels form also during deglaciation under cold-based conditions (Kleman, 1992; Dyke, 1993; Hättestrand and Stroeven, 2002; Jansson et al., 2002). Meltwater landforms have therefore been used in our reconstruction primarily where the final deglaciation occurred under cold-based conditions (Kleman, 1992; Kleman et al., 1997, 2006; Kleman and Hättestrand, 1999) (Fig. 4).

2.1.3. Ice-marginal formations

Along the margins of ice sheets, there are several processes by which sediment exits the ice and becomes part of the glacier foreland (Boulton et al., 1985). The sediment frequently becomes concentrated in ice-marginal formations, including end moraines and glaciofluvial deposits that generally mirror the shape and position of former ice margins (Fig. 5). These formations occur commonly along the entire Fennoscandian Ice Sheet margin and indicate either interruptions in ice sheet retreat or re-advances following the LGM. Particularly extensive ice-marginal formations

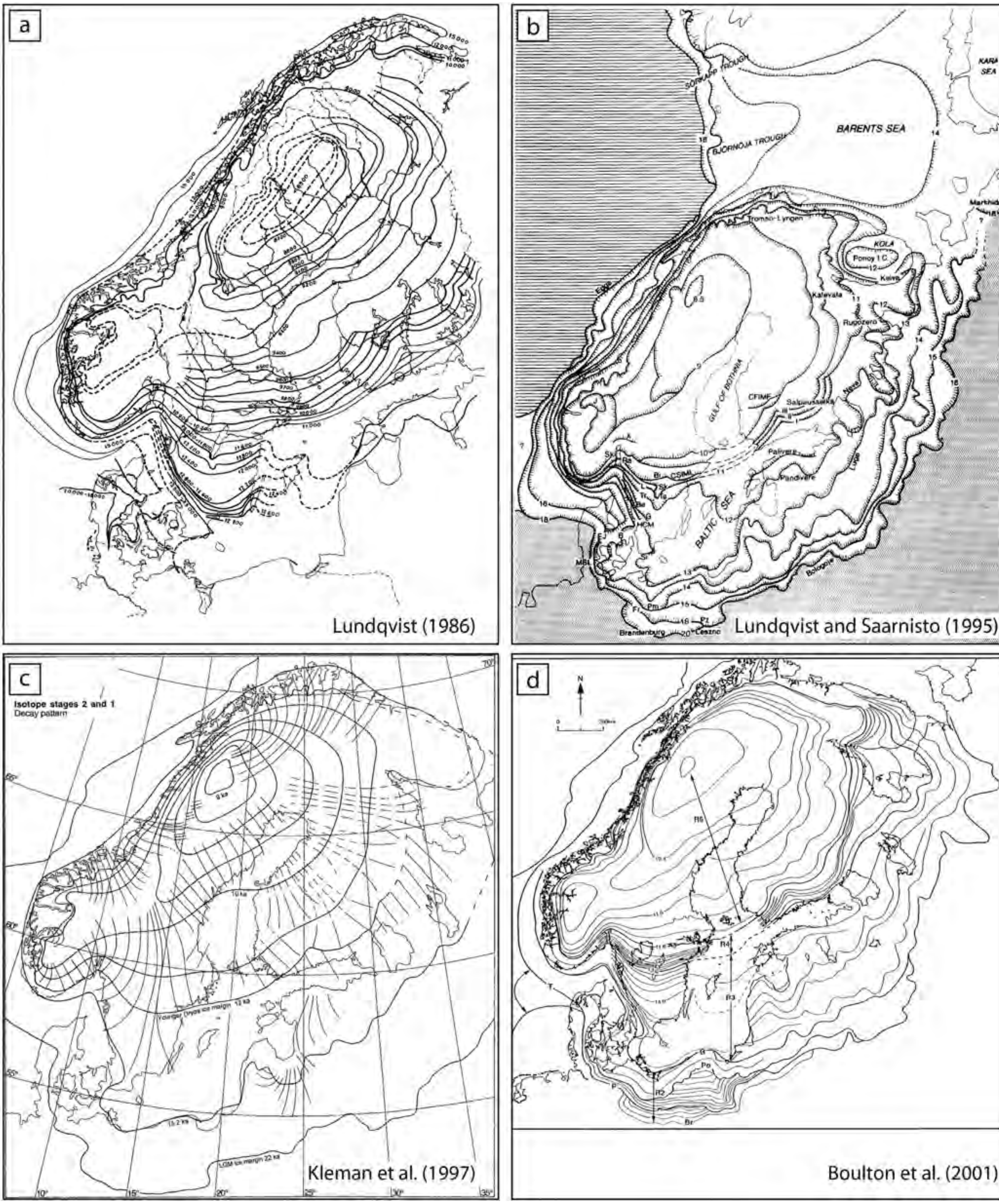

Fig. 2. Four reconstructions of the deglaciation pattern of the Fennoscandian Ice Sheet by a) Lundqvist (1986), b) Lundqvist and Saarnisto (1995), c) Kleman et al. (1997), and d) Boulton et al. (2001).

characterize the eastern and southern ice sheet limits, through Russia, the Baltic countries, Poland, Germany, Denmark, and into Norway (Fig. 6). Hence, series of these formations can be traced inwards from local glacial maximum positions to Younger Dryas positions (Fig. 5), which mark the last ice sheet-wide interruption in margin retreat before complete deglaciation. Where ice-marginal formations are punctuated by gaps of non-deposition or meltwater stream erosion, they can often be extrapolated to each

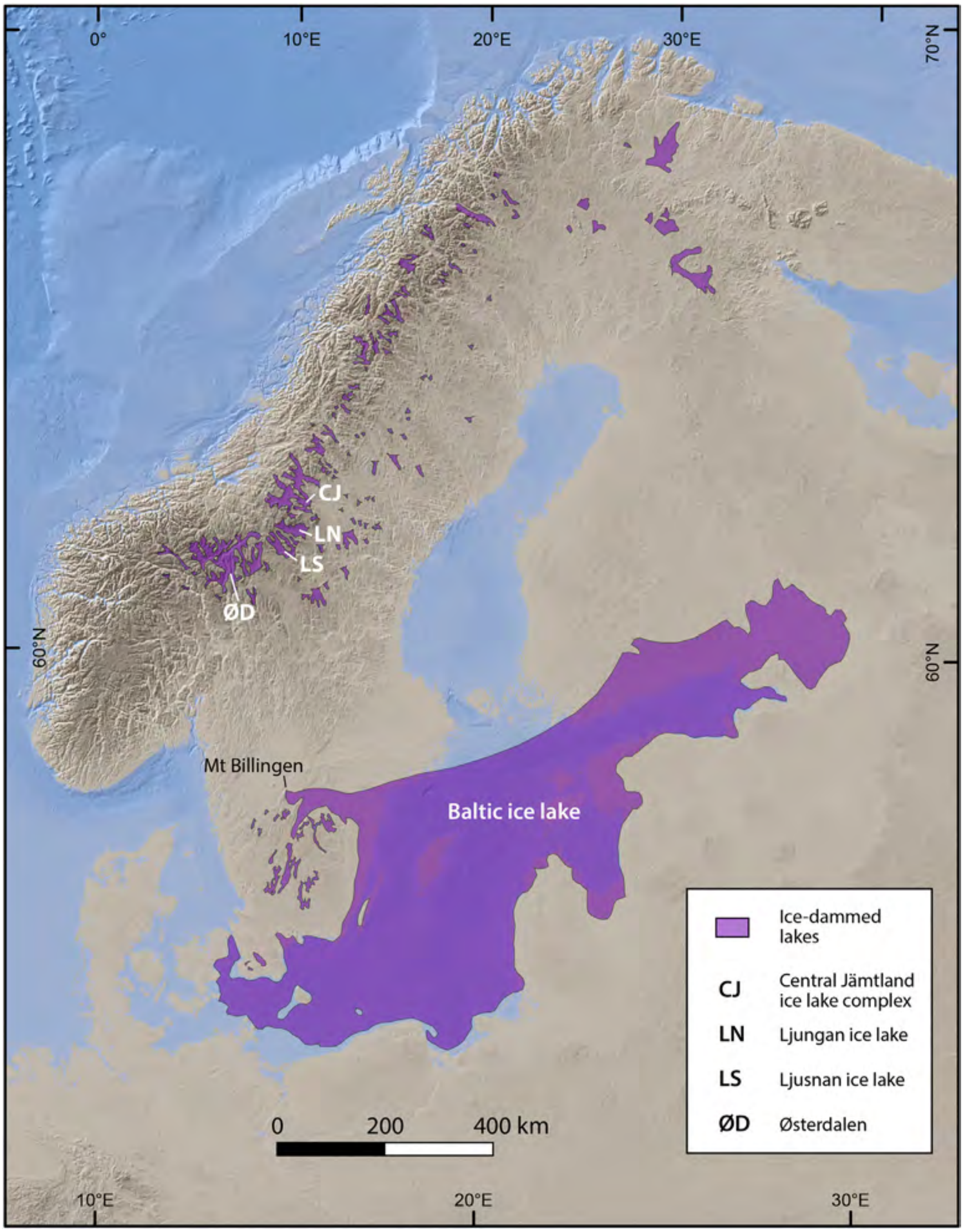

Fig. 3. Glacial lakes in Fennoscandia used to constrain the ice margin retreat pattern. The Baltic Ice Lake existed during the Younger Dryas, until it finally drained at its northwestern extremity, Mount Billingen, at 11,620 cal years BP (Stroeven et al., 2015). Additional smaller glacial lakes existed before the Younger Dryas, but we have made no attempt to make a systematic inventory of them, because we rely predominantly on ice-marginal formations to guide our deglaciation reconstruction. The position of the final narrow ice ridge joining residual ice in southern Norway with the main dome in the north (cf. 10.2 cal kyr BP, Fig. 9), is constrained by glacial lakes having been dammed in opposite directions. The period with ice-dammed lakes in existence along the mountain backbone is short, around 600 years. The drainage of some of the lakes has been traced and dated in the clay varve chronology (De Geer, 1940; Borell and Offerberg, 1955; Fözö, 1980; Strömberg, 1989).

other assuming lateral ice sheet continuity. To guide pre-Younger Dryas deglaciation patterns of the Fennoscandian Ice Sheet, we have compiled moraine positions from maps (Fig. S1, Supplementary dataset). Post-Younger Dryas ice-marginal formations are much rarer and so only guide deglaciation patterns regionally, and they can indicate both interruptions of the ice margin retreat and re-advances up to late Preboreal, 10,500 cal years BP (Sveian et al., 1979).

2.1.4. *Eskers*

Eskers are ridges of coarse-grained sorted sediment deposited in meltwater tunnels at the base of an ice sheet. They can be single ridges or form networks of several parallel ridges. Eskers can be short (hundreds of meters) and straight but more typically are long and winding and can extend for hundreds of kilometers and be tens of meters high (De Geer, 1897; Lundqvist, 1979; Storrar et al., 2014). Because eskers are such recognizable and sizeable landforms, they have been accurately mapped from aerial photographs, and reliable esker maps exist for individual countries (Lundqvist, 1959) as well as for larger regions such as northern Fennoscandia (Nordkalott Project, 1986). For our deglaciation reconstruction of the Fennoscandian Ice Sheet, we present an ice sheet-wide esker map for shield areas, where they are abundant (Fig. 5). The map is compiled from existing publications (Nordkalott Project, 1986; Niemelä et al., 1993; Hättestrand, 1998; Bargel et al., 1999; Hättestrand and Clark, 2006a; NGU, 2014) and managed in ArcGIS. The esker pattern on

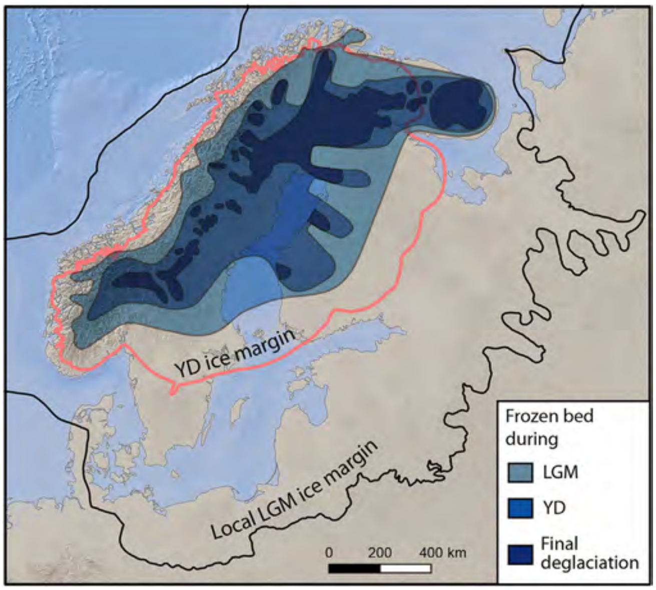

Fig. 4. The shrinkage of the cold-based core area of the Fennoscandian Ice Sheet during deglaciation from its local LGM maximum position (Kleman, 1992; Kleman et al., 1997, 2006; Kleman and Hättestrand, 1999; Hättestrand and Clark, 2006b). The outer blue envelope represents the inferred minimum cold-based extent at LGM. The innermost envelope represents areas inferred to have had cold-based conditions until local deglaciation. The intermediate envelope shows how ice streams in northern Norway, Finland, and the collapse event following a surge in the Gulf of Bothnia (Strömberg, 1989; Lundqvist, 2007; Kleman and Applegate, 2014; Greenwood et al., in press), extended wet-based conditions into the ice sheet in a corridor-like pattern during the decay phase. At any given point in time, the border zone between warm- and cold-based conditions was probably mosaic-like in sheet flow areas (Kleman et al., 1999; Kleman and Glasser, 2007).

Fig. 5 provides a generalized pattern because of the relatively small scales of the source maps, and short eskers (including subglacially engorged eskers) are therefore not included or used for the deglaciation reconstruction. Eskers that formed over the sedimentary bedrock areas west, south, and east of the Baltic Sea are generally smaller and shorter than those over shield areas, and esker compilations generally cover only minor areas (e.g., Rattas, 2007). As eskers have been shown to form within limited distances of the contemporaneous ice margin (Hebrand and Åmark, 1989; Kleman et al., 1997), and because water flow directions follow the overburden pressure regime, we use the direction of eskers to guide the overall shape of former ice sheet margins. In our reconstruction, ice sheet margins are always drawn perpendicular to the esker long-axes. It should be noted, however, that there are areas where eskers could not be used for our reconstruction because they did not form during the last deglaciation but, rather, formed during earlier deglaciations. This is the case, for example, in extensive areas of northern Sweden (Lagerbäck and Robertsson, 1988), and Finland (Johansson and Kujansuu, 1995), where eskers of a pre-LGM deglaciation (Helmens et al., 2000) are cross-cut by younger esker systems, are covered by tills, and have kettle-holes with interstadial sediments, all which indicate that these eskers escaped erosion during the last deglaciation through sustained cold-based conditions. In these areas, other meltwater landforms, such as ice-dammed lake traces and marginal meltwater channels, were used to reconstruct retreat of the Fennoscandian Ice Sheet during the last deglaciation.

2.1.5. Lineations

The most widely utilised subglacial landform for ice sheet reconstructions is the glacial lineation (Fairchild, 1907; Linton, 1963; Punkari, 1982; Boulton and Clark, 1990a, b; Kleman, 1992; Clark, 1993; Kleman et al., 1997). Lineations are elongated landforms that form parallel to ice flow and are usually referred to as drumlins. Because lineations can be formed through depositional and erosional processes, they may be comprised of diamicts, sorted sediments, and/or bedrock (cf. review by Stokes et al., 2011). Although larger landforms may have formed during multiple glaciations (Hättestrand et al., 2004), and although later generations of lineations do not necessarily erase older lineations (Kleman, 1992), the association of lineations with other deglacial landforms implies that most of these inform the ice flow direction, and therefore the ice surface slope, just prior to deglaciation. Lineations are a particularly useful complement to the directional information contained in eskers because they often form in swarms hundreds of kilometers in extent and may contain tens of thousands of elements (Hättestrand et al., 1999, 2004; Dellgar Hagström, 2006; Clark et al., 2009a). We have employed the lineation database of Kleman et al. (1997, Fig. 3) in our reconstruction of the last deglaciation of the Fennoscandian Ice Sheet.

2.1.6. Striae

Striae represent the finest-scale imprint of ice flow on bedrock. On outcrops where more than one set of striae are preserved, their cross-cutting relationships may reveal the evolution of ice flow directions (Erdmann, 1868; Lundqvist, 1969) and indicate the ice flow direction closest in time to deglaciation. Lineations and striae both record the ice-flow direction at the time of formation, and could therefore be expected to yield the same information regarding ice flow-evolution. In reality, there are important differences in the information provided by the two data types (Kleman, 1990). Lineations are typically formed from a glacial deposit, and their spatial arrangement means that the continuity and extent of a flow pattern can be visually judged. Striae, on the other hand, are purely erosional bedrock forms and constitute detailed point data even though large collections of striae observations, with less precision than for lineations, still can give a visual imprint of flow patterns. Importantly though, the maximum "time depth" is larger for striae than for lineations. This is because a rock outcrop typically provides facets or steps that are sheltered during later ice flow and may therefore locally preserve older striae. No corresponding local protection mechanisms exists for lineations, except for protection from erosion under cold-based conditions (Kleman et al., 2002), and so preservation of older directional information decreases more directly as a function of subsequent ice flow velocity and duration.

An important property of the composite striae record is that the locally youngest striae may, in some places, indicate deglacial ice flow directions in areas lacking lineation swarms. We have used compilations of striae (first pioneered by Sefström, 1836) to extract the youngest ice flow direction in areas where such information is otherwise absent (Ljungner, 1943). These areas are predominantly along the Gulf of Bothnia (Fig. 6) where the youngest sets of striae indicate the re-advance of an ice lobe (Lundqvist, 2007) and in northwestern Sweden where meltwater landforms and striae can be used to construct final deglaciation ice flow directions in areas characterized by cold-based ice (Kleman, 1990).

2.2. Chronology

No dating technique is applicable in every field setting, whether it be due to limits on the materials available to date or the timescale spanned by the method itself. Consequently, a range of geochronological tools are employed and the most important methods in the Fennoscandian context are as follows.

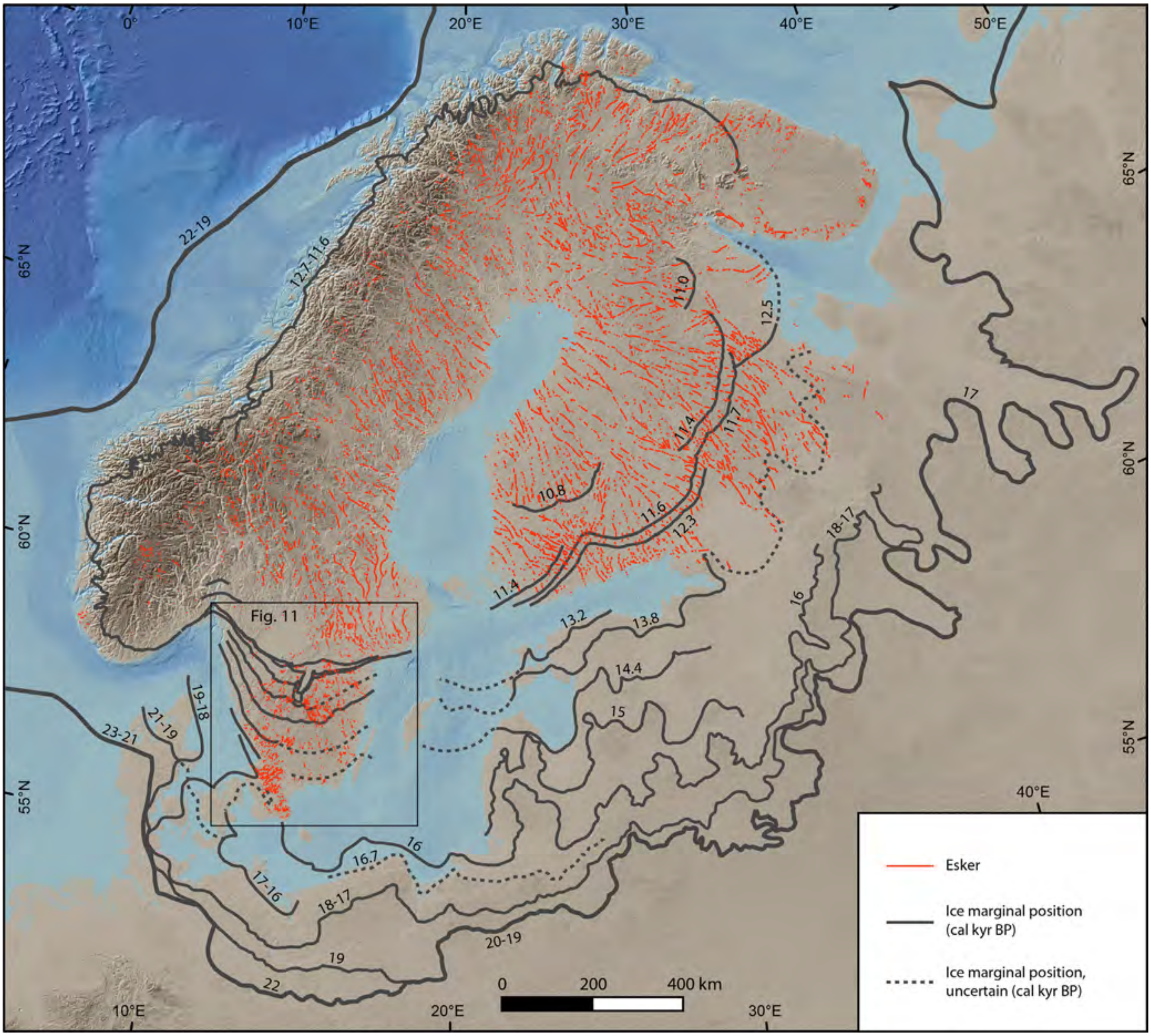

Fig. 5. Prominent eskers and ice-marginal positions in the area evacuated by the Fennoscandian Ice Sheet since the LGM. Note that the esker data only covers shield areas, where eskers form continuous esker chains that are useful for reconstructing the deglaciation. Eskers in non-shield areas have been omitted since they are short, infrequent, and add little to the deglaciation information provided by the generally rich record of ice-marginal positions in these areas. The overwhelming majority of mapped eskers date from the last deglaciation (Nordkalott Project, 1986; Niemelä et al., 1993; Hättestrand, 1998; Bargel et al., 1999; Hättestrand and Clark, 2006a; NGU, 2014). For ice-marginal formations in the southern and eastern sectors of the Fennoscandian Ice Sheet, we have relied primarily on literature of the past 15 years (Fig. S1, Supplementary dataset). Where published data have been in conflict, we have employed minimum-complexity assumptions for spatial (and thereby chronological) correlation of data, assessing spatial, morphological, chronological, and glaciological relationships and probabilities. For southern Sweden (black box, Fig. 11) we have made amendments to existing moraine maps through interpretation of LiDAR-generated DEM data. Landforms and ages (in cal kyr BP) from Sollid et al. (1973), Houmark-Nielsen and Kjær (2003), Demidov et al. (2006), Hättestrand and Clark (2006b), Rise et al. (2006), Raukas et al. (2010), Mangerud et al. (2011), Saarse et al. (2012), Marks (2012), Lasberg and Kalm (2013), Anjar et al. (2014), Bjarnadóttir et al. (2014), Briner et al. (2014), Rinterknecht et al. (2014), Stokes et al. (2014), and Svendsen et al. (2015).

2.2.1. Radiocarbon dating

Radiocarbon dating of organic material has traditionally been the key chronological tool for defining the timing of deglaciation (e.g., Dyke, 2004). With glacier retreat, new terrain becomes ice free and available for the production, storage, and preservation of organic material in pro-glacial sedimentary archives. With a half-life of 5730 ± 40 years for ^{14}C, which limits its application to about the last ~50–40 kyr, radiocarbon dating provides chronological constraint on the Fennoscandian Ice Sheet deglaciation (c. 24–10 kyr).

We have compiled a database of 335 published ^{14}C ages of relevance for the deglaciation of the Fennoscandian Ice Sheet (Table 1, Fig. 7, Supplementary dataset). The ^{14}C ages are primarily derived from basal sediment in lakes and peat cores and include measurements on both bulk sediment and terrestrial macrofossils. One-third of the ^{14}C dates in our compilation, mainly from the western and southeastern sectors of the Fennoscandian Ice Sheet, are derived from sub-till sediment samples. Organic material in these samples pre-dates the glacial advance to the LGM configuration and subsequent retreat to the sample site, and they therefore represent maximum ages of deglaciation.

All radiocarbon ages have been calibrated using OxCal 4.2

Fig. 6. Map of the Fennoscandian Ice Sheet deglaciation domain with ice-marginal formations and place names mentioned in the main text.

(Bronk Ramsey, 2009) and the Intcal13 curve (Reimer et al., 2013). All marine samples were corrected for a marine reservoir effect, by applying a correction of 300–800 years, according to the original publications (Supplementary dataset), for the presence of old carbon derived from the marine environment (Mangerud and Gulliksen, 1975).

2.2.2. Varves, Swedish Time Scale (STS)

The strength of the clay varve chronology, if the varve measuring sites are closely spaced, is that retreat of the ice margin can be resolved more accurately than with any other correlation method, regardless of whether the varve chronology is floating in time or is of calendar-year quality. Fig. 8 exemplifies the level of detail that can be achieved using clay varve correlations. Isochrons are drawn on the basis of clay varve correlations using the age of the oldest varve. In this way the STS should be internally robust for 2400 years of Late Glacial time (Table 2, -2250 to +140 STS varve years or 12,340 to 9950 cal yrs BP; Bergström, 1968; Fözö, 1980; Kristiansson, 1986; Strömberg, 1989, 1990, 1994, 2005; Brunnberg, 1995; Wohlfarth et al., 1998). To obtain a complete varve chronology, connecting the Late Glacial varve sequence with postglacial varves that extend to the present (Cato, 1987), over 1300

Table 1
Publications with radiocarbon dates included in the Supplementary dataset, including the number of samples (N).

Publications	N	Publications	N
Aas and Faarlund (1988)	1	Larsen et al. (2006)	5
Abrahamsen and Readman (1980)	1	Larsen et al. (2014)	1
Alm (1993)	2	Lasberg and Kalm (2013)	6
Alstadsæter (1982)	2	Liiva et al. (1966)	1
Andersen (1975)	1	Lindén et al. (2006)	4
Antonsson et al. (2006)	1	Möller et al. (2013)	8
Arppe and Karhu (2010)	3	Nese and Lauritzen (1996)	2
Bang-Andersen (2003)	2	Noe-Nygaard and Heiberg (2001)	1
Bennike and Jensen (1995)	2	Nydal et al. (1972)	1
Berglund (1995)	5	Olsen (1997)	2
Berglund (2005)	2	Olsen (2000)	1
Berglund et al. (1976)	3	Olsen (2002)	2
Bergman et al. (2004)	1	Olsen (2004, unpublished)	1
Bergman et al. (2005)	2	Olsen et al. (1996)	5
Bergstrøm (1975)	2	Olsen et al. (2001)	40
Bitinas et al. (2002)	3	Olsen et al. (2013b)	18
Björck and Digerfeldt (1982a)	2	Putkinen and Lunkka (2008)	4
Björck and Digerfeldt (1982b)	1	Repo and Tynni (1967)	1
Björck and Digerfeldt (1986)	1	Repo and Tynni (1969)	2
Björck and Digerfeldt (1991)	1	Repo and Tynni (1971)	4
Björck and Möller (1987)	1	Richardt (1996)	1
Blake and Olsen (1999)	5	Rinterknecht et al. (2006)	47
Corner et al. (2001)	3	Rosén (2005)	4
Digerfeldt (1979)	1	Rosén et al. (2001)	2
Donner et al. (1978)	3	Rotnicki and Borówka (1995)	2
Dreimanis and Zelčs (1995)	15	Rubensdotter (2006)	3
Eilertsen et al. (2005)	16	Saarse et al. (2009)	2
Ek (2004)	1	Saarse et al. (2012)	1
Eronen (1976)	2	Sandgren et al. (1999)	1
Göttlich et al. (1983)	1	Segerström and von Stedingk (2003)	4
Håkansson (1970)	1	Seidenkrantz and Knudsen (1993)	1
Håkansson (1975)	2	Šeirienė et al. (2006)	2
Håkansson (1978)	1	Seppä and Birks (2002)	1
Håkansson (1982)	1	Seppä and Weckström (1999)	1
Håkansson (1987)	3	Seppä et al. (2004)	2
Hammarlund et al. (2004)	1	Seppä et al. (2012)	3
Heikkilä and Seppä (2003)	1	Shemesh et al. (2001)	1
Heinsalu and Veski (2007)	1	Snyder et al. (1997)	2
Helmens et al. (2000)	1	Snyder et al. (2000)	1
Hilldén (1979)	3	Stančikaitė et al. (2008)	3
Houmark-Nielsen and Kjær (2003)	3	Stankowska and Stankowski (1988)	2
Jensen et al. (2002)	2	Svedhage (1985)	1
Johnsen et al. (2010)	1	Svensson (1989)	4
Johnson and Ståhl (2010)	5	Tolonen and Ruuhijärvi (1976)	1
Klovning and Hafsten (1965)	1	Valen et al. (1996)	2
Korsager et al. (2003)	1	Vorren (1978)	2
Kramarska (1998)	2	Vorren and Alm (1999)	1
Krog and Tauber (1974)	2	Vorren et al. (1988)	2
Lagerlund and Houmark-Nielsen (1993)	1	Vorren et al. (2013)	5
Larsen et al. (1999)	1	Wohlfarth et al. (1999)	1
		Zernitskaya et al. (2007)	1

sites have been measured. Despite these efforts, based on AMS ^{14}C dates on terrestrial macrofossils embedded in the varves (Wohlfarth, 1996), ^{14}C-dated marker horizons in Swedish lacustrine deposits, central-European tree-ring chronologies, and Greenland ice core records (Björck et al., 1996), it has been shown that hundreds of varves are missing, most probably in the postglacial section of the STS. Estimates of the number of missing varves have varied over time but are generally about 700–900 (Strömberg, 1994; Andrén et al., 2002).

We use the catastrophic drainage of the Baltic Ice Lake, 35 years before the start of the Holocene (Andrén et al., 2002), as an event that can be used to tie the STS to ice core records (Andrén et al., 1999, 2002; Björck et al., 2001), and we specifically explore its link to the NGRIP ice core record (Stroeven et al., 2015). The NGRIP ice core record has been layer-counted across the Younger Dryas/Preboreal (Holocene) transition, yielding an age of 11,700 ± 99 cal years b2k (Walker et al., 2009; Rasmussen et al., 2014), or 11,650 cal years BP. Detailed statistical comparisons between the ^{14}C record in tree rings and the ^{10}Be record in ice cores across this boundary (Muscheler et al., 2008, 2014) imply that the ice core record may be 65 years too old. The best estimate of the start of the Holocene is 11,585 cal years BP and the drainage, being 35 years older (Andrén et al., 2002), is therefore pinned to 11,620 cal years BP (Stroeven et al., 2015). The timing of the Baltic Ice Lake drainage occurred at STS -1530 (Björck et al., 2001; Andrén et al., 2002) or 10,770 varve years BP, which instils an age difference of 850 years between the two annual records (Table 2). Fig. 8 shows the constraints that the STS varve record offers to ice marginal positions between 13,390 cal years BP (North of Vimmerby; Kristiansson, 1986; Wohlfarth et al., 1998), and 9950 cal years BP (Pauträsk; Bergström, 1968) even though our connection between the robust part of the record and the Kristiansson-Wohlfarth section of the record (black series in Fig. 8) remains challenging.

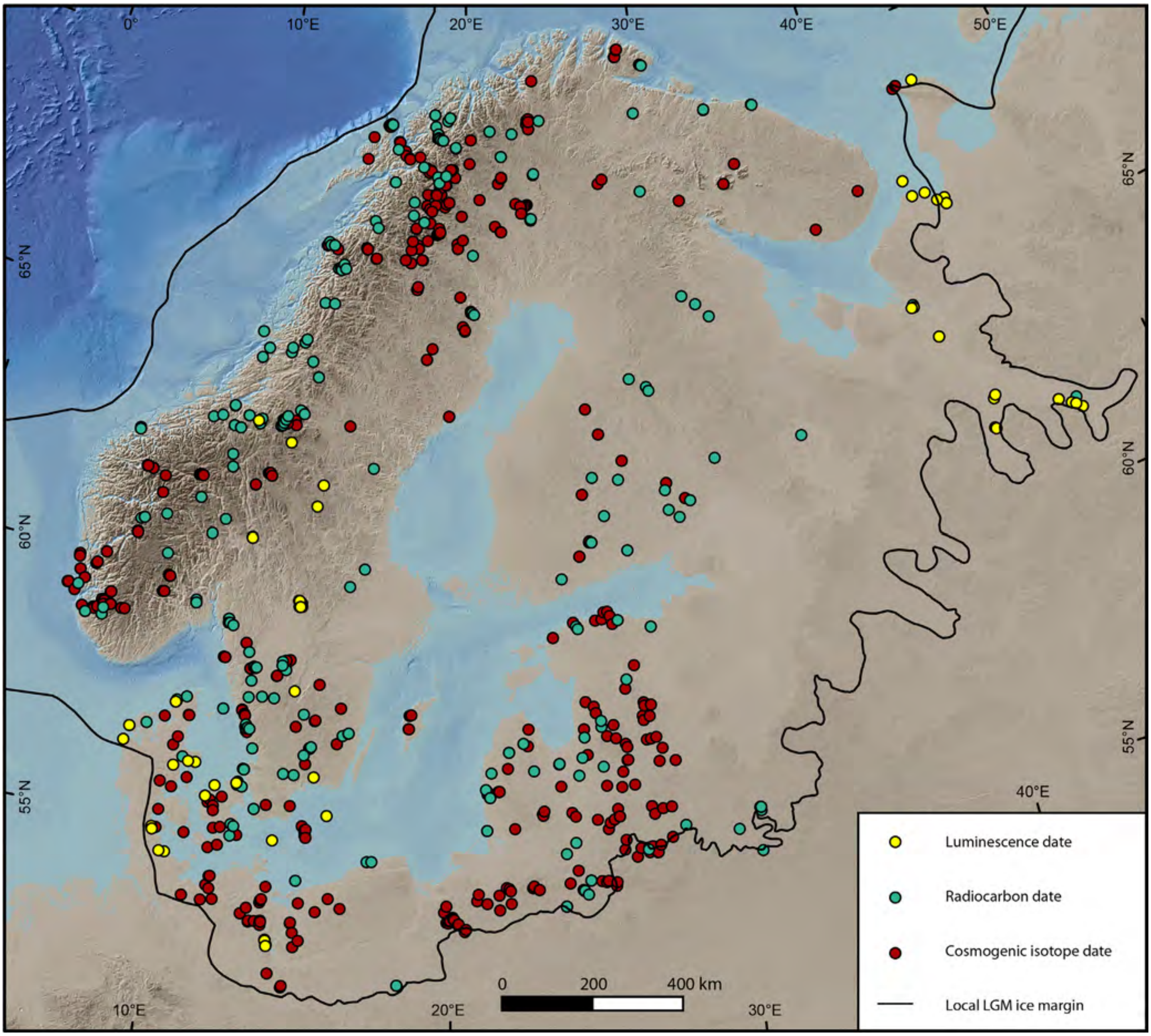

Fig. 7. Locations of optically-stimulated luminescence, radiocarbon, and cosmogenic isotope samples included in the chronological database that is part of the deglaciation reconstruction (Tables 1, 3 and 4; Supplementary dataset). Cosmogenic isotope samples have resulted in both ^{10}Be and ^{26}Al dates.

2.2.3. Optically-stimulated luminescence (OSL) dating

OSL dating enables direct dating of sediment deposition and burial, and it can potentially yield accurate minimum ages of deglaciation. However, in practice it appears that some OSL ages are older than the expected deglaciation age for sites in Fennoscandia (Alexanderson and Murray, 2012b; Johnsen et al., 2012). Because this is probably due to incomplete bleaching of, especially, subglacial till and proximal glaciofluvial sediment samples (Alexanderson, 2007; Alexanderson and Murray, 2012a), most of the 138 OSL samples that are part of the deglaciation reconstruction (Table 3), concern minimum age constraints for distal glaciofluvial, lacustrine, and eolian sediment samples (Fig. 7; Larsen et al., 1999, 2006, 2014; Strickertsson and Murray, 1999; Lyså et al., 2001, 2011, 2014; Houmark-Nielsen, 2003; Houmark-Nielsen and Kjær, 2003; Kjær et al., 2003a; Kortekaas and Murray, 2007; Kortekaas et al., 2007; Johnsen et al., 2010; Lüthgens et al., 2011; Alexanderson and Murray, 2012b).

2.2.4. Cosmogenic nuclide exposure dating

Cosmogenic surface exposure dating of glacial landforms and deposits has become a key tool for defining glacier and ice sheet chronologies. We present a compilation of published and new ^{10}Be ($n = 786$) and ^{26}Al ($n = 74$; eight of these have no corresponding ^{10}Be measurements) exposure ages for the area covered by the LGM Fennoscandian Ice Sheet (Table 4, Fig. 7; Supplementary dataset). The exposure ages are derived from sampled bedrock surfaces ($n = 284$), glacial boulders ($n = 474$), and cobble/pebble/sediment ($n = 36$). All samples with potential importance for the deglaciation chronology have been included, including samples from bedrock surfaces that have been preserved under cold-based ice (Fabel et al., 2002; Stroeven et al., 2002b; Linge et al., 2006a; Darmody et al., 2008). Most of the new, previously unpublished samples ($n = 132$) are from northern Sweden and Norway ($n = 84$), plus some from the Kola Peninsula, Russia (Fig. 6; $n = 15$), Finland ($n = 17$), and east-central ($n = 4$), west-central ($n = 5$), and

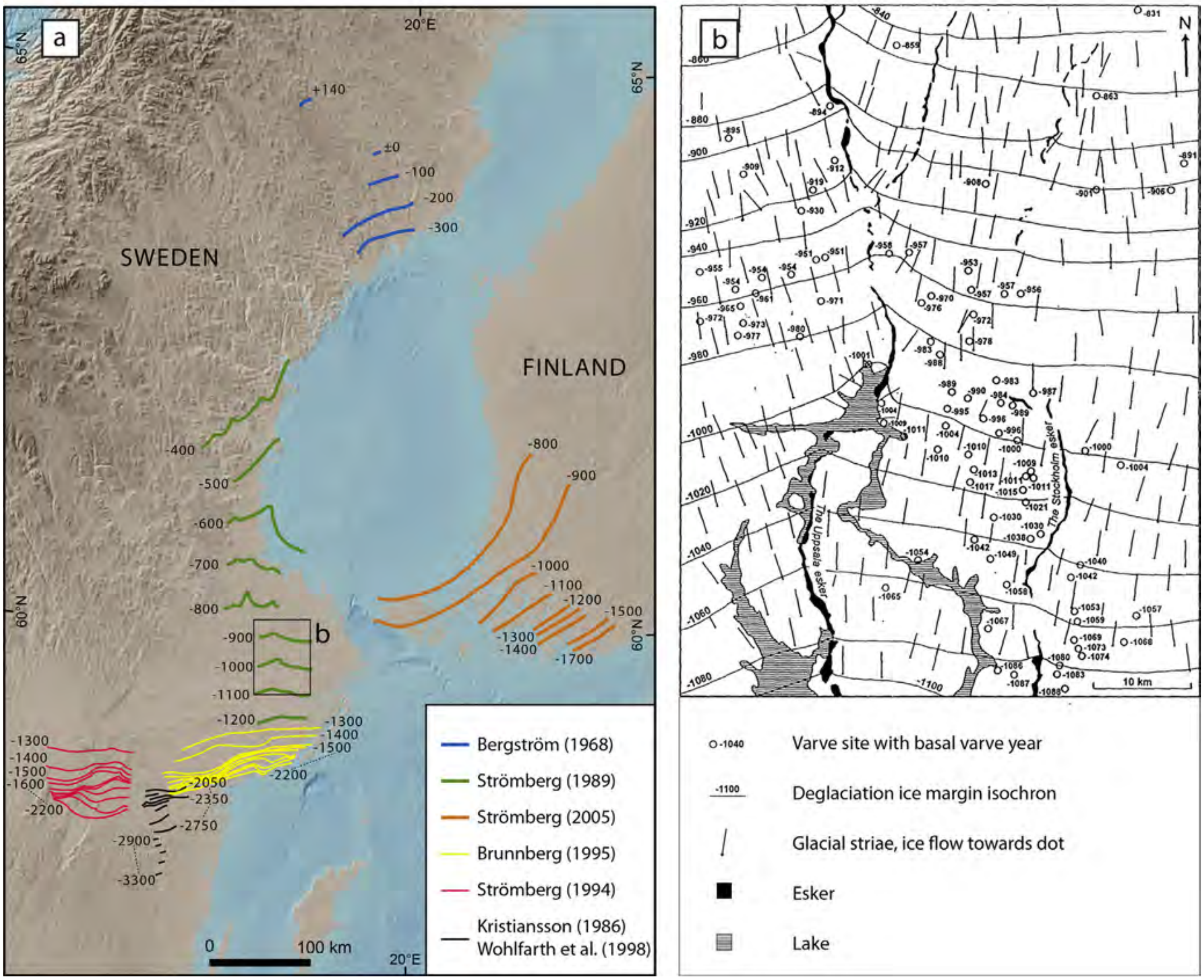

Fig. 8. a) Compilation of the Late Glacial clay varve chronologies in Sweden and Finland that are used in this study (Table 2). The Swedish Time Scale (STS) is expressed as varve years before (negative values) and after (positive values) the "zero-year" in the revised and corrected STS (Bergström, 1968; Strömberg, 1985b, 1989, 1990, 1994, 2005; Kristiansson, 1986; Cato, 1987; Brunnberg, 1995; Wohlfarth et al., 1998). The framework may be considered as a two-part chronology, one with "glacial" varves, deposited before a "zero-year" (De Geer, 1940), and one with "postglacial" varves, deposited after this "zero-year" (Lidén, 1938). Hence, the varve ±0 has been an "anchor point" for all past revisions of the STS. The age of the zero-year varve, STS ±0, is c. 10,090 cal years BP based on the adopted correlation of the STS with the Greenland ice core record (Stroeven et al., 2015, Table 2). The ice recession lines of Strömberg (1994) in west-central Sweden have been corrected, and the "floating" varve chronology by Kristiansson (1986) has been correlated with the STS, as proposed by Wohlfarth et al. (1993) and Brunnberg (1995). The ice-marginal lines in Finland are based on Strömberg (1990, 2005), which include new varve measurements north of the Second Salpausselkä Moraine (Ss II). The post-Younger Dryas recessional lines of the varve chronology are considered robust. However, the chronology is less robust between STS c. -2300 and −2600, i.e. during the early part of the Younger Dryas, because ice front oscillations may have eroded already deposited varves. b) Locally, short varve sequences require a dense pattern of varve measuring sites to get reliable correlations between varve diagrams. Because, for the area shown here, the distance between measuring sites had to be restricted to only a few kilometres, the resulting pattern of ice margin retreat becomes highly detailed. Modified from Strömberg (1989).

southwestern Sweden ($n = 9$). These new samples have been prepared following standard procedures (Fabel et al., 2002, 2006; Stroeven et al., 2002a, 2002b, 2011, in review) and were measured at PRIME Lab, ANSTO, and SUERC over the years 2000–2008 (see Supplementary dataset).

Data for exposure age calculations has been compiled from the original publications and recalculated with a consistent production rate and scaling scheme. We use the reported sample thickness, sample density (adopting 2.65 g cm^{-3} where not otherwise stated), and topographic shielding and we assume zero surface erosion. An important refinement in our compilation is ^{10}Be standardization. With the ^{10}Be AMS standard calibration of Nishiizumi et al. (2007), it became clear that previously assumed isotope ratios of AMS standards, and reported ^{10}Be concentrations based on those standards, deviate by up to 14% from the new Nishiizumi et al. (2007) standard. We have made an effort to track the applied standardization for all ^{10}Be samples and we regard our dataset as the best available for the Fennoscandian Ice Sheet region. All exposure ages have been calculated using a modified version of the CRONUS calculator (Balco et al., 2008), with the nuclide specific LSD$_n$ production rate scaling scheme (Lifton et al., 2014), the regional Scandinavian reference ^{10}Be production rate of 3.95 ± 0.10 atoms g^{-1} yr^{-1} (Stroeven et al., 2015), and the corresponding reference ^{26}Al production rate of 26.71 ± 1.60 atoms g^{-1} yr^{-1}. Exposure ages for the CRONUS scaling schemes (Balco et al., 2008) and the two LSD scaling schemes (Lifton et al., 2014), using the regional Scandinavian ^{10}Be reference production rate, are listed in the Supplementary dataset. The exposure ages of the various

Table 2
Conversion of the Swedish Time Scale (STS) to cal yrs BP.

STS (Fig. 8)[a]	Varve yrs BP[b]	cal yrs BP[c]
+140	9100	9950
±0	9240	10,090
−1400	10,640	11,490
−1500	10,740	11,590
−1530	10,770	11,620
−2200	11,440	12,290
−2250	11,490	12,340
−3300	12,540	13,390

[a] The Swedish Time Scale, STS, was proposed by Gerard De Geer (1935, 1940). He defined clay varves deposited before the zero-year, ±0, as glacial varves (negative values), and varves deposited after the zero-year as postglacial varves (positive values).
[b] Conversion to varve yrs BP is based on a connection of the floating STS to the present by Cato (1987), using 9240 varve years for the zero-year varve, relative to 1950 (BP).
[c] Conversion to cal yrs BP is based on the connection of the STS to the NGRIP Greenland ice core chronology using the timing of the Baltic Ice Lake Drainage (STS c. -1530; Andrén et al., 2002) which correlates to c. 11,620 cal years BP in the ice core record (Stroeven et al., 2015), thus requiring a further revision of c. 850 years.

scaling schemes generally agree well and all CRONUS scaling scheme exposure ages are within 7.1% of the LSD scaling exposure ages.

3. Methodology

The outlines of ice sheet retreat isochrons are primarily based on the pattern of eskers and ice-marginal positions (Fig. 5). Retreat isochrons that are drawn perpendicular to esker long-axes (Kleman et al., 2006) tend to produce smooth contours. Isochrons based on ice-marginal positions, however, account for the irregular and often lobate nature of ice margins as expressed in remnant deglacial landforms and commonly yield highly irregular retreat contours. Some of the margins are smoother interpreted positions between more detailed dated ice-marginal formations to allow for a consistent 1000 year contouring. As far as we know, the retreat pattern never violates these principles of reconstruction and ‘youngest sets’ of lineations and striae typically conform to the presented retreat pattern. While eskers form an almost continuous pattern in the shield areas they are scarce in the mountains (Fig. 5), probably because of persistent cold-based conditions. In areas characterised by cold-based deglaciation, ice sheet retreat is reconstructed with the use of lateral channels (Kleman, 1992; Hättestrand, 1998) and ice-dammed lakes. Where thawing occurred shortly before the retreating ice margin passed through these cold-based regions, faint lineations in the till sheet and glacial striae on bedrock are also used to reconstruct ice sheet retreat (Clarhäll and Kleman, 1999; Harbor et al., 2006).

The deglaciation timing is almost entirely based on published constraints and correlations. However, the quality of, and detail provided by, the constraints differ across the glaciated domain. For ice-marginal positions older than 13 cal kyr BP, the chronology is largely constrained by radiocarbon, OSL, and cosmogenic nuclide-derived ages (Fig. 7; Supplementary dataset). For the 17–13 cal kyr BP deglaciation of southern Sweden, we also couple the radiocarbon and cosmogenic nuclide data for ice-marginal positions to climatic events recorded in Greenland ice cores (for a detailed explanation, see section 5.2). For ice-marginal positions younger than 13 cal kyr BP, we use the timing of the retreat of the Fennoscandian Ice Sheet from its Younger Dryas position in southern Sweden and Finland as a starting point to build the chronology. When the ice sheet retreated from the northern tip of Mount Billingen, the Baltic Ice Lake (Fig. 3) catastrophically drained to the Kattegatt (Fig. 6; Lundqvist, 1921; Johansson, 1926). The event has been dated to 11,620 ± 100 cal years BP using radiocarbon and by correlating this event in the STS with the Pleistocene/Holocene boundary in the NGRIP ice core (Stroeven et al., 2015). We use the internally-consistent varve record between c. 12,340 (Korsberga; Strömberg, 1994) and 9950 (Pauträsk; Bergström, 1968) cal years BP (Table 2, Fig. 8) to guide the pace of retreat for this part of the record. Strömberg (1990, 2005) connected the varve record in southern Finland, across Åland (Fig. 6), to the STS, thereby allowing further geochronological control on ice-marginal positions (Fig. 8). Final deglaciation in the Sarek Mountains of northwestern Sweden (Fig. 6) occurred after 9.7 cal kyr BP, in general agreement with the clay varve record and ages derived using radiocarbon and cosmogenic nuclides.

Hence, the method of reconstructing isochrons used here differs between pre- and post-Younger Dryas periods. For regions that were deglaciated before the Younger Dryas, ages of ice-marginal positions were derived from published data. In cases where published ages for mapped ice-marginal formations were inconsistent, groups of samples with consistent ages, or consistent ages using different dating techniques, were considered more reliable than individual ages. In the final step of reconstructing time slices that were 1 kyr apart, some mapped ice-marginal formations were used directly while others were visually interpolated from adjacent ice-marginal formations, generally assuming a steady retreat rate, but giving due consideration to topography. For regions that were deglaciated after the Younger Dryas, clay varve chronology was used to construct retreat isochrons. This was achieved by adopting the principle that isochrons extrapolated away from established ice-marginal positions (Fig. 8) should always be perpendicular to youngest deglaciation ice flow traces, as indicated by eskers, glacial lineations, and striations, and using constraints provided by ice-dammed lakes and meltwater channels. The pace of retreat as derived from the youngest part of the varve record was used to construct the last two isochrons, and the final age of deglaciation was cross-checked against published deglaciation ages.

4. Results

4.1. Deglaciation overview

We present a deglaciation map of the Fennoscandian Ice Sheet

Table 3
Publications with OSL dates included in the Supplementary dataset, including the number of samples (N).

Publications	N	Publications	N
Alexanderson and Henriksen (in press)	12	Larsen et al. (1999)	14
Alexanderson and Murray (2012b)	30	Larsen et al. (2006)	6
Houmark-Nielsen (2003)	7	Larsen et al. (2014)	8
Houmark-Nielsen and Kjær (2003)	6	Livingstone et al. (2015)	2
Johnsen et al. (2012)	7	Lüthgens et al. (2011)	7
Kjær et al. (2003a)	7	Lyså et al. (2011)	4
Kortekaas and Murray (2007)	2	Lyså et al. (2014)	24
Kortekaas et al. (2007)	1	Strickertsson and Murray (1999)	1

Table 4
Publications with cosmogenic dates included in the Supplementary dataset, including the number of ^{10}Be and ^{26}Al samples.

Publications	^{10}Be	^{26}Al	Publications	^{10}Be	^{26}Al
Alexanderson and Fabel (2015)	8	–	Linge et al. (2006a)	41	–
Anjar et al. (2014)	23	–	Linge et al. (2006b)	6	–
Briner et al. (2014)	34	–	Linge et al. (2007)	25	–
Brook et al. (1996)	4	4	Mangerud et al. (2013)	34	–
Darmody et al. (2008)	2	2	Matthews et al. (2008)	3	3
Fabel et al. (2002)	13	2	Nesje et al. (2007)	16	–
Fabel et al. (2006)	19	17	Paasche et al. (2006)	2	–
Fjellanger et al. (2006)	11	–	Rinterknecht et al. (2004)	9	–
Goehring et al. (2008)	69	–	Rinterknecht et al. (2005)	41	–
Goehring et al. (2012)	8	–	Rinterknecht et al. (2006)	95	–
Goodfellow et al. (2014)	2	2	Rinterknecht et al. (2012)	5	–
Harbor et al. (2006)	3	2	Rinterknecht et al. (2014)	21	–
Hättestrand et al. (2004)	1	–	Shakesby et al. (2008)	5	5
Heine et al. (2009)	6	–	Stroeven et al. (2002a)	3	–
Houmark-Nielsen et al. (2012)	35	–	Stroeven et al. (2002b)	4	3
Jansen et al. (2014)	19	–	Stroeven et al. (2006)	3	–
Johnsen et al. (2009)	6	–	Stroeven et al. (2011)	12	2
Johnsen et al. (2010)	6	–	Stroeven et al. (2015)	10	–
Larsen et al. (2012)	17	–	Svendsen et al. (2015)	18	–
Li et al. (2005)	14	–	Tschudi et al. (2000)	4	–
Li et al. (2008)	–	1	This study	127	31

with isochrons marking every 1000 years between 22 and 13 cal kyr BP and every hundred years between 11.6 and 9.7 cal kyr BP (Fig. 9; Video, Supplementary dataset). Abundant literature attests to the difficulties in resolving the dynamic behaviour of the Fennoscandian Ice Sheet during the Younger Dryas chronozone, although two to three extensive end moraine belts indicate standstills and re-advances of the ice sheet along most of its margin during this period (Rainio et al., 1995; Lundqvist, 2004; Mangerud et al., 2011; Putkinen et al., 2011). The onset of the Younger Dryas in Scandinavia is delayed by 100 years relative to the Greenland ice core record (GS-1; 12.8–11.7 cal kyr BP; Lohne et al., 2013). Hence, we denote the net retreat distance during the Younger Dryas as an ice-marginal zone spanning 12.7–11.6 cal kyr BP, rather than a series of individual and specific ice marginal positions. The ice marginal zone straddles the last extensive zone of end moraines (including the Ra Moraine system in Norway, the Middle-Swedish end moraine zone, the Salpausselkä I and II moraines in Finland, and the Koitere and probably Rugozero moraines in Russia; Figs. 5 and 6) and it divides a period of retreat interspersed with standstills and re-advances since the LGM from a period with fewer interruptions in retreat up to final deglaciation in the northwestern Swedish Mountains.

The radiocarbon, OSL, and cosmogenic ^{10}Be and ^{26}Al exposure ages included in our deglaciation reconstruction are presented in the Supplementary dataset. Of the 335 radiocarbon samples, 223 yield minimum age constraints for deglaciation because they are part of the post-glacial environment and 112 yield maximum age constraints for deglaciation because they are from sub-till samples. Calibrated radiocarbon ages range from 7.2 ± 0.1 cal kyr BP to 27.7 ± 0.1 cal kyr BP for minimum age-constraint samples and from 16.3 ± 0.7 cal kyr BP to 33.5 ± 0.5 cal kyr BP for sub-till samples. While 125 OSL samples are from sediment layers that were deposited contemporaneously with or postdate the timing of local ice extent, and yield minimum age constraints for deglaciation, 13 are from sub-till samples, yielding maximum age constraints for deglaciation. OSL ages range from 5.9 ± 0.7 kyr to 131.0 ± 8.0 kyr for minimum age-constraint samples, and from 15.1 ± 1.3 kyr to 25.3 ± 1.6 kyr for maximum age-constraint samples. The recalculated ^{10}Be (^{26}Al) exposure ages range from 1.1 ± 0.3 kyr to 456 ± 20 kyr (7.8 ± 0.5 kyr to 107 ± 4.6 kyr) with 74% (59%) of the ages falling in the time window between 9 kyr and 22 kyr. The new ^{10}Be and ^{26}Al exposure ages from Sweden, Norway, and Finland are generally similar to previously published exposure ages, with some sites yielding well-clustered exposure ages in the deglaciation age range and others, primarily located in the north and at high altitude, yielding ages significantly older than the last deglaciation due to cosmogenic inheritance.

4.2. Deglaciation history and dynamics

We have subdivided the Fennoscandian Ice Sheet domain into four sectors (Fig. 10) to guide our presentation of the deglaciation history and dynamics of the entire ice sheet. This subdivision is guided by topography and ice sheet deglaciation dynamics.

4.2.1. The western sector

The Norwegian shelf was deglaciated between the local LGM and 14–15 cal kyr BP (Andersen, 1979, 1981; Sollid and Torp, 1984). Because of the high-precipitation coastal setting, the ice sheet margin in this sector responded rapidly to climatic variations. The most distinct climate variation, the Younger Dryas cold interval, produced the most laterally-continuous moraines (Lundqvist, 1990; Andersen et al., 1995a, 1995b). Stratigraphical evidence for Younger Dryas re-advances of c. 40–50 km have been reported from southwestern to northern Norway (Mangerud, 1977; Andersen et al., 1995b; Bergstrøm et al., 2005; Mangerud et al., 2011). There is limited evidence for ice marginal positions during the Allerød that could shed light on the pre-Younger Dryas ice sheet geometry and illustrate to what extent the ice sheet had retreated. Estimates of ice sheet retreat rely on observations of Allerød sediments, predominantly marine sediments, that were overrun by the Younger Dryas ice sheet (Lohne et al., 2007; Mangerud et al., 2011). Mangerud (1977), for example, reports an estimated minimum retreat of 40 km in the Bergen area (Fig. 6), which implies extensive ice free coastal areas in western Norway during the Allerød. Similar inferences come from the Stavanger area (Fig. 6) and are summarized by Lohne et al. (2007). Observations from the south coast of Norway and the Oslo area reveal less extensive Younger Dryas re-advances of <18 km (Sørensen, 1992; Bergstrøm, 1995). It is thought that the more maritime setting of the western margin, and its proximity to an Atlantic moisture supply, may explain why re-advances on the western margin were more extensive than

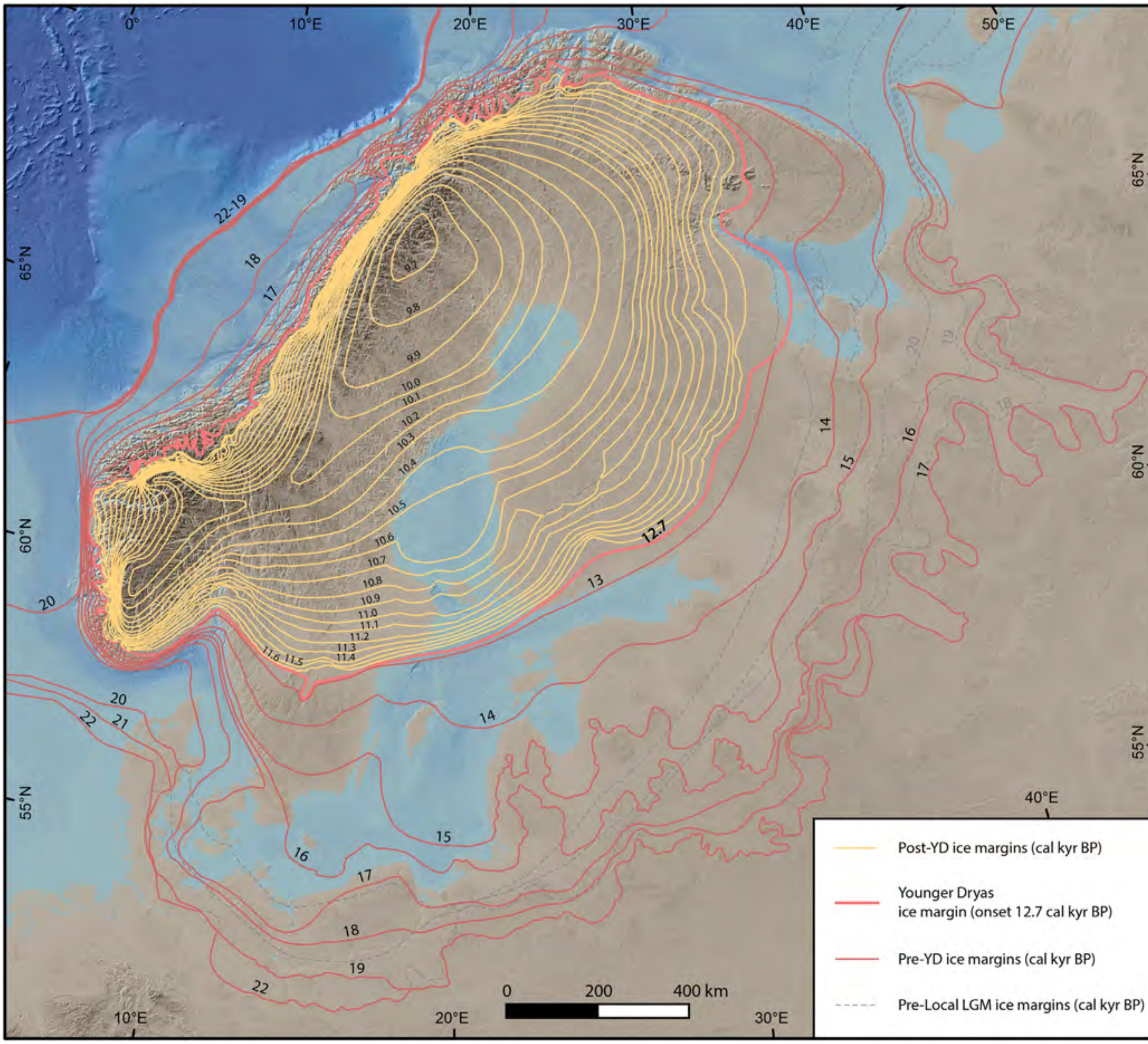

Fig. 9. Deglaciation pattern and chronology for the Fennoscandian Ice Sheet. Ice margins are given at 1-kyr intervals before the Younger Dryas (12.7–11.6 cal kyr BP), that is from local LGM to 13 cal kyr BP. Post-Younger Dryas margins are shown at 100-year intervals (11.6–9.7 cal kyr BP). Ice margins south and east of the Baltic Sea follow established ice-marginal formations (Figs. 5 and 6) and show lobate outlines related to bedrock type, local topography, and the formation of ice streams. The less lobate ice margin on the Scandinavian Peninsula (set in shield rocks) is partly a result of the reconstruction technique, and partly reflects a difference in ice dynamics. Ice-marginal formations did not form during the rapid final retreat. Consequently, the ice margin is reconstructed transverse to the youngest documented flow traces (predominantly eskers; Fig. 5), and is also constrained by marginal meltwater channels and ice-dammed lakes.

elsewhere. In contrast to both younger and older moraines that occur in many valleys, the Younger Dryas moraines can frequently be traced over intervening uplands, with a notable exception for mid-Norway where the Younger Dryas ice margin is poorly mapped in forested and alpine areas. Prominent moraines and associated ice-marginal formations deposited after the Younger Dryas, observed in fjords and coastal valleys (Sveian et al., 1979; Corner, 1980; Andersen et al., 1981; Nesje and Rye, 1990; Rye et al., 1997), reflect standstills or minor re-advances which record a response of the dynamic western margin of the Fennoscandian Ice Sheet to the Preboreal oscillation (PBO). Accurate cartographic representation of the dynamic fluctuations at the western ice sheet margin is exceedingly difficult at the ice sheet-scale because of the relatively high degree of topographic complexity over short spatial scales. Hence, we have simplified our depiction as one of slow but steady retreat over the course of the deglaciation.

4.2.2. The southern sector

The uniform retreat from the local LGM configuration in the southern sector, including the Main Stationary Line in Denmark, the Brandenburg in northern Germany, and the Lezno in Poland (Houmark-Nielsen and Kjær, 2003; Marks, 2012; Rinterknecht et al., 2014) was interrupted by two Young Baltic advances creating the East Jylland and Bælthav ice-marginal formations in Denmark (Fig. 6; Stephan, 2001; Kjær et al., 2003a, b). We follow Houmark-Nielsen and Kjær (2003) in correlating the East Jylland with the Frankfurt and Poznan ice-marginal formations in Germany and Poland, and the Bælthav ice-marginal formation with the

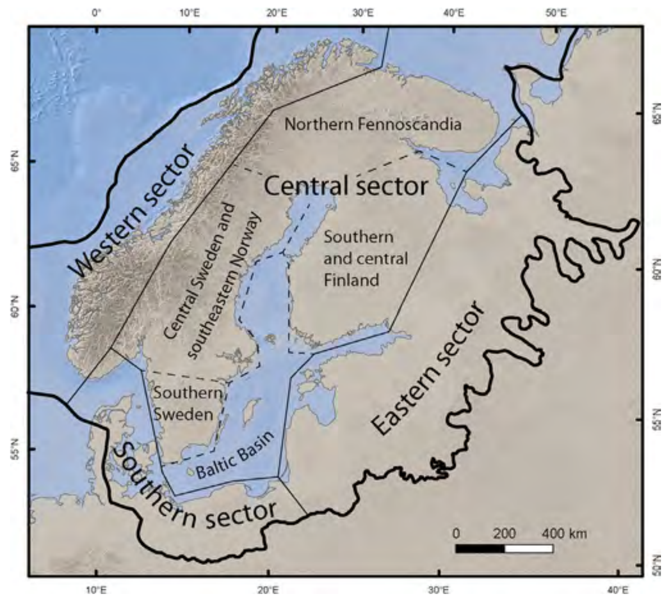

Fig. 10. The Fennoscandian Ice Sheet area divided into four geographical and ice-dynamical sectors which are discussed individually in the text. The Central sector is further subdivided into five regions because of internal differences in ice dynamics during deglaciation.

Pomeranian ice-marginal formation in Germany (Fig. 6). The Young Baltic advances show a highly lobate ice margin including a northerly flow direction in some inter-island straits. A comparison between the 16 and 14 cal kyr BP ice margin configurations in Fig. 9 clearly shows the remarkable contrast in retreat rates of the slow terrestrial margin retreat in western and southern Sweden and the rapid retreat of the calving ice margin in the Baltic Basin following the Young Baltic advances (Duphorn et al., 1979). This may be explained by the 16 cal kyr BP position representing an over-extended ice margin, related to the previous surge in the southernmost Baltic Basin. A thin surge lobe would be highly susceptible to rapid calving and break-up.

4.2.3. The eastern sector

The local LGM was attained as early as 19 cal kyr BP in the southern part of the eastern sector (and has been correlated with the East Jylland-, Frankfurt-, and Poznan ice-marginal formations) and as late as 17 cal kyr BP in the northern part of the eastern sector (Kalm, 2012; Larsen et al., 2014; Lyså et al., 2014), which broadly correlates with the Bælthav- and Pomeranian ice-marginal formations (e.g., Houmark-Nielsen and Kjær, 2003). From its local LGM extent, the ice margin retreated into a depression spanning the entire length from northern Germany to Lake Onega in western Russia (Fig. 6; Rainio et al., 1995). This led to the formation of a number of ice-dammed lakes in Poland, Lithuania, Latvia, Estonia and Russia, and later the formation of the Baltic Ice Lake (Fig. 3). The latter had its outlets in the Öresund and Storebælt depressions (Figs. 3 and 6) across a landbridge between Denmark and Sweden. Although the Baltic Ice Lake persisted until the end of the Younger Dryas, at approximately 11,620 ± 100 cal years BP (Stroeven et al., 2015), it may have drained once previously at c. 13.0 cal kyr BP (Björck, 2008; Björck et al., 1996; Bodén et al., 1997).

4.2.4. The central sector

4.2.4.1. Southern Sweden. The deglaciation of southern Sweden before the onset of the Younger Dryas was characterised by a predominantly terrestrial and slow (<150 m yr^{-1}) ice marginal retreat. This retreat was repeatedly interrupted by still-stands and minor re-advances (Lundqvist and Wohlfarth, 2001), as indicated by a series of ice-marginal formations that are particularly well developed on the western side of the peninsula (Fig. 11). In contrast, there is only one significant ice-marginal formation on the eastern side of the peninsula; the Vimmerby Moraine (Agrell et al., 1976; Malmberg Persson et al., 2007; Johnsen et al., 2009), and there has been no conclusive correlation between it and the ice-marginal formations on the western side. LiDAR elevation data, which has recently become available over southern Sweden (Dowling et al., 2013), has enabled the identification of these ice-marginal formations over longer lateral extents than could previously be identified. For example, the Vimmerby Moraine has a clear morphological continuation to the west and can be connected to the Berghem Moraine (Fig. 11). This physical evidence supports what has previously been suspected by others (e.g., Anjar et al., 2014), and it provides, for the first time, a strong spatial link between the deglaciation chronologies on the western and eastern sides of southern Sweden (see 5.2.). A well-developed pattern of esker systems and ubiquitous glacial lineations indicate that basal conditions were mostly warm-based in southern Sweden during deglaciation. However, parts of southern Sweden probably remained cold-based up until final deglaciation, resulting in limited subglacial erosion, as indicated by numerous pre-LGM glacial deposits in the area (Lemdahl et al., 2013), and extensive ribbed moraine fields (Kleman and Hättestrand, 1999; Möller, 2010).

4.2.4.2. Central Sweden and southeastern Norway. Here the ice-margin retreat was mostly terrestrial. The topography ranges from high-relief, over the plateaus and mountains of south-central Norway, to low-relief in central Sweden. The ice sheet was generally wet-based and left a ubiquitous record of striae, till lineations and eskers, which enables an accurate reconstruction of the ice margin retreat pattern compared with other sectors, although dating constraints are scarce from the inner areas (Fig. 7). The deglacial landform pattern reveals that the southwestern sector of the Fennoscandian Ice Sheet retreated towards the mountains of south-central Norway while the southeastern sector continued its northward retreat, yielding a narrow ice ridge (saddle) at 10.2 cal kyr BP that connected residual ice in south-central Norway to the main ice sheet remnant in the north. This saddle was an obstruction to meltwater drainage and large ice-dammed lakes consequently formed in Østerdalen (Nedre Glåmsjø ice lake) and adjacent valleys in Norway (Fig. 3), the drainage of which has been described by Garnes and Bergersen (1980) and Longva and Thoresen (1991). During this ice sheet configuration the Ljungan-, Ljusnan-, and the central Jämtland complex of ice-dammed lakes began to develop in west-central Sweden, on the east side of the bordering topographic ice sheet saddle (Lundqvist, 1969, 1972, 1973; Borgström, 1989).

4.2.4.3. Southern and central Finland. The most conspicuous glacial landforms are three lobate ridges, from outer to inner – the Salpausselkä (Ss) I, II, and III moraines, respectively (Fig. 6). Ss I and II are considered to be of Younger Dryas age (Donner, 1978, 2010; Rainio et al., 1995; Rinterknecht et al., 2004) and are therefore synchronous with the Younger Dryas moraines in Norway, Sweden and Russia (Rainio et al., 1995). From the pattern of lineations immediately distal to the ridges, retreat of the Fennoscandian Ice Sheet just prior to the deposition of the Ss I and II displayed a non-lobate structure. The well-developed drumlin zones proximal to the Salpausselkä moraines indicate that laterally well-constrained ice streams developed early in the Younger Dryas, feeding the fan-like flow structure of advancing ice sheet lobes. There is stratigraphical indication that a substantial re-advance of the ice

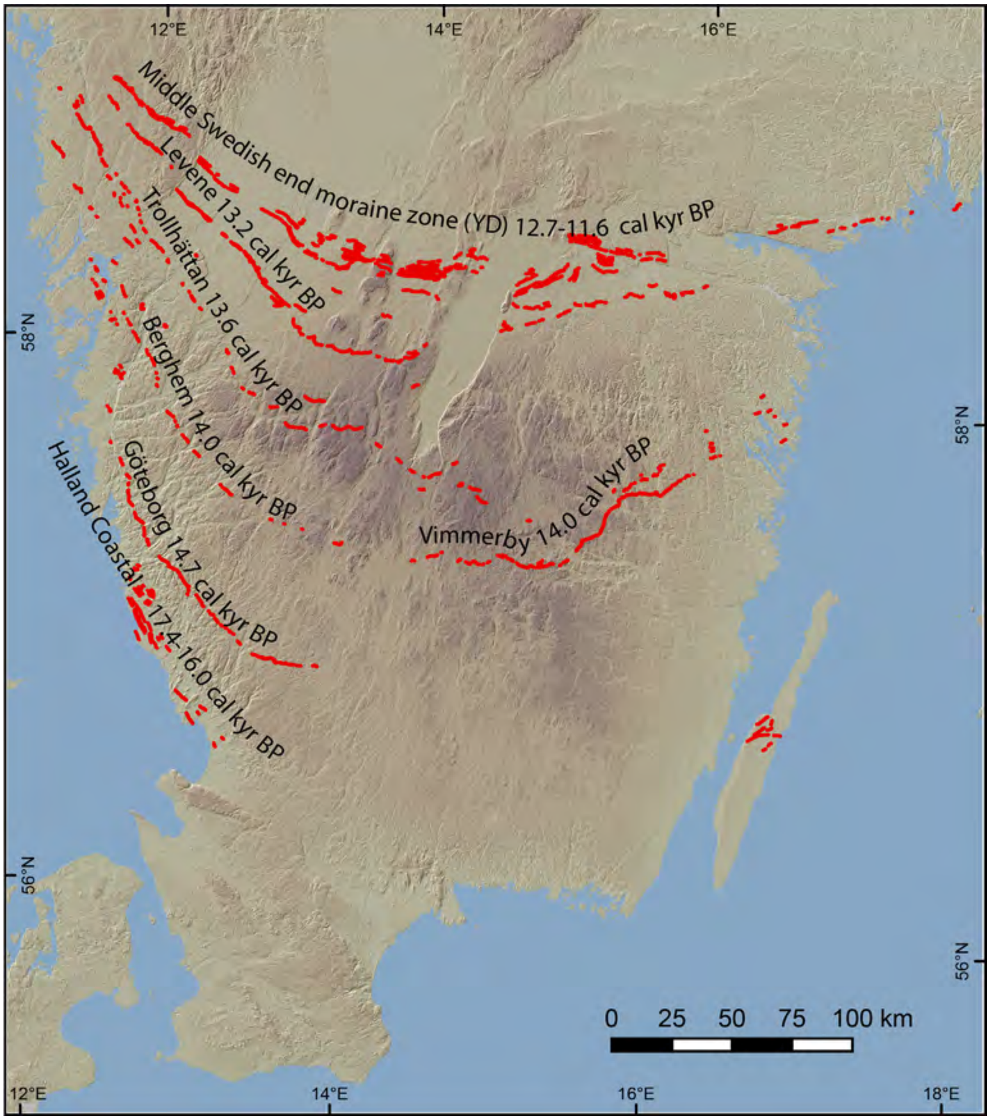

Fig. 11. Major end moraine belts in southern Sweden mapped from LiDAR data (Swedish national elevation model "GSD-Höjddata, grid 2+", with a 2 m horizontal resolution). The moraine pattern correlates well with earlier maps (e.g., Lundqvist and Wohlfarth, 2001), although we demonstrate, for the first time, that there is a morphological continuation of the Berghem Moraine across southern Sweden to the Vimmerby Moraine. The age assignments (in cal kyr BP) are based on radiocarbon dates (summarized in Lundqvist and Wohlfarth, 2001), cosmogenic isotope dates (Larsen et al., 2012; Anjar et al., 2014), and, primarily, correlations with the Greenland ice core event stratigraphy (Rasmussen et al., 2014; see also Table 5, Fig. 13).

margin, up to 50 km (Rainio, 1993), occurred as part of the building of the Ss I Moraine. The two feeder ice streams (Punkari, 1995) transported large volumes of ice and were probably instrumental in shifting the dispersal centre of the ice sheet to the west during the Younger Dryas (Kleman et al., 1997). Areas between these ice streams, such as coastal Ostrobothnia, were subjected to slow and probably cold-based sheet flow, which preserved older landforms and organic deposits (Niemelä and Tynni, 1979; Salonen et al., 2008; Pitkäranta et al., 2014).

4.2.4.4. The Baltic Basin. The Baltic Basin is around 1500 km long and bathymetrically separated into many sub-basins (Fig. 1). Although water depths remain generally shallower than 100 m, three of the basins reach depths of 250–460 m. Retreat of the ice sheet mostly occurred with the ice margin orientated perpendicular to the long axis of the Baltic Basin. Ice sheet retreat deviates from this pattern only in the Gulf of Bothnia where it retreated obliquely to the basin long axis towards the location of the final ice remnants in the northern Swedish mountains (Andrén, 1990). In the absence of published regional flow traces on the Baltic Sea floor, the ice dynamics in the basin have been mostly inferred from clay varves, and striae and other landforms yielding ice-marginal positions and flow traces on adjacent coasts (Hörnsten, 1964; Bergström, 1968; Fözö, 1980; Lundqvist, 1987; Strömberg, 1989). In contrast to North America, where rapid calving in the interior basin of Hudson Bay divided the ice sheet in discrete smaller remnants (Dyke, 2004), no such separation seems to have occurred in Fennoscandia.

Retreat along the Baltic Basin started with the decay or collapse of the extended terminal lobe of the Bælthav Young Baltic ice stream, at around 16.5 cal kyr BP. This lobe extended northwards into the Storebælt and Öresund straits, and was sufficiently thin for its flow pattern to be governed by the modest topographic relief of the southern Baltic Basin, where present-day water depths remain <100 m. Retreat through the southern and central Baltic Basin, up to the Younger Dryas position, took approximately 4000 years. The lobate moraines east and south of the Baltic Basin are indicative of ice streaming in the deeper parts of the basin, particularly east of Gotland (Fig. 6). During the Younger Dryas, the ice margin appears to have stabilized around 150 km south of Åland, although its precise location remains elusive (Noormets and Flodén, 2002). North of Åland, the rate of retreat sharply increased, and it appears that at least one major surge occurred in the Gulf of Bothnia, at around 10.8 cal kyr BP (Sandegren, 1929; Strömberg, 1989; Lundqvist, 2007; Kleman and Applegate, 2014). This was possibly caused by a sudden and widespread change in subglacial conditions from cold- to warm-based (Strömberg, 1989; Kleman and Applegate, 2014). A relatively deep basin in the seafloor south of Umeå (Fig. 6) may have been the initiation point for this surge, as evidenced by a convergence of striae on the coast towards this depression, and new geomorphological data from the central Gulf of Bothnia floor showing typical signs of ice streaming, such as highly elongated glacial lineations (Greenwood et al., in press).

Perhaps coeval to surging in the Gulf of Bothnia, the ice sheet margin in Finland surged as well. Initially, retreat proceeded towards the northwest, but it was interrupted by a standstill and readvance indicated by the Central Finland Ice-Marginal Formation, CFIMF (Rainio et al., 1986). The CFIMF (Figs. 5, 6 and 9) is limited to Central Finland. It consists of large glaciofluvial deposits (plateaux and ridges) and end moraines. Stratigraphical evidence, differing patterns of striae and eskers on proximal and distal sides, and its lobate outline, are all consistent with an ice margin advance through surging. Inwards from this location, ice margin retreat proceeded towards the northwest, and appears to have been rapid and uninterrupted by dynamic events, such as renewed ice streaming. The ice sheet retreated onshore at around 10 cal kyr BP.

4.2.4.5. The final deglaciation of northern Fennoscandia. Although deglacial landforms and deposits are common in northern Fennoscandia, inherited deglacial landforms and deposits are regionally important (Lagerbäck and Robertsson, 1988; Kleman, 1990; Hättestrand, 1998). On many western and northern uplands only a Late Quaternary weathering mantle is present (Goodfellow et al., 2014), capping a non-glacial bedrock morphology (Kleman and Stroeven, 1997; Goodfellow et al., 2008). Although repeated glaciations on the Kola Peninsula, Russia, have left almost no lithostratigraphical record (Niemelä et al., 1993), there is a discernible deglaciation record from meltwater landforms (Hättestrand and Clark, 2006a, 2006b; Hättestrand et al., 2007). In much of northern Fennoscandia, the Late Weichselian till is a thin (1–3 m) veneer atop older glacial and non-glacial deposits (Nordkalott Project, 1986; Kleman et al., 2008). The pre-Late Weichselian glacial landscape in northern Sweden and Finland is the most important inherited element in the Fennoscandian glacial landscape. It consists of widespread Veiki moraine (dead ice topography), as well as drumlins and eskers indicating a regional ice flow towards the southeast (Hoppe, 1959; Lagerbäck, 1988; Kleman, 1992; Hättestrand, 1998; Kleman et al., 2006). The deglacial landform imprint of mainly lineations and eskers is locally well-developed, such as in northern Norway and throughout northeastern Sweden, where this landform assemblage can be traced inland to the position of the last ice remnant in the northern Swedish mountains (Nordkalott Project, 1986; Hättestrand et al., 1999; Dellgar Hagström, 2006; Stroeven et al., 2011). Widespread deglaciation landforms also occur inland from the Bothnian coast (Fig. 5). In this area, abundant De Geer moraines indicate deglaciation at a calving ice margin (Hoppe, 1948). Towards the interior areas of northern Sweden, deglacial landforms are less developed, especially inland of a series of subglacial fluvial gorges cut at the highest coastline (Jansen et al., 2014), and they are often superimposed on landforms of Early Weichselian age. Glacial lakes constrain 10.1–9.7 cal kyr BP marginal positions on the eastern side of the Scandinavian Mountains and, during the earliest Holocene, most of the river valleys in northern Sweden were locations for repeated drainage events in response to ice margin failures (Elfström, 1987). The last remnant of the Fennoscandian Ice Sheet vanished after 9.7 cal kyr BP in the eastern Sarek Mountains of northern Sweden (Lundqvist, 1986; Kleman, 1990; Kleman et al., 1997; Boulton et al., 2001).

5. Discussion

The deglaciation chronology of the Fennoscandian Ice Sheet presented here is consistent with the last two published deglaciation chronologies by Kleman et al. (1997) and Boulton et al. (2001), and adds considerable new detail. Our reconstruction is based on additional geomorphological constraints, including many publications addressing the distribution and chronology of marginal positions in the eastern sector (Fig. S1, Supplementary dataset), which were poorly covered, and a first compilation of eskers across the glaciated domain (Fig. 5). Compared to the previous reconstructions, there are now more abundant radiometric constraints, including cosmogenic nuclide constraints which were unavailable at the time (Supplementary dataset). Hence, our reconstruction is much improved for the southern and eastern ice sheet sectors. Below, we discuss some of these aspects and analyse their implication for ice sheet dynamics.

5.1. Uncertainty in the timing of ice sheet deglaciation

The position of the LGM ice margin around the perimeter of the Fennoscandian Ice Sheet is relatively well established (Ehlers and Gibbard, 2004), even if opinions can diverge on when the local maximum position was attained. However, one area where considerable uncertainties persist regarding the LGM extent of the ice sheet is in northwestern Russia. Here, different reconstructions, even those published in the last 10 years, place the LGM ice margin hundreds of kilometres apart. We have largely adopted the LGM-reconstruction suggested by Larsen et al. (2014) and Lyså et al. (2014). They base their suggested ice marginal outline and chronology on a recent mapping of marginal moraines by Fredin et al. (2012) and a new dataset of OSL and radiocarbon ages from below and above LGM sediments (Lyså et al., 2014; see Supplementary dataset). Combined, these data indicate that the LGM ice margin was located further east than previously suggested (Fredin et al., 2012; Larsen et al., 2014; Lyså et al., 2014), and peaked at a later time than for the rest of the ice sheet perimeter, at around 17–15 cal kyr BP (Larsen et al., 1999; Lyså et al., 2014).

Fig. 12 shows the deviation of individual sample ages from the reconstructed deglaciation age for that location. The scatter in ages is significant (Fig. 12b–e) and, consequently, a large number of sample ages do not match the reconstructed deglaciation chronology. Of the radiocarbon ages, only 12% (0%) of the minimum (maximum) ages overlap within uncertainties with the reconstructed age whereas 71% (2%) reside within a time window of ±2 kyr around the reconstructed deglaciation age. Of the OSL ages, 29% (31%) of the minimum (maximum) ages overlap within uncertainties with the reconstructed age and 54% (31%) reside within a time window of ±2 kyr around the reconstructed deglaciation age. Of the ^{10}Be (^{26}Al) exposure ages, 27% (28%) overlap within uncertainties with the reconstructed age and 51% (41%) reside within a time window of ±2 kyr around the reconstructed deglaciation age. These numbers help illustrate the relatively poor fit of individual sample ages to the reconstructed deglaciation age and highlight the challenges associated with dating ice margin retreat using these techniques. The radiocarbon ages yield better results than the cosmogenic and OSL ages. Individual sample ages show

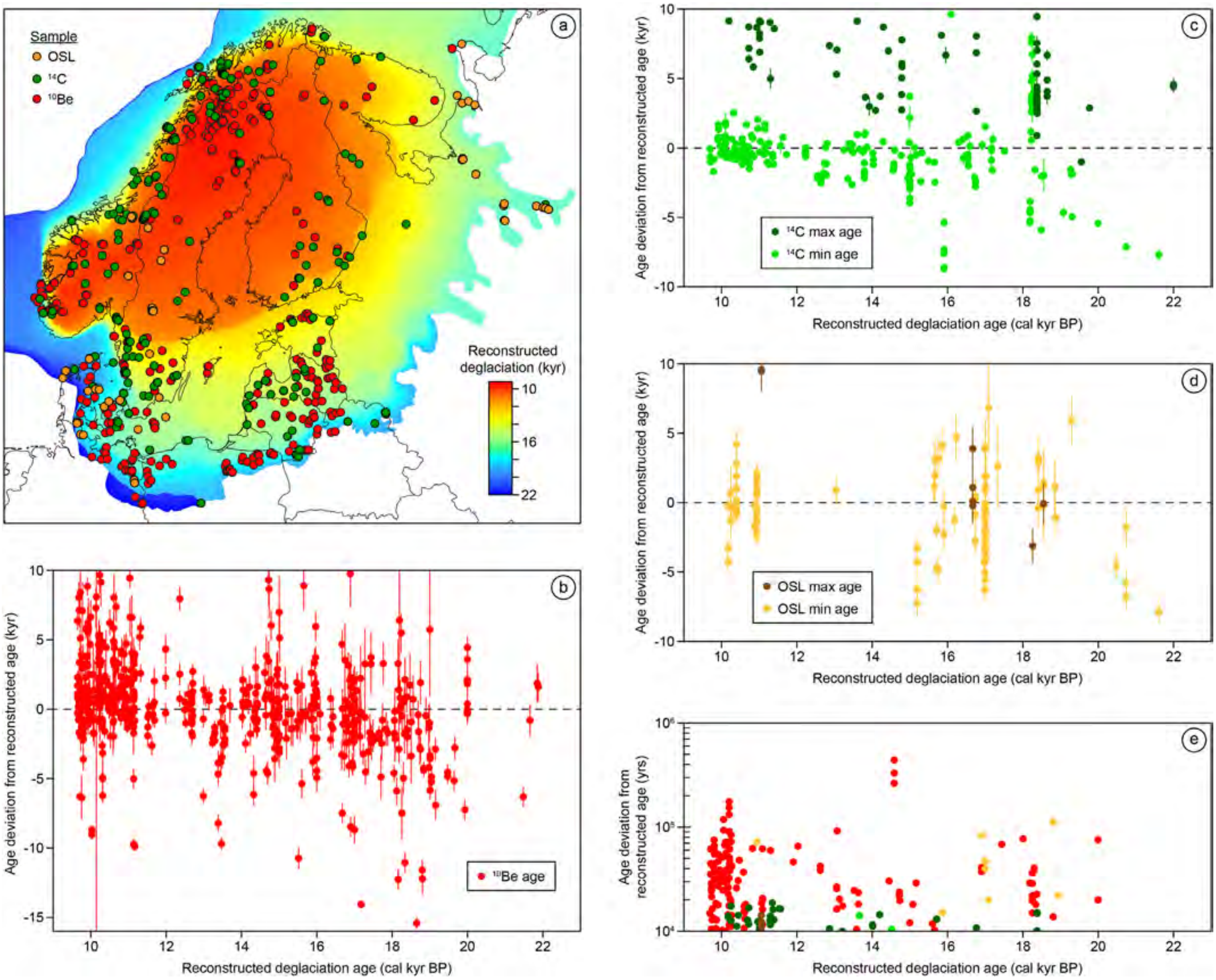

Fig. 12. Age differences between the reconstructed deglaciation age (Fig. 9) and individual cosmogenic (^{10}Be), radiocarbon (^{14}C), and OSL ages (Supplementary dataset). a) Interpolated deglaciation reconstruction including ^{10}Be, ^{14}C, and OSL sample locations within the local LGM domain. b) Deviation from the reconstructed deglaciation age for ^{10}Be exposure ages (sample age minus reconstructed age). c) Deviation from the reconstructed deglaciation age for ^{14}C ages (sample age minus reconstructed age). d) Deviation from the reconstructed deglaciation age for OSL ages (sample age minus reconstructed age). e) Deviation of >10 kyr from the reconstructed deglaciation age for OSL, ^{14}C, and ^{10}Be ages (sample age minus reconstructed age).

more disparity with the reconstructed age in the early part of the deglaciation than in the latter part of the deglaciation. However, this is not generally true for cosmogenic ages because inheritance is a problem for many samples collected from surfaces preserved under cold-based non-erosive ice (e.g., Fabel et al., 2002; Stroeven et al., 2002b; Goehring et al., 2008).

The spatial and chronological uncertainties for the deglaciation reconstruction vary across the paleo-ice sheet domain. Generally, the uncertainties are lowest for the post-Younger Dryas deglaciation, which is well constrained by geomorphology and the clay-varve chronology. Distal to the Younger Dryas margin the uncertainties increase progressively with the largest uncertainties attained for the eastern and southeastern sectors of the LGM configuration. It is difficult to estimate the uncertainties because the reconstruction is based on a range of geomorphological and chronological data with highly different characteristics and problems potentially causing errors in the reconstruction. While the uncertainty for the post-Younger Dryas deglaciation is in the range of 100–500 years, the uncertainty in the earlier part of the deglaciation chronology is much higher, perhaps 500–2000 years.

5.2. A climatic imprint on Fennoscandian ice margin behaviour: a southern Sweden case study

We consider the GRIP/GISP2/NGRIP harmonized Greenland ice core record of Rasmussen et al. (2014), dated by annual layer counting, as the best calendar-year record of the Younger Dryas climatic event, which left a prominent glacial geological record in Fennoscandia (Lundqvist, 1990; Andersen et al., 1995a). According to Rasmussen et al. (2014), this climatic event spans the period 12.8–11.7 cal kyr BP in the Greenland ice core record (Fig. 13). The same record also shows five cold phases in the period leading up to the Younger Dryas (18–12.8 cal kyr BP), which is largely coincident with Greenland interstadial 1 and is the time during which southern Sweden became deglaciated (Hillefors, 1969; Berglund, 1976; Lundqvist and Wohlfarth, 2001). The deposition of the patchy Halland Coastal moraine belt, which is laterally confined to about 75 km, was followed by the deposition of four more-continuous and laterally-extensive end moraine belts, the Göteborg, Berghem-Vimmerby, Trollhättan, and Levene (Table 5, Figs. 5, 6 and 11). Each of these five moraine belts appears to have generally formed in response to a stand-still or re-advance of the Fennoscandian Ice Sheet. We have not identified evidence, such as deviating striae patterns or lobate margin outlines, which would indicate that these moraines are a result of internal ice sheet dynamics (surge moraines). An exception is the central part of the Vimmerby Moraine, which has a lobate outline with a splaying pattern of glacial lineations on its proximal side. However, considering the clear lateral continuation of the Vimmerby Moraine to the Berghem Moraine, ice-dynamic oscillation appears to have occurred on only a minor part of the continuous Berghem-Vimmerby ice-marginal formation. Hence, the South Swedish moraines may offer the possibility to directly link the proxy climatic record of Greenland to southern Swedish glacial geology.

The Halland Coastal Moraine belt (Caldenius, 1942; Fernlund, 1993) is the oldest in Sweden. It differs from the other moraine belts in southern Sweden because, rather than being a semi-continuous single or double ridge, it is a zone up to 15 km wide with numerous parallel moraines. Individual segments are rarely more than a few kilometers long and some resemble De Geer, or washboard, moraines. The Halland Coastal Moraine belt is estimated to have an age of 18–16 cal kyr BP based on radiocarbon ages (Lundqvist and Wohlfarth, 2001), and 17.0 ± 0.9 to 16.8 ± 1.0 cal kyr BP according to recent cosmogenic isotope dating (Anjar et al., 2014; Larsen et al., 2012). Within error margins, these ages correspond with the onset of Greenland interstadial GS-2.1a at 17.4 ka (Rasmussen et al., 2014).

The Göteborg Moraine (Hillefors, 1975) is a well-defined ice-marginal formation and, where it runs parallel to the west coast of Sweden, it also approximates the marine limit. Consequently, there may be some dynamic control on the location of this moraine segment. The 700 years preceding the GI-1d event comprises the warm Bölling phase (GI-1e; Fig. 13), during which climatically-controlled moraine formation appears unlikely. We therefore assign the Göteborg Moraine a youngest possible age of 14.7 cal kyr BP (Table 5), which marks the final cold stage of stadial GS-2.1. It has been suggested that the Göteborg Moraine continues eastward into a hummocky moraine zone on the southern Swedish highlands (e.g., Möller, 2010; Anjar et al., 2014) and similarly that other west-Swedish ice marginal formations continue eastwards into hummocky moraine equivalents on the southern Swedish highlands (e.g., Lundqvist and Wohlfarth, 2001). However, the new LiDAR coverage of southern Sweden leads us to question this linkage eastwards of the Göteborg Moraine. Using this data we find that,

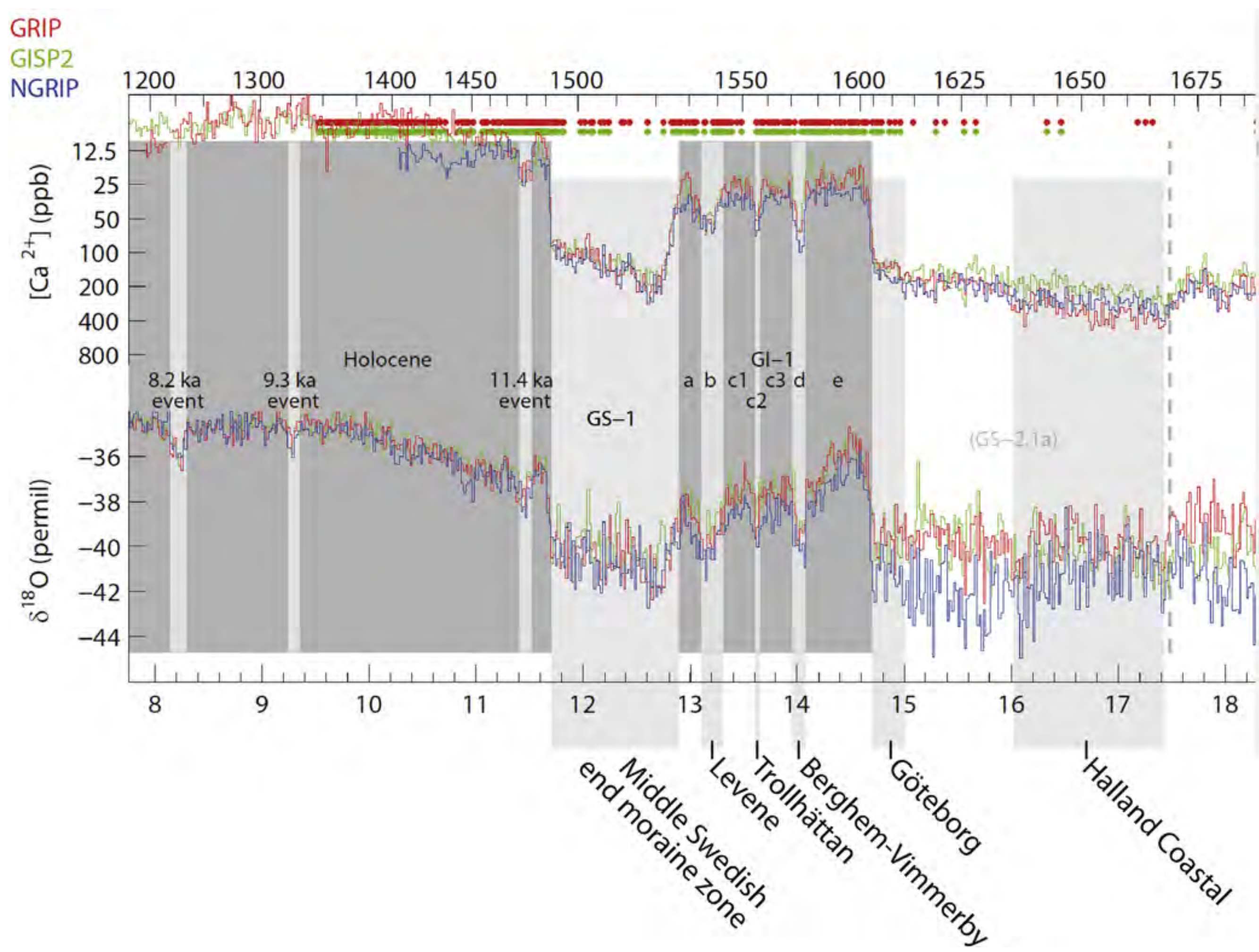

Fig. 13. Subset of the Greenland ice core event stratigraphy (from Rasmussen et al., 2014, Fig. 1), with, indicated, the proposed correlation of the south Swedish end moraine belts with ice core cold stages (Fig. 11). Not indicated, but mentioned in the text, is evidence of the response of the Fennoscandian Ice Sheet to the “11.4 ka event”, or the Preboreal oscillation, in Norway and in Finland (Ss III). (For interpretation of the references to colour in this figure legend, the reader is referred to the web version of this article.)

Table 5
Southern Swedish moraine chronology from radiocarbon and varve dating (Lundqvist and Wohlfarth, 2001) and cosmogenic nuclide dating (Larsen et al., 2012; Anjar et al., 2014). We infer a slightly different chronology (this study) based on a one-to-one matching with cold phases in the harmonized Greenland ice core record of Rasmussen et al. (2014). Ages expressed in cal kyr BP.

Moraine	Lundqvist and Wohlfarth (2001)	Anjar et al. (2014)	Larsen et al. (2012)	Rasmussen et al. (2014)	This study
Levene	13.4	13.8 ± 0.8	13.6 ± 0.9	13.2 (GI-1b)	13.2
Trollhättan	14.2–13.4			13.6 (GI-1c2)	13.6
Berghem[a]	14.4–14.2			14.0 (GI-1d)	14.0
Vimmerby[a]		14.6–14.5			14.0
Göteborg	15.4–14.5	16.1 ± 0.9	16.2 ± 0.9	15.0–14.7 (GS-2.1a)	14.7
Halland Coastal	18.0–16.0	17.0 ± 0.9	16.8 ± 1.0	17.4–16.0	17.4–16.0

[a] In this study the Berghem Moraine is correlated with the Vimmerby Moraine.

where the Göteborg Moraine laps onto the southern Swedish highlands hummocky moraine zone, it appears as one or two distinct moraine ridges superimposed on a hummocky moraine zone that lacks clear proximal and distal borders. Hence, there are no morphologically-based arguments to support a genetic relationship between them.

The most logical correlation for the Berghem-Vimmerby Moraine is the GI-1d cold phase at 14.0 cal kyr BP (Fig. 13). There is, however, a discrepancy between the varve chronology in Fig. 8 and the age assignment of the Vimmerby Moraine in Fig. 11. According to the varve chronology, deglaciation from the Vimmerby Moraine occurred at c.13.5 cal kyr BP, whereas absolute dating and our Greenland ice sheet correlation indicate that the combined Berghem-Vimmerby line is no younger than 14.0 cal kyr BP. Presently, these two data sets appear irreconcilable and, because of the difficulties in extending the varve chronology across the Younger Dryas zone, we have chosen to adhere to the radiocarbon chronology in southeastern Sweden, rather than the varve chronology. New clay varve locations south of the Younger Dryas zone, not yet connected to the STS and where tephra (Vedde ash) has been found, may help to resolve this issue (MacLeod et al., 2014).

The Trollhättan Moraine is smaller and less continuous than the Berghem-Vimmerby and Göteborg moraines. We consider a correlation between the relatively small Trollhättan Moraine and a short-lived and low-magnitude cold phase (event GI-1c2; Fig. 13), to be most plausible. Cold event GI-1c2 postdates the GI-1d cold phase by about 400 years (Table 5).

The Levene Moraine and its extension in the Oslofjord area, the Onsøy Moraine (Fig. 6; Sørensen, 1992), is the youngest of the four ice-marginal formations. These moraines are especially important because of their lateral extent (>250 km). They form a narrow belt located 5–20 km outside Younger Dryas-age ice-marginal formations (Berglund, 1979; Hillefors, 1979; Lundqvist and Wohlfarth, 2001). The Levene Moraine likely reflects the ice sheet margin reacting to a short-lived climatic deterioration of regional significance, shortly before the Younger Dryas event. The regional character of this climate event is further illustrated by ice margin deposits of 13.1–13.2 cal kyr BP in Central Norway about 20 km outside local Younger Dryas moraines (Olsen et al., 2013a). A comparison with the harmonized Greenland ice core record indicates that it correlates with a short, sharp, cold phase in Greenland interstadial 1 (event GI-1b; Table 5, Fig. 13) at around 13.2 cal kyr BP.

Our chronology is based on the premise that there is a correlation between the southern Swedish ice-marginal formations and the harmonized Greenland ice core cold stages. If this is correct, we argue that the correlation scheme as presented in Table 5 is the most likely and also fits within 200 years of the error margins of available radiocarbon ages for the moraines, as summarized in Lundqvist and Wohlfarth (2001). This chronology for the southern Swedish ice-marginal formations is younger than recently suggested by Larsen et al. (2012) and Anjar et al. (2014) on the basis of cosmogenic exposure ages. However, sampling of the Göteborg Moraine for the Larsen et al. (2012) study was done on the portion of this moraine that approximates the marine limit and which is closely juxtaposed to, and possibly merges with, the Halland Coastal Moraine belt. This portion of the moraine appears to have been dynamically controlled and the ice margin may have persisted at this location throughout GS-2.1a (Fig. 13). The Anjar et al. (2014) age assignments for some locations in southern-most Sweden are incompatible with age assignments for ice marginal positions in northern Germany and Denmark. OSL, ^{14}C, and other cosmogenic isotope data indicate that the ice margin at this time was positioned close to the northern coasts of Germany and Poland (Marks, 2012), and in eastern Denmark (Houmark-Nielsen and Kjær, 2003), respectively. Our reconstruction conforms to this latter, more extensive, data set.

5.3. Climatic and dynamic controls on moraine formation: the Younger Dryas case study

From the record of ice-marginal formations, we infer that the ice sheet margin periodically halted in its retreat or re-advanced. An important question when utilizing such ice-marginal formations for the tracing of retreat patterns, is what controlled the interruption in retreat? The two end member answers are full climatic control, with essentially unchanged ice dynamics, and dynamic control, irrespective of climatic trends. Interruptions in retreat through dynamic controls typically result in ice margin advances as part of surges. Moraines that form from surges are well-known from the periphery of Vatnajökull, Iceland, and other major surging glaciers (Evans and Rea, 1999; Benediktsson et al., 2010; Schomacker et al., 2014). The Younger Dryas cold period resulted in an almost continuous belt of ice-marginal formations, which we analyse in terms of the controls behind the margin response.

We regard the Younger Dryas moraines in Norway and Sweden as classical examples of the effect of climatically controlled ice margin responses, i.e. they mark standstills, sometimes with minor to modest re-advances immediately prior to moraine formation. In Sweden, there is no evidence in the landform record for ice streaming proximal to the Younger Dryas moraines or for major lobation (which is an indicator of strong lateral velocity gradients caused by ice streaming; Stokes and Clark, 1999). The extreme topographic relief of Norway renders simultaneous surging in a large number of outlets as an extremely unlikely scenario.

The situation with regards to the Salpausselkä moraines in Finland is, however, more complex. The Ss I and Ss II moraines (Fig. 5) are also of approximately Younger Dryas age, with Ss I likely being formed at the start of the Younger Dryas cold period (Rainio et al., 1995). Thus, they are broadly linked to a major cold event and have traditionally been seen as correlatives to the Younger Dryas moraines in Norway and Sweden. Ss II continues northeastward in the Koitere Moraine and probably also further in the Rugozero Moraine (Fig. 6; Rainio et al., 1995). This continuity, over a 1000 km of ice margin distance, and with, at least, the Koitere Moraine fronting a sector of the ice sheet with little evidence for fast ice flow dynamics, supports the inference of climatic control for the formation of Ss II. The occurrence of paired deltas with an elevation difference of 26–28 m, immediately north of the Ss II, and in all likelihood reflecting the late Younger Dryas drainage of the Baltic Ice Lake, firmly anchors the Ss II to a Younger Dryas age (Donner, 1978, 2010; Saarnisto and Saarinen, 2001). Hence, we also regard the Ss II as a robust part of the circum-Fennoscandian Younger Dryas ice-marginal formation.

We note that Ss I, in contrast to Ss II, only fronts the two major lobes in southern Finland and does not continue in a northeasterly direction (Fig. 5). Although it appears that the Ss I is of early Younger Dryas age (Rainio et al., 1995), we suspect that its formation is not directly related to the Younger Dryas climatic cooling. Based on the pattern of landforms proximal to the Ss I, we instead infer that it represents a surge moraine, located at the outermost position of ice sheet lobes that indicate the development of two ice streams. In contrast, the striae record immediately distal of the Ss I indicates that sheet flow immediately precede the Ss I event. This indicates that fast ice flow that formed the feeder ice streams commenced shortly before the Younger Dryas, during the late Allerød.

We propose that pronounced warming and surface melting during the Allerød warm period triggered the onset of ice streaming, which resulted in the formation of Ss I as a surge moraine. We further consider it plausible that this phase of ice streaming continued throughout the Younger Dryas cold period, preventing fast collapse of the lobes, and that Ss II, and possibly also Ss III, were formed during climatically-controlled standstills during the retreat from the non-climatically controlled Ss I. In summary, our view, represented in the deglaciation map (Fig. 9), is that the Ss I and Ss II moraines fall within the Younger Dryas chronozone, and that only Ss II and Ss III are climatically controlled moraines and, in that sense, Ss II is directly correlative to the Norwegian and Swedish Younger Dryas moraines.

Ss III is a c. 10 km-wide ice-marginal formation composed of end moraines, glaciofluvial ridges, and deltas. After formation of the Ss I and Ss II during the Younger Dryas, a rapid deglaciation commenced and persisted for c. 130 years until, in south-western Finland, it was interrupted by slow retreat, standstill, and re-advance of the ice margin during c. 160 years (Strömberg, 2005). A re-advance of the ice margin is indicated by the end moraine stratigraphy (Salonen, 1990). No retarded retreat of the ice margin has been recorded in Sweden (Brunnberg, 1995), even though large glaciofluvial deposits 20–25 km south of Stockholm were suggested to be correlatives (Nilsson, 1968). A more likely counterpart to Ss III is the Jaamankangas-Pielisjärvi formation in northern Karelia (Figs. 5 and 6; Rainio et al., 1995).

We regard this temporary halt in retreat, and limited re-advance, to be the result of colder conditions during the short-lived Preboreal oscillation (PBO) or “11.4 ka event” (Rasmussen et al., 2014, Fig. 13). Björck et al. (1997) first proposed a formation of Ss III during the PBO, a short-lived event that commenced 300 years after the end of the Younger Dryas, even though there was a mismatch between the timing of the event in the ice core (GRIP), dendrochronology, and varve chronologies (Björck et al., 1996). However, with the new timing of the PBO in the Greenland ice core event stratigraphy of Rasmussen et al. (2014), the PBO is dated at 11.47–11.35 cal kyr BP, only about 130–250 years after the end of the Younger Dryas, and is therefore well aligned with varve evidence for the age of Ss III.

5.4. Bedrock control on the behaviour of ice sheet margins: a northwestern Russia case study

Ice sheet margins in the southern and northeastern sectors of the Fennoscandian Ice Sheet differ in style from ice margins in shield bedrock areas. In the latter, margins tend to be slightly curved, such as is the case with most of the Younger Dryas ice margin. This contrasts with the pre-Younger Dryas ice-marginal formations deposited in non-shield areas, which reflect ice margins that were much more topographically controlled and therefore show a more lobate pattern (Kalm and Gorlach, 2014). In the southern sector, such lobes typically extended tens of kilometres beyond adjacent ice margins, with a maximum of up to 100 km for ice lobes southeast of the Baltic Basin. In the eastern sector, ice lobes extended several hundreds of kilometres beyond the adjacent ice margin. There were three major lobes of this type located in the Dvina, Vologda, and Rybinsk basins (Fig. 6), and these are uniquely long for the Fennoscandian Ice Sheet. This situation is analogous to the southern margin of the Laurentide Ice Sheet, where ice marginal retreat started at 23 kyr (Ullman et al., 2015), with the exception of two ice lobes hundreds of kilometres long (Des Moines lobe and James lobe; Clayton and Moran, 1982), which attained their LGM maximum position long after adjacent ice margins, because of ice-dynamical factors rather than climatic drivers. For the ice lobes in NW Russia, Larsen et al. (2014) argued that the advances were due to ice-bed decoupling caused by a combination of successive damming of pro-glacial lakes and ice overriding waterlain sediments and tills with low shear strength. This enabled fast-flowing low-gradient ice lobes to expand into the exceptionally wide valleys and basins of the northwestern Russian Plain. We note also that these three major ice lobes at the eastern Fennoscandian Ice Sheet margin extended beyond major basins (the White Sea, Lake Onega and Lake Ladoga; Fig. 6). These basins provided the low-shear sediments and probably acted as conduits for fast ice flow, feeding the lobes with ice from interior parts of the ice sheet, possibly as a result of thawing at the ice sheet bed during early deglaciation. We infer that these dynamic ice sheet responses led to an overstretching of the ice sheet surface profile as it created the ice lobes. Given the extremely low ice surface gradients, and the warm climate following these expansions, the ice-marginal retreat following the expansion occurred uninterrupted by stillstands and possibly included local areal down-wasting.

5.5. Retreat rate across different sectors

Retreat rates for different sectors of the ice sheet for the post-16 cal kyr BP evolution differ drastically. Total retreat distances towards the two final retreat centers (Figs. 9 and 14) for the southern and eastern sectors of the ice sheet during this period were on the order of 1500 km, whereas retreat distances on the high-elevation and maritime Norwegian margin during the same period amounted to roughly 150 km. Moreover, the western margin was also much closer to a state of equilibrium during overall ice sheet retreat as witnessed by several standstills and concomitant pulses of moraine formation in response to minor climatic deteriorations, such as occurred during the Preboreal (Sveian et al., 1979; Corner, 1980; Sollid and Torp, 1984). No correlative moraines exist on the eastern flank; here, only the Younger Dryas was a climatic cooling of sufficient magnitude to temporarily halt the recession.

In Fig. 14 we compare ice sheet retreat rates along three southern and eastern transects since local LGM. A clear, and climatically governed, pattern is apparent in all three profiles. Retreat rates were variable and high, mostly in the 50–200 m yr^{-1} range, between 17 and 13 cal kyr BP, very slow or absent retreat

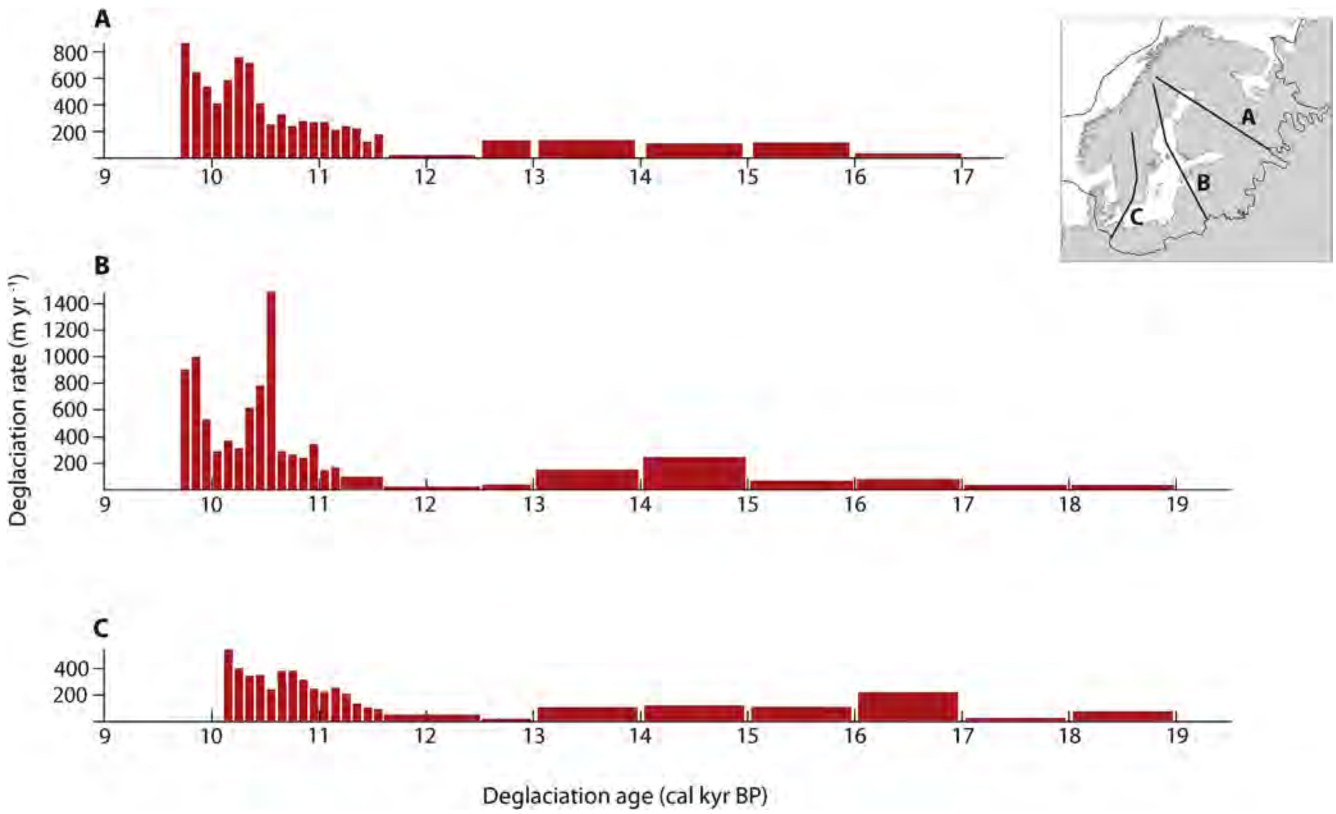

Fig. 14. Ice sheet retreat rates (in m yr^{-1}) along three southern and eastern transects since local LGM. Although retreat rates along the three profiles differ in detail, a slow or absent retreat during the Younger Dryas (12.8–11.7 cal kyr BP) is apparent in all three profiles. The peak retreat rate at 10.3–10.4 cal kyr BP in profile A was probably caused by a retreat of the ice margin across a bed with a reverse slope (deepening water up-ice) at the eastern side of the Gulf of Bothnia. Similarly, the very rapid retreat seen in profile B, across the Gulf of Bothnia at 10.5–10.6 cal kyr BP, was related to retreat in deep water, and possibly also reflects a rapid disintegration of a post-surge ice lobe.

during the Younger Dryas, and rapid retreat of 200–1600 m yr^{-1} until final deglaciation. Retreat rates were highest where the ice sheet margin terminated offshore and retreated across a bed with a reverse slope (deepening water up-ice) and over bathymetric basins.

5.6. Correlation across the Baltic Basin

Inside the Younger Dryas position, correlation of ice margins across the Baltic Basin is fairly straightforward, using high-precision clay varve archives (Strömberg, 1990, 2005). Distances across the water are also shorter than in the southern Baltic Basin. Outside the Younger Dryas zone, correlations across the Baltic Basin are more difficult to make (De Geer, 1935). This is because of chronological uncertainties and the topographical complexity of the basin floor. The ice-marginal formations in coastal Estonia, Latvia, and Lithuania indicate a lobe extending southwards in the Baltic Basin during the 16–14 cal kyr BP period. On the opposing coast, in eastern Sweden, eskers and striae indicate a SW–NE oriented ice margin during the same period, i.e. a calving bay configuration that is difficult to reconcile with the evidence from the eastern side. We suggest that a southward-directed lobe was confined to the deeper eastern part of the southern Baltic Basin and that the ice margin had a pronounced change of direction between Gotland and the Swedish mainland. The overall configuration of closely-spaced ice-marginal formations in southern Sweden between c 17 and 13 cal kyr BP and widely-spaced ice marginal formations in the same period on the other side of the Baltic Basin, indicates that southern Sweden was a hinge point which fixed the swinging gate of the Baltic Basin deglaciation (cf. with reconstruction of the deglaciation pattern in the Ross Sea Basin by Conway et al., 1999).

6. Conclusions

Understanding ice sheet deglaciation processes and rates is of considerable importance given current and projected melting of the Greenland and Antarctic ice sheets. We have compiled and synthesized published geomorphological data for eskers, ice-marginal formations, lineations, marginal meltwater channels, striae, ice-dammed lakes, and geochronological data from radiocarbon, varve, optically-stimulated luminescence, and cosmogenic nuclide dating, to provide reconstructions of ice sheet extents for deglaciation of the Fennoscandian Ice Sheet, in the form of calendar-year time-slices. This is summarized as a deglaciation map of the Fennoscandian Ice Sheet (Fig. 9), with isochrons marking every 1000 years between 22 and 13 cal kyr BP and every hundred years between 11.6 and final ice decay after 9.7 cal kyr BP. We estimate that the uncertainty for the post-Younger Dryas deglaciation is 100–500 years, while the uncertainty in the earlier part of the deglaciation chronology is perhaps 500–2000 years.

The ice margin morphology in plan view varies between sectors; shield areas tend to produce straight or slightly curved ice margins, even where there is a considerable topographic relief. Ice margins in non-shield areas, on the other hand, tend to be highly lobate because of the strong topographic steering that shallow topographic depressions exert on low-gradient marginal areas on deformable beds and sediments with high pore-water pressures. An extreme example of the latter is in NW Russia, where ice lobes hundreds of kilometers long extended to their farthest LGM position well into the deglaciation period for the ice sheet as a whole.

Deglaciation patterns vary across the Fennoscandian Ice Sheet, reflecting both differences in climatic and geomorphic settings as well as differences in ice sheet basal thermal conditions and terrestrial versus marine termination. The ice sheet margin in the high-precipitation coastal setting of the western sector responded sensitively to climatic variations leaving a detailed record of prominent moraines and ice-marginal deposits in many fjords and coastal valleys. The southern sector includes a major contrast in retreat rates of the slow terrestrial margin retreat in western and southern Sweden and the rapid retreat of the calving ice margin in the Baltic Basin. Our reconstructions are consistent with much of the published research. However, the synthesis of a large amount of existing and new data support refined reconstructions in some areas. For example, (i) the LGM extent of the ice sheet in north-western Russia was located far east and it peaked at a later time than the rest of the ice sheet perimeter, at around 17–15 cal kyr BP; and (ii) using new LiDAR data over southern Sweden to correlate moraines, and coupling the timing of moraine formation to cold periods in the Greenland ice core, we propose a slightly different chronology.

Retreat rates vary by as much as an order of magnitude in different sectors of the ice sheet, with the lowest rates on the high-elevation and maritime Norwegian margin. Retreat rates compared to the climatic information provided by the NGRIP ice-core record show a general correspondence between retreat rate and climatic forcing, although a close match between retreat rate and climate is unlikely because of other controls, such as topography and marine versus terrestrial termination. Thus, although many of the ice marginal features can be interpreted as straightforward responses to climate variations as recorded in ice cores, in some cases the relationships are more complex. For example, we conclude that rapid warming and surface melting during the Allerød warm period triggered the onset of ice streaming upstream of the Salpausselkä I moraine in Finland, and that it represents a surge moraine.

Overall, the time slice reconstructions of Fennoscandian Ice Sheet deglaciation from 22 to 9.7 cal kyr BP (Fig. 9; provided as shape files in the Supplementary dataset) provide an important dataset for understanding the contexts that underlie spatial and temporal patterns in retreat of the Fennoscandian Ice Sheet, and are an important resource for testing and refining ice sheet models. Future work is needed to improve the chronological control in areas where dating is sparse, and to test the new interpretations provided in parts of this paper.

Acknowledgements

We thank Chris Clark and an anonymous reviewer for useful constructive criticism that improved the clarity of the paper. Swedish Research Council Grants G-AA/GU 12034-300 and G-AA/GU 12034-301 to Stroeven and National Science Foundation Grants OPP-9818162 and OPP-0138486 to Harbor provided partial support for this work. The Swedish Research Council (2007-15) and Granholmsstiftelse at Stockholm University generously supported Stroeven to host the first of a couple of deglaciation workshops at the Tarfala Research Station in late March–April 2007. Jansen was supported by a UK NERC fellowship (NE/EO14143/1). We thank Helena Alexanderson, John Clague, Timothy Johnsen, Yingkui Li, and Kurt Lambeck for their contribution to the 2007 workshop. The field data has been collected with the help of Ingmar Borgström (2000), Magnus Johansson (2001), Torbjörn Dahlgren (2002), Karin Ebert (2002), Angelica Feurdean (2002), Barbara Wohlfarth (2002), Svante Björck (2003), Eva Sahlin (2003), Vasily Kolka (2004), and Alexandru T. Codilean (2009). We received considerable support at three accelerator facilities (PrimeLab, ANSTO, and SUERC), and we are most grateful to staff at these facilities. Fig. 2c was reprinted from the Journal of Glaciology with permission of the International Glaciological Society.

Appendix A. Supplementary data

Supplementary data related to this article can be found at http://dx.doi.org/10.1016/j.quascirev.2015.09.016.

References

Aas, B., Faarlund, T., 1988. Postglasiale skoggrenser i sentrale sørnorske fjelltrakter. ^{14}C-datering av subfossile furu- og bjørkerester. Nor. Geogr. Tidsskr. 42, 25–61.
Abrahamsen, N., Readman, P.W., 1980. Geomagnetic variations recorded in older (≥ 23 000 B.P.) and Younger *Yoldia* Clay (~ 14 000 B.P.) at Nørre Lyngby, Denmark. Geophys. J. R. Astron. Soc. 62, 329–344.
Agassiz, L., 1840. Études sur les Glaciers. Neuchatel, pp. 1–346.
Agrell, H., Friberg, N., Oppgården, R., 1976. The Vimmerby line - an ice-margin zone in north-eastern Småland. Sven. Geogr. Årsb. 52, 71–91.
Aitken, M.J., 1998. An Introduction to Optical Dating. The Dating of Quaternary Sediments by the Use of Photon-stimulated Luminescence. Oxford University Press, Oxford, New York, Tokyo, pp. 1–267.
Alexanderson, H., 2007. Residual OSL signals from modern Greenlandic river sediments. Geochronometria 26, 1–9.
Alexanderson, H., Fabel, D., 2015. Holocene chronology of the Brattforsheden delta and inland dune field, SW Sweden. Geochronometria 42, 1–16.
Alexanderson, H., Henriksen, M., 2015. A short-lived aeolian event during the Early Holocene in southeastern Norway. Quat. Geochronol. (in press).
Alexanderson, H., Murray, A.S., 2012a. Luminescence signals from modern sediments in a glaciated bay, NW Svalbard. Quat. Geochronol. 10, 250–256.
Alexanderson, H., Murray, A.S., 2012b. Problems and potential of OSL dating Weichselian and Holocene sediments in Sweden. Quat. Sci. Rev. 44, 37–50.
Alm, T., 1993. Øvre Æråsvatn - palynostratigraphy of a 22,000 to 10,000 BP lacustrine record on Andøya, northern Norway. Boreas 22, 171–188.
Alstadsæter, I., 1982. The deglaciation and vegetational history of a former ice-damned lake area at Skåbu, Nord-Fron, southern Norway. Norges Geol. Unders. 373, 39–43.
Andersen, B.G., 1975. Glacial geology of northern Nordland, North Norway. Norges Geol. Unders. Bull. 320, 1–74.
Andersen, B.G., 1979. The deglaciation of Norway 15,000–10,000 B.P. Boreas 8, 79–87.
Andersen, B.G., 1980. The deglaciation of Norway after 10,000 B.P. Boreas 9, 211–216.
Andersen, B.G., 1981. Late Weichselian ice sheets in Eurasia and Greenland. In: Denton, G.H., Hughes, T.J. (Eds.), The Last Great Ice Sheets. John Wiley & Sons, New York, pp. 3–66.
Andersen, S., Pedersen, S.S., 1998. Israndlinjer i Norden. TemaNord 1998:584. Nordisk Ministerråd, Copenhagen, pp. 1–372.
Andersen, B.G., Bøen, F., Nydal, R., Rasmussen, A., Vallevik, P.N., 1981. Radiocarbon dates of marginal moraines in Nordland, North Norway. Geogr. Ann. 63, 155–160.
Andersen, B.G., Lundqvist, J., Saarnisto, M., 1995a. The Younger Dryas margin of the scandinavian ice sheet - an introduction. Quat. Int. 28, 145–146.
Andersen, B.G., Mangerud, J., Sørensen, R., Reite, A., Sveian, H., Thoresen, M., Bergström, B., 1995b. Younger Dryas ice-marginal deposits in Norway. Quat. Int. 28, 147–169.
Anderson, E.C., Libby, W.F., Weinhouse, S., Reid, A.F., Kirshenbaum, A.D., Grosse, A.V., 1947. Radiocarbon from cosmic radiation. Science 105, 576–577.
Andrén, T., 1990. Till Stratigraphy and Ice Recession in the Bothnian Bay. Department of Quaternary Research Report 18. University of Stockholm, pp. 1–59.
Andrén, T., Björck, J., Johnson, S., 1999. Correlation of Swedish glacial varves with the Greenland (GRIP) oxygen isotope record. J. Quat. Sci. 14, 361–371.
Andrén, T., Lindeberg, G., Andrén, E., 2002. Evidence of the final drainage of the Baltic Ice Lake and the brackish phase of the Yoldia Sea in glacial varves from the Baltic Sea. Boreas 31, 226–238.
Anjar, J., Larsen, N.K., Håkansson, L., Möller, P., Linge, H., Fabel, D., Xu, S., 2014. A ^{10}Be-based reconstruction of the last deglaciation in southern Sweden. Boreas 43, 132–148.
Antonsson, K., Brooks, S.J., Seppä, H., Telford, R.J., Birks, H.J.B., 2006. Quantitative palaeotemperature records inferred from fossil pollen and chironomid assemblages from Lake Gilltjärnen, northern central Sweden. J. Quat. Sci. 21, 831–841.
Applegate, P.J., Urban, N.M., Laabs, B.J.C., Keller, K., Alley, R.B., 2010. Modeling the statistical distributions of cosmogenic exposure dates from moraines. Geosci. Model Dev. 3, 293–307.
Applegate, P.J., Urban, N.M., Keller, K., Lowell, T.V., Laabs, B.J.C., Kelly, M.A., Alley, R.B., 2012. Improved moraine age interpretations through explicit matching of geomorphic process models to cosmogenic nuclide measurements from single landforms. Quat. Res. 77, 293–304.
Arnold, J.R., Libby, W.F., 1949. Age determinations by radiocarbon content: Checks with samples of known age. Science 110, 678–680.

Arppe, L., Karhu, J.A., 2010. Oxygen isotope values of precipitation and the thermal climate in Europe during the middle to late Weichselian ice age. Quat. Sci. Rev. 29, 1263–1275.
Balco, G., Schaefer, J.M., 2006. Cosmogenic-nuclide and varve chronologies for the deglaciation of southern New England. Quat. Geochronol. 1, 15–28.
Balco, G., Stone, J.O., Lifton, N.A., Dunai, T.J., 2008. A complete and easily accessible means of calculating surface exposure ages or erosion rates from ^{10}Be and ^{26}Al measurements. Quat. Geochronol. 3, 174–195.
Bang-Andersen, S., 2003. Southwest Norway at the Pleistocene/Holocene transition: landscape development, colonization, site types, settlement patterns. Nor. Archaeol. Rev. 36, 5–25.
Bard, E., Broecker, W.S., 1992. The Last Deglaciation: Absolute and Radiocarbon Chronologies. Global Environmental Change. Springer-Verlag, Berlin.
Bard, E., Hamelin, B., Fairbanks, R.G., Zindler, A., 1990. Calibration of the ^{14}C timescale over the past 30,000 years using mass spectrometric U-Th ages from Barbados corals. Nature 345, 405–410.
Bard, E., Raisbeck, G.M., Yiou, F., Jouzel, J., 1997. Solar modulation of cosmogenic nuclide production over the last millennium: comparison between ^{14}C and ^{10}Be records. Earth Planet. Sci. Lett. 150, 453–462.
Bargel, T., Huttunen, T., Johansson, P., Jokinen, S., Lagerbäck, R., Mäkinen, K., Nenonen, K., Olsen, L., Svedlund, J.-O., Väänänen, T., Wahlroos, J.-E., 1999. Maps of Quaternary Geology in Central Fennoscandia, Sheet 2: Glacial Geomorphology and Palaeohydrography, Scale 1:1 000 000. Geological Surveys of Finland (Espoo), Norway (Trondheim) and Sweden (Uppsala).
Barnekow, L., Possnert, G., Sandgren, P., 1998. AMS ^{14}C chronologies of Holocene lake sediments in the Abisko area, northern Sweden - a comparison between dated bulk sediment and macrofossil samples. GFF 120, 59–67.
Benediktsson, Í.Ö., Schomacker, A., Lokrantz, H., Ingólfsson, Ó., 2010. The 1890 surge end moraine at Eyjabakkajökull, Iceland: a re-assessment of a classic glaciotectonic locality. Quat. Sci. Rev. 29, 484–506.
Bennike, O., Jensen, J.B., 1995. Near-shore Baltic ice Lake deposits in Fakse Bugt, southeast Denmark. Boreas 24, 185–195.
Berglund, B.E., 1976. The Deglaciation of Southern Sweden. Presentation of a Research Project and a Tentative Radiocarbon Chronology. Department of Quaternary Geology Report 10. University of Lund, pp. 1–67.
Berglund, B.E., 1979. The deglaciation of southern Sweden 13,500-10,000 B.P. Boreas 8, 89–117.
Berglund, M., 1995. The Late Weichselian Deglaciation, Vegetational Development and Shore Displacement in Halland, Southwestern Sweden. Lund University. LUNDQUA Thesis 35.
Berglund, M., 2005. The Holocene shore displacement of Gästrikland, eastern Sweden: a contribution to the knowledge of Scandinavian glacio-isostatic uplift. J. Quat. Sci. 20, 519–531.
Berglund, B.E., Håkansson, S., Lagerlund, E., 1976. Radiocarbon-dated mammoth (*Mammuthus primigenius Blumenbach*) finds in South Sweden. Boreas 5, 177–191.
Bergman, J., Wastegård, S., Hammarlund, D., Wohlfarth, B., Roberts, S.J., 2004. Holocene tephra horizons at Klocka Bog, west-central Sweden: aspects of reproducibility in subarctic peat deposits. J. Quat. Sci. 19, 241–249.
Bergman, J., Hammarlund, D., Hannon, G.E., Barnekow, L., Wohlfarth, B., 2005. Deglacial vegetation succession and Holocene tree-limit dynamics in the Scandes Mountains, west-central Sweden: stratigraphic data compared to megafossil evidence. Rev. Palaeobot. Palynology 134, 129–151.
Bergström, R., 1968. Stratigrafi och isrecession i södra Västerbotten. Sveriges Geol. Unders. C634, 1–76.
Bergstrøm, B., 1975. Deglasiasjonsforløpet i Aurlandsdalen og områdene omkring, Vest-Norge. Norges Geol. Unders. 317, 33–68.
Bergstrøm, B., 1995. Stratigraphical evidence of a considerable Younger Dryas glacier advance in southeastern Norway. Nor. Geol. Tidsskr. 75, 127–136.
Bergstrøm, B., Olsen, L., Sveian, H., 2005. The Tromsø-Lyngen glacier readvance (early Younger Dryas) at Hinnøya-Ofotfjorden, northern Norway: a reassessment. Norges Geol. Unders. Bull. 445, 73–88.
Bitinas, A., Damušytė, A., Stančikaitė, M., Aleksa, P., 2002. Geological development of the Nemunas River Delta and adjacent areas, West Lithuania. Geol. Q. 46, 375–389.
Bjarnadóttir, L.R., Winsborrow, M.C.M., Andreassen, K., 2014. Deglaciation of the central Barents Sea. Quat. Sci. Rev. 92, 208–226.
Björck, S., 2008. The late Quaternary development of the Baltic Sea. In: BACC Author Team (Ed.), Assessment of Climate Change for the Baltic Sea Basin. Springer-Verlag Berlin Heidelberg, pp. 398–407.
Björck, S., Digerfeldt, G., 1982a. Late Weichselian shore displacement at Hunneberg, southern Sweden, indicating complex uplift. Geol. Fören. Stockh. Förh. 104, 131–155.
Björck, S., Digerfeldt, G., 1982b. New ^{14}C dates from Hunneberg supporting the revised deglaciation chronology of the Middle Swedish end moraine zone. Geol. Fören. Stockh. Förh. 103, 395–404.
Björck, S., Digerfeldt, G., 1986. Late Weichselian-early Holocene shore displacement west of Mt. Billingen, within the middle Swedish end moraine zone. Boreas 15, 1–18.
Björck, S., Digerfeldt, G., 1991. Allerød- Younger Dryas sea level changes in southwestern Sweden and their relation to the Baltic Ice Lake development. Boreas 20, 115–133.
Björck, S., Möller, P., 1987. Late Weichselian environmental history in southeastern Sweden during the deglaciation of the Scandinavian Ice Sheet. Quat. Res. 28, 1–37.
Björck, S., Kromer, B., Johnsen, S., Bennike, O., Hammarlund, D., Lemdahl, G., Possnert, G., Rasmussen, T.L., Wohlfarth, B., Hammer, C.U., Spurk, M., 1996. Synchronized terrestrial-atmospheric deglacial records around the North Atlantic. Science 274, 1155–1160.
Björck, S., Rundgren, M., Ingólfsson, O., Funder, S., 1997. The Preboreal oscillation around the Nordic Seas: terrestrial and lacustrine responses. J. Quat. Sci. 12, 455–465.
Björck, J., Possnert, G., Schoning, K., 2001. Early Holocene deglaciation chronology in Västergötland and Närke, southern Sweden — biostratigraphy, clay varve, ^{14}C and calendar year chronology. Quat. Sci. Rev. 20, 1309–1326.
Blake, K.P., Olsen, L., 1999. Deglaciation of the Svartisen area, northern Norway, and isolation of a large ice mass in front of the Fennoscandian Ice Sheet. Nor. Geogr. Tidsskr. 53, 1–16.
Bodén, P., Fairbanks, R.G., Wright, J.D., Burckle, L.H., 1997. High-resolution isotope records from southwest Sweden: the drainage of the Baltic Ice Lake and Younger Dryas ice margin oscillations. Paleoceanography 12, 39–49.
Borell, R., Offerberg, J., 1955. Geokronologiska undersökningar inom Indalsälvens dalgång mellan Bergeforsen och Ragunda. Sveriges Geol. Unders. Ca 31, 1–24.
Borgström, I., 1989. Meddelanden från Naturgeografiska institutionen vid Stockholms universitet. Terrrängformerna och den glaciala utvecklingen i södra fjällen: Geomorphology and Glacial History of the Middle Swedish Mountains, vol. A234. Department of Physical Geography. Stockholm University, Stockholm, pp. 1–133.
Boulton, G.S., Clark, C.D., 1990a. A highly mobile Laurentide ice sheet revealed by satellite images of glacial lineations. Nature 346, 813–817.
Boulton, G.S., Clark, C.D., 1990b. The Laurentide ice-sheet through the last glacial cycle: the topology of drift lineations as a key to the dynamic behaviour of former ice-sheets. Trans. R. Soc. Edinb. Earth Sci. 81, 327–347.
Boulton, G., Hagdorn, M., 2006. Glaciology of the British Isles Ice Sheet during the last glacial cycle: form, flow, streams and lobes. Quat. Sci. Rev. 25, 3359–3390.
Boulton, G.S., Smith, G.D., Jones, A.S., Newsome, J., 1985. Glacial geology and glaciology of the last mid-latitude ice sheets. J. Geol. Soc. Lond. 142, 447–474.
Boulton, G.S., Hulton, N., Vautravers, M., 1995. Ice-sheet models as tools for palaeoclimatic analysis: the example of the European ice sheet through the last glacial cycle. Ann. Glaciol. 21, 103–110.
Boulton, G.S., Dongelmans, P., Punkari, M., Broadgate, M., 2001. Palaeoglaciology of an ice sheet through a glacial cycle: the European ice sheet through the Weichselian. Quat. Sci. Rev. 20, 591–625.
Briner, J.P., Bini, A.C., Anderson, R.S., 2009. Rapid early Holocene retreat of a Laurentide outlet glacier through an Arctic fjord. Nat. Geosci. 2, 496–499.
Briner, J.P., Svendsen, J.I., Mangerud, J., Lohne, Ø.S., Young, N.E., 2014. A ^{10}Be chronology of south-western Scandinavian Ice Sheet history during the Lateglacial period. J. Quat. Sci. 29, 370–380.
Bronk Ramsey, C., 2009. Bayesian analysis of radiocarbon dates. Radiocarbon 51, 337–360.
Brook, E.J., Nesje, A., Lehman, S.J., Raisbeck, G.M., Yiou, F., 1996. Cosmogenic nuclide exposure ages along a vertical transect in western Norway: Implications for the height of the Fennoscandian ice sheet. Geology 24, 207–210.
Brunnberg, L., 1995. Clay-varve Chronology and Deglaciation during the Younger Dryas and Preboreal in the Easternmost Part of the Middle Swedish Ice Marginal Zone. Department of Quaternary Research, Quaternaria A2. Stockholm University, Stockholm, pp. 1–94.
Budd, W.F., Smith, I.N., 1982. Large-scale numerical modelling of the Antarctic Ice Sheet. Ann. Glaciol. 3, 42–49.
Caldenius, C., 1942. Gotiglaciala israndsstadier och jökelbäddar i Halland. Förelöpande meddelande. Geol. Fören. Stockh. Förh. 64, 163–183.
Cato, I., 1987. On the definitive connection of the Swedish Time Scale with the present. Sveriges Geol. Unders. Ca 68, 1–55.
Church, J.A., Clark, P.U., Cazenave, A., Gregory, J.M., Jevrejeva, S., Levermann, A., Merrifield, M.A., Milne, G.A., Nerem, R.S., Nunn, P.D., Payne, A.J., Pfeffer, W.T., Stammer, D., Unnikrishnan, A.S., 2013. Sea level change. Contribution of Working Group I to the Fifth Assessment Report of the Intergovernmental Panel on Climate Change. In: Stocker, T.F., Qin, D., Plattner, G.-K., Tignor, M., Allen, S.K., Boschung, J., Nauels, A., Xia, Y., Bex, V., Midgley, P.M. (Eds.), Climate Change 2013: the Physical Science Basis. Cambridge University Press, Cambridge, United Kingdom and New York, NY, USA.
Clarhäll, A., Kleman, J., 1999. Distribution and glaciological implications of relict surfaces on the Ultevis plateau, northwestern Sweden. Ann. Glaciol. 28, 202–208.
Clark, C.D., 1993. Mega-scale glacial lineations and cross-cutting ice-flow landforms. Earth Surf. Process. Landforms 18, 1–29.
Clark, C.D., Hughes, A.L.C., Greenwood, S.L., Spagnolo, M., Ng, F.S.L., 2009a. Size and shape characteristics of drumlins, derived from a large sample, and associated scaling laws. Quat. Sci. Rev. 28, 677–692.
Clark, P.U., Dyke, A.S., Shakun, J.D., Carlson, A.E., Clark, J., Wohlfarth, B., Mitrovica, J.X., Hostetler, S.W., McCabe, A.M., 2009b. The last glacial maximum. Science 325, 710–714.
Clark, C.D., Hughes, A.L.C., Greenwood, S.L., Jordan, C., Sejrup, H.P., 2012. Pattern and timing of retreat of the last British-Irish Ice Sheet. Quat. Sci. Rev. 44, 112–146.
Clason, C.C., Applegate, P.J., Holmlund, P., 2014. Modelling Late Weichselian evolution of the Eurasian ice sheets forced by surface meltwater-enhanced basal sliding. J. Glaciol. 60, 29–40.
Clayton, L., Moran, S.R., 1982. Chronology of late Wisconsinan glaciation in middle North America. Quat. Sci. Rev. 1, 55–82.
Conway, H., Hall, B.L., Denton, G.H., Gades, A.M., Waddington, E.D., 1999. Past and

future grounding-line retreat of the West Antarctic Ice Sheet. Science 286, 280–283.
Corner, G.D., 1980. Preboreal deglaciation chronology and marine limits of the Lyngen-Storfjord area, Troms, North Norway. Boreas 9, 239–249.
Corner, G.D., Kolka, V.V., Yevzerov, V.Y., Møller, J.J., 2001. Postglacial relative sea-level change and stratigraphy of raised coastal basins on Kola Peninsula, northwest Russia. Glob. Planet. Change 31, 155–177.
Darmody, R.G., Thorn, C.E., Seppälä, M., Campbell, S.W., Li, Y.K., Harbor, J., 2008. Age and weathering status of granite tors in Arctic Finland (~ 68° N.). Geomorphology 94, 10–23.
Davis, J.L., Mitrovica, J.X., Scherneck, H.-G., Fan, H., 1999. Investigations of Fennoscandian glacial isostatic adjustment using modern sea level records. J. Geophys. Res. B 104, 2733–2747.
De Geer, G., 1884. Om möjligheten af att införa en kronologi för Istiden. Geol. Fören. Stockh. Förh. 7, 3.
De Geer, G., 1896. Skandinaviens geografiska utveckling efter istiden. Sveriges Geol. Unders. Ser. C. 161, 1–160.
De Geer, G., 1897. Om rullstensåsarnas bildningssätt. Geol. Fören. Stockh. Förh. 19, 366–388.
De Geer, G., 1912. A geochronology of the last 12 000 years. In: Proceedings of the 11th International Geological Congress 1910, Stockholm, pp. 243–253.
De Geer, G., 1935. The transbaltic extension of the Swedish Time Scale. Geogr. Ann. 17, 533–549.
De Geer, G., 1940. Geochronologia Sueccia principles. K. Sven. Vetensk. Handl. III 18 (6), 1–367.
Dellgar Hagström, M., 2006. The Kiruna Swarm in Northern Fennoscandia : a Landform Analysis of an Ice Flow Bed. Bachelors Thesis in Physical Geography, N-62. Department of Physical Geography and Quaternary Geology, Stockholm University, Stockholm, pp. 1–20.
Demidov, I.N., Houmark-Nielsen, M., Kjaer, K.H., Larsen, E., 2006. The last Scandinavian Ice Sheet in northwestern Russia: ice flow patterns and decay dynamics. Boreas 35, 425–443.
Denton, G.H., Hughes, T.J., 1981. The Last Great Ice Sheets, vol. 1–484. Wiley-Interscience, New York, pp. 1–484.
Denton, G.H., Hughes, T.J., 2002. Reconstructing the antarctic ice sheet at the last glacial maximum. Quat. Sci. Rev. 21, 193–202.
Digerfeldt, G., 1979. The highest shore-line on Hunneberg, southern Sweden. Geol. Fören. Stockh. Förh. 101, 49–64.
Donner, J.J., 1978. The Dating of the Levels of the Baltic Ice Lake and the Salpausselkä Moraines in South Finland. Societas Scientiarum Fennica. In: Commentationes Physico-mathematicae, vol. 48, pp. 11–38.
Donner, J., 2010. The Younger Dryas age of the Salpausselkä moraines in Finland. Bull. Geol. Soc. Finl. 82, 69–80.
Donner, J.J., Alhonen, P., Eronen, M., Jungner, H., Vuorela, I., 1978. Biostratigraphy and radiocarbon dating of the Holocene lake sediments of Työtjärvi and the peats in the adjoining bog Varrassuo west of Lahti in southern Finland. Ann. Bot. Fenn. 15, 258–280.
Dowling, T.P.F., Alexanderson, H., Moller, P., 2013. The new high-resolution LiDAR digital height model ('Ny Nationell Höjdmodell') and its application to Swedish Quaternary geomorphology. GFF 135, 145–151.
Dreimanis, A., Zelčs, V., 1995. Pleistocene stratigraphy of Latvia. In: Ehlers, J., Kozarski, S., Gibbard, P.L. (Eds.), Glacial Deposits in North-East Europe. Balkema, pp. 105–113.
Duphorn, K., Kögler, F.-C., Stay, B., 1979. Late-glacial varved clays in the Bornholm Basin and Hanö Bay. Boreas 8, 137–140.
Dyke, A.S., 1993. Landscapes of cold-centered late Wisconsinan ice caps, Arctic Canada. Prog. Phys. Geogr. 17, 223–247.
Dyke, A.S., 2004. An outline of North American deglaciation with emphasis on central and northern Canada. In: Ehlers, J., Gibbard, P.L. (Eds.), Quaternary Glaciations- Extent and Chronology, Part II. Elsevier, pp. 373–424.
Dyke, A.S., Moore, A., Robertson, L., 2003. Deglaciation of North America. Geological Survey of Canada. Open File 1574 (CD ROM).
Ehlers, J., Gibbard, P.L., 2004. Quaternary Glaciations: Extent and Chronology, Part I: Europe. Elsevier, Amsterdam.
Eilertsen, R., Corner, G.D., Aasheim, O., 2005. Deglaciation chronology and glaciomarine successions in the Malangen-Målselv area, northern Norway. Boreas 34, 233–251.
Ek, L.-G., 2004. The Establishment of Norway Spruce (*Picea Abies (L.) Karst.*) on Two Mountains in the Åre Area – a Follow-up of the Macrofossil Finds on Mount Åreskutan. Swedish University of Agricultural Sciences. Student thesis.
Elfström, Å., 1987. Large boulder deposits and catastrophic floods: a case study of the Båldakatj area, Swedish Lapland. Geogr. Annaler. Series A Phys. Geogr. 69, 101–121.
Erdmann, A., 1868. Sveriges qvartära bildningar. Sveriges Geol. Unders. Ser. C. 1, 1–297.
Eronen, M., 1976. A radiocarbon-dated Ancylus transgression site in south-eastern Finland. Boreas 5, 65–76.
Evans, D.J.A., Rea, B.R., 1999. Geomorphology and sedimentology of surging glaciers: a land-systems approach. Ann. Glaciol. 28, 75–82.
Fabel, D., Stroeven, A.P., Harbor, J., Kleman, J., Elmore, D., Fink, D., 2002. Landscape preservation under Fennoscandian ice sheets determined from in situ produced ^{10}Be and ^{26}Al. Earth Planet. Sci. Lett. 201, 397–406.
Fabel, D., Harbor, J., Dahms, D., James, A., Elmore, D., Horn, L., Daley, K., Steele, C., 2004. Spatial patterns of glacial erosion at a valley scale derived from terrestrial cosmogenic Be-10 and Al-26 concentrations in rock. Ann. Assoc. Am. Geogr. 94, 241–255.
Fabel, D., Fink, D., Fredin, O., Harbor, J., Land, M., Stroeven, A.P., 2006. Exposure ages from relict lateral moraines overridden by the Fennoscandian ice sheet. Quat. Res. 65, 136–146.
Fairchild, H.L., 1907. Drumlins of central New York. N. Y. State Mus. Bull. 111, 391–443.
Favier, L., Durand, G., Cornford, S.L., Gudmundsson, G.H., Gagliardini, O., Gillet-Chaulet, F., Zwinger, T., Payne, A.J., Le Brocq, A.M., 2014. Retreat of Pine Island Glacier controlled by marine ice-sheet instability. Nat. Clim. Change 4, 117–121.
Fernlund, J.M.R., 1993. The long-singular ridges of the Halland Coastal Moraines, south-western Sweden. J. Quat. Sci. 8, 67–78.
Fjellanger, J., Sørbel, L., Linge, H., Brook, E.J., Raisbeck, G.M., Yiou, F., 2006. Glacial survival of blockfields on the Varanger Peninsula, northern Norway. Geomorphology 82, 255–272.
Fözö, I., 1980. Ådalen. Den geologiska utvecklingen vid slutet av istiden. Länsstyrelsen, Västernorrlands län, pp. 1–64.
Fredin, O., Rubensdotter, L., van Welden, A., Larsen, E., Lyså, A., 2012. Distribution of ice marginal moraines in NW Russia. J. Maps 8, 236–241.
Frödin, G., 1913. Bidrag till västra Jämtlands senglaciala geologi. Sveriges Geol. Unders. C 246, 1–236.
Fuchs, M., Owen, L.A., 2008. Luminescence dating of glacial and associated sediments: review, recommendations and future directions. Boreas 37, 636–659.
Garnes, K., Bergersen, O.F., 1980. Wastage features of the inland ice sheet in central South Norway. Boreas 9, 251–269.
Goehring, B.M., Brook, E.J., Linge, H., Raisbeck, G.M., Yiou, F., 2008. Beryllium-10 exposure ages of erratic boulders in southern Norway and implications for the history of the Fennoscandian Ice Sheet. Quat. Sci. Rev. 27, 320–336.
Goehring, B.M., Lohne, Ø.S., Mangerud, J., Svendsen, J.I., Gyllencreutz, R., Schaefer, J., Finkel, R., 2012. Late glacial and Holocene ^{10}Be production rates for western Norway. J. Quat. Sci. 27, 89–96.
Goodfellow, B.W., Stroeven, A.P., Hättestrand, C., Kleman, J., Jansson, K.N., 2008. Deciphering a non-glacial/glacial landscape mosaic in the northern Swedish mountains. Geomorphology 93, 213–232.
Goodfellow, B.W., Stroeven, A.P., Fabel, D., Fredin, O., Derron, M.-H., Bintanja, R., Caffee, M.W., 2014. Arctic–alpine blockfields in the northern Swedish Scandes: late Quaternary – not Neogene. Earth Surf. Dyn. 2, 383–401.
Gosse, J.C., Phillips, F.M., 2001. Terrestrial in situ cosmogenic nuclides: theory and application. Quat. Sci. Rev. 20, 1475–1560.
Göttlich, K., Hornburg, P., König, D., Schwaar, J., Vorren, K.-D., 1983. Untersuchungen an einem Palsen mit Kieselgurschichten bei Kautokeino, Nord-Norwegen. Nor. J. Geogr. 37, 1–31.
Greenwood, S.L., Clark, C.D., Hughes, A.L.C., 2007. Formalising an inversion methodology for reconstructing ice-sheet retreat patterns from meltwater channels: application to the British Ice Sheet. J. Quat. Sci. 22, 637–645.
Greenwood, S.L., Clason, C.C., Mikko, H., Nyberg, J., Peterson, G., Smith, C.A., 2015. Integrated use of LiDAR and multibeam bathymetry reveals onset of ice streaming in the northern Bothnian Sea. GFF. http://dx.doi.org/10.1080/11035897.2015.1055513 (in press).
Gyllencreutz, R., Mangerud, J., Svendsen, J.I., Lohne, Ø., 2007. DATED – a GIS-based Reconstruction and Dating Database of the Eurasian Deglaciation. Special Paper 46. Geological Survey of Finland, pp. 113–120.
Hajdas, I., 2008. Radiocarbon dating and its applications in Quaternary studies. Eiszeitalt. Ggw. 57, 2–24.
Håkansson, S., 1970. University of Lund radiocarbon dates III. Radiocarbon 12, 534–552.
Håkansson, S., 1975. University of Lund radiocarbon dates VIII. Radiocarbon 17, 174–195.
Håkansson, S., 1978. University of Lund radiocarbon dates XI. Radiocarbon 20, 416–435.
Håkansson, S., 1982. University of Lund radiocarbon dates XV. Radiocarbon 24, 194–213.
Håkansson, S., 1987. University of Lund radiocarbon dates XX. Radiocarbon 29, 353–379.
Hammarlund, D., Velle, G., Wolfe, B.B., Edwards, T.W.D., Barnekow, L., Bergman, J., Holmgren, S., Lamme, S., Snowball, I., Wohlfarth, B., Possnert, G., 2004. Palaeolimnological and sedimentary responses to Holocene forest retreat in the Scandes Mountains, west-central Sweden. Holocene 14, 862–876.
Hang, T., 1997. Clay varve chronology in the Eastern Baltic area. GFF 119, 295–300.
Harbor, J., Stroeven, A.P., Fabel, D., Clarhäll, A., Kleman, J., Li, Y.K., Elmore, D., Fink, D., 2006. Cosmogenic nuclide evidence for minimal erosion across two subglacial sliding boundaries of the late glacial Fennoscandian ice sheet. Geomorphology 75, 90–99.
Hättestrand, C., 1998. The glacial geomorphology of central and northern Sweden. Sveriges Geol. Unders. Ca 85, 1–47.
Hättestrand, C., Clark, C.D., 2006a. The glacial geomorphology of Kola Peninsula and adjacent areas in Murmansk Region, Russia. J. Maps 30–42.
Hättestrand, C., Clark, C.D., 2006b. Reconstructing the pattern and style of deglaciation of Kola Peninsula, NE Fennoscandian Ice Sheet. In: Knight, P.G. (Ed.), Glaciology and Earth's Changing Environment. Blackwell Publishing Ltd, Oxford, pp. 199–201.
Hättestrand, C., Stroeven, A.P., 2002. A relict landscape in the centre of Fennoscandian glaciation: geomorphological evidence of minimal Quaternary glacial erosion. Geomorphology 44, 127–143.
Hättestrand, C., Goodwillie, D., Kleman, J., 1999. Size distribution of two cross-cutting drumlin systems in northern Sweden: a measure of selective erosion

and formation time length. Ann. Glaciol. 28, 146–152.
Hättestrand, C., Kosche, S., Näslund, J.-O., Fabel, D., Stroeven, A.P., 2004. Drumlin formation time - evidence from northern and central Sweden. Geogr. Ann. 86A, 155–167.
Hättestrand, C., Kolka, V., Stroeven, A.P., 2007. The Keiva ice marginal zone on the Kola Peninsula, northwest Russia: a key component for reconstructing the palaeoglaciology of the northeastern Fennoscandian Ice Sheet. Boreas 36, 352–370.
Hebrand, M., Åmark, M., 1989. Esker formation and glacier dynamics in eastern Skåne and adjacent areas, southern Sweden. Boreas 18, 67–81.
Heikkilä, M., Seppä, H., 2003. A 11,000 yr palaeotemperature reconstruction from the southern boreal zone in Finland. Quat. Sci. Rev. 22, 541–554.
Hein, A.S., Hulton, N.R.J., Dunai, T.J., Sugden, D.E., Kaplan, M.R., Xu, S., 2010. The chronology of the Last Glacial Maximum and deglacial events in central Argentine Patagonia. Quat. Sci. Rev. 29, 1212–1227.
Heine, K., Reuther, A.U., Thieke, H.U., Schulz, R., Schlaak, N., Kubik, P.W., 2009. Timing of Weichselian ice marginal positions in Brandenburg (northeastern Germany) using cosmogenic in situ ^{10}Be. Z. Geomorphol. N. F. 53, 433–454.
Heinsalu, A., Veski, S., 2007. The history of the Yoldia Sea in Northern Estonia: palaeoenvironmental conditions and climatic oscillations. Geol. Q. 51, 295–306.
Helmens, K.F., Räsänen, M.E., Johansson, P.W., Jungner, H., Korjonen, K., 2000. The last interglacial-glacial cycle in NE fennoscandia: a nearly continuous record from Sokli (Finnish Lapland). Quat. Sci. Rev. 19, 1605–1623.
Heyman, J., 2014. Paleoglaciation of the Tibetan Plateau and surrounding mountains based on exposure ages and ELA depression estimates. Quat. Sci. Rev. 91, 30–41.
Heyman, J., Stroeven, A.P., Harbor, J.M., Caffee, M.W., 2011. Too young or too old: evaluating cosmogenic exposure dating based on an analysis of compiled boulder exposure ages. Earth Planet. Sci. Lett. 302, 71–80.
Hilldén, A., 1979. Deglaciationen i trakten av Berghemsmoränen öster om Göteborg. Lund University, pp. 1–130 (PhD thesis).
Hillefors, Å., 1969. Västsveriges glaciala historia och morfologi, Meddelanden från Lunds Universitets Geografiska Institution. Avhandling 60, 1–319.
Hillefors, Å., 1975. Contribution to the knowledge of the deglaciation of western Sweden with special reference to the Gothenburg Moraine. Sven. Geogr. Årsb. 51, 70–81.
Hillefors, Å., 1979. Deglaciation models from the Swedish west coast. Boreas 8, 153–169.
Holmlund, P., Fastook, J., 1995. A time dependent glaciological model of the Weichselian Ice Sheet. Quat. Int. 27, 53–58.
Hoppe, G., 1948. Isrecessionen från Norrbottens kustland i belysning av de glaciala formelementen. Geographica 20, 1–112.
Hoppe, G., 1959. Glacial morphology and inland ice recession in northern Sweden. Geogr. Ann. 41, 193–212.
Hörnsten, Å., 1964. Ångermanlands kustland under isavsmältningsskedet. Preliminärt meddelande. Geol. Fören. Stockh. Förh. 86, 181–205.
Houmark-Nielsen, M., 2003. Signature and timing of the Kattegat Ice Stream: onset of the Last Glacial Maximum sequence at the southwestern margin of the Scandinavian Ice Sheet. Boreas 32, 227–241.
Houmark-Nielsen, M., Kjær, K.H., 2003. Southwest Scandinavia, 40–15 kyr BP: palaeogeography and environmental change. J. Quat. Sci. 18, 769–786.
Houmark-Nielsen, M., Linge, H., Fabel, D., Schnabel, C., Xu, S., Wilcken, K.M., Binnie, S., 2012. Cosmogenic surface exposure dating the last deglaciation in Denmark: Discrepancies with independent age constraints suggest delayed periglacial landform stabilisation. Quat. Geochronol. 13, 1–17.
Hubbard, A., 1999. High resolution modelling of the Advance of the Younger Dryas ice sheet and its climate in Scotland. Quat. Res. 52, 27–43.
Hughes, T., 1975. The West Antarctic Ice Sheet: Instability, disintegration, and initiation of ice ages. Rev. Geophys. Space Phys. 13, 502–526.
Hughes, A.L.C., Greenwood, S.L., Clark, C.D., 2011. Dating constraints on the last British-Irish Ice Sheet: a map and database. J. Maps 156–183.
Huntley, D.J., Godfrey-Smith, D.I., Thewalt, M.L.W., 1985. Optical dating of sediments. Nature 313, 105–107.
Huybrechts, P., 1993. Glaciological modeling of the late Cenozoic east antarctic ice sheet: Stability or dynamism? Geogr. Ann. 75A, 221–238.
Ivy-Ochs, S., Kerschner, H., Reuther, A., Maisch, M., Sailer, R., Schaefer, J., Kubik, P.W., Synal, H.-A., Schlüchter, C., 2006. The Timing of Glacier Advances in the Northern European Alps Based on Surface Exposure Dating with Cosmogenic ^{10}Be, ^{26}Al, ^{36}Cl, and ^{21}Ne. Special Papers 415. Geological Society of America, pp. 43–60.
Jackson Jr., L.E., Clague, J.J., 1991. The Cordilleran Ice Sheet - 150 years of exploration and discovery. Geogr. Phys. Quat. 45, 269–280.
Jakobsson, M., Björck, S., Alm, G., Andrén, T., Lindeberg, G., Svensson, N.-O., 2007. Reconstructing the Younger Dryas ice dammed lake in the Baltic Basin: bathymetry, area and volume. Glob. Planet. Change 57, 355–370.
Jansen, J.D., Codilean, A.T., Stroeven, A.P., Fabel, D., Hättestrand, C., Kleman, J., Harbor, J.M., Heyman, J., Kubik, P.W., Xu, S., 2014. Inner gorges cut by subglacial meltwater during Fennoscandian ice sheet decay. Nat. Commun. 5, 3815. http://dx.doi.org/10.1038/ncomms4815.
Jansson, K.N., 2003. Early Holocene glacial lakes and ice marginal retreat pattern in Labrador/Ungava, Canada. Palaeogeogr. Palaeoclimatol. Palaeoecol. 193, 473–501.
Jansson, K.N., Kleman, J., Marchant, D.R., 2002. The succession of ice-flow patterns in north-central Quebec-Labrador, Canada. Quat. Sci. Rev. 21, 503–523.
Jensen, C., Kuiper, J.G.J., Vorren, K.-D., 2002. First post-glacial establishment of forest trees: early Holocene vegetation, mollusc settlement and climate dynamics in central Troms, North Norway. Boreas 31, 285–301.
Johansson, S., 1926. Baltiska issjöns tappning. Geol. Fören. Stockh. Förh. 48, 186–263.
Johansson, P., Kujansuu, R., 1995. Observations on Three Subglacial Drainage Systems (Eskers) of Different Ages in Savukoski, Eastern Finnish Lapland. Special Paper 20. Geological Survey of Finland, pp. 83–93.
Johnsen, T.F., Alexanderson, H., Fabel, D., Freeman, S.P.H.T., 2009. New ^{10}Be cosmogenic ages from the Vimmerby Moraine confirm the timing of Scandinavian ice sheet deglaciation in southern Sweden. Geogr. Ann. 91A, 113–120.
Johnsen, T.F., Fabel, D., Stroeven, A.P., 2010. High-elevation cosmogenic nuclide dating of the last deglaciation in the central Swedish mountains: implications for the timing of tree establishment. In: Johnsen, T.F. (Ed.), Late Quaternary Ice Sheet History and Dynamics in Central and Southern Scandinavia. Stockholm University. PhD thesis.
Johnsen, T.F., Olsen, L., Murray, A., 2012. OSL ages in central Norway support a MIS 2 interstadial (25–20 ka) and a dynamic Scandinavian ice sheet. Quat. Sci. Rev. 44, 96–111.
Johnson, M.D., Ståhl, Y., 2010. Stratigraphy, sedimentology, age and palaeoenvironment of marine varved clay in the Middle Swedish end-moraine zone. Boreas 39, 199–214.
Joughin, I., Smith, B.E., Medley, B., 2014. Marine ice sheet collapse potentially under way for the Thwaites Glacier Basin, West Antarctica. Science 344, 735–738.
Kalm, V., 2012. Ice-flow pattern and extent of the last Scandinavian Ice Sheet southeast of the Baltic Sea. Quat. Sci. Rev. 44, 51–59.
Kalm, V., Gorlach, G., 2014. Impact of bedrock surface topography on spatial distribution of Quaternary sediments and on the flow pattern of late Weichselian glaciers on the East European Craton (Russian Plain). Geomorphology 207, 1–9.
Kjær, K.H., Demidov, I.N., Larsen, E., Murray, A., Nielsen, J.K., 2003a. Mezen Bay—a key area for understanding Weichselian glaciations in northern Russia. J. Quat. Sci. 18, 73–93.
Kjær, K.H., Houmark-Nielsen, M., Richardt, N., 2003b. Ice-flow patterns and dispersal of erratics at the southwestern margin of the last Scandinavian Ice Sheet: Signature of palaeo- ice streams. Boreas 32, 130–148.
Kleman, J., 1990. On the use of glacial striae for reconstruction of paleo-ice sheet flow patterns. Geogr. Ann. 72A, 217–236.
Kleman, J., 1992. The palimpsest glacial landscape in northwestern Sweden - late Weichselian deglaciation landforms and traces of older west-centered ice sheets. Geogr. Ann. 74A, 305–325.
Kleman, J., 1994. Preservation of landforms under ice sheets and ice caps. Geomorphology 9, 19–32.
Kleman, J., Applegate, P.J., 2014. Durations and propagation patterns of ice sheet instability events. Quat. Sci. Rev. 92, 32–39.
Kleman, J., Glasser, N.F., 2007. The subglacial thermal organisation (STO) of ice sheets. Quat. Sci. Rev. 26, 585–597.
Kleman, J., Hättestrand, C., 1999. Frozen-bed Fennoscandian and Laurentide ice sheets during the Last Glacial Maximum. Nature 402, 63–66.
Kleman, J., Stroeven, A.P., 1997. Preglacial surface remnants and Quaternary glacial regimes in northwestern Sweden. Geomorphology 19, 35–54.
Kleman, J., Hättestrand, C., Borgström, I., Stroeven, A., 1997. Fennoscandian paleoglaciology reconstructed using a glacial geological inversion model. J. Glaciol. 43, 283–299.
Kleman, J., Fastook, J., Stroeven, A.P., 2002. Geologically and geomorphologically constrained numerical model of Laurentide Ice Sheet inception and build-up. Quat. Int. 95–96, 87–98.
Kleman, J., Hättestrand, C., Stroeven, A.P., Jansson, K.N., De Angelis, H., Borgström, I., 2006. Reconstruction of palaeo-ice sheets-inversion of their glacial geomorphological record. In: Knight, P.G. (Ed.), Glacier Science and Environmental Change. Blackwell Publishing, Malden, MA, USA, pp. 192–198.
Kleman, J., Stroeven, A.P., Lundqvist, J., 2008. Patterns of Quaternary ice sheet erosion and deposition in Fennoscandia and a theoretical framework for explanation. Geomorphology 97, 73–90.
Kleman, J., Jansson, K., De Angelis, H., Stroeven, A.P., Hättestrand, C., Alm, G., Glasser, N., 2010. North American Ice Sheet build-up during the last glacial cycle, 115-21 kyr. Quat. Sci. Rev. 29, 2036–2051.
Klovning, I., Hafsten, U., 1965. An Early Post-glacial pollen profile from Flåmsdalen, a tributary valley to the Sognefjord, western Norway. Nor. Geol. Tidsskr. 45, 333–338.
Kopp, R.E., Mitrovica, J.X., Griffies, S.M., Yin, J.J., Hay, C.C., Stouffer, R.J., 2010. The impact of Greenland melt on local sea levels: a partially coupled analysis of dynamic and static equilibrium effects in idealized water-hosing experiments. Clim. Change 103, 619–625.
Korsager, B., Bennike, O., Houmark-Nielsen, M., 2003. *Salix polaris* leaves dated at 14.3 ka BP from northern Jylland, Denmark. Bull. Geol. Soc. Den. 50, 151–155.
Kortekaas, M., Murray, A.S., 2007. Using luminescence to determine palaeoenvironmental change in the Bornholm basin; some preliminary data. In: Kortekaas, M. (Ed.), Post-Glacial History of Sea-level and Environmental Change in the Southern Baltic Sea. Lund University. PhD thesis.
Kortekaas, M., Murray, A.S., Sandgren, P., Björck, S., 2007. OSL chronology for a sediment core from the southern Baltic Sea: a continuous sedimentation record since deglaciation. Quat. Geochronol. 2, 95–101.
Kramarska, R., 1998. Origin and development of the Odra Bank in the light of the geologic structure and radiocarbon dating. Geol. Quaterly 42, 277–288.
Kristiansson, J., 1986. The Ice Recession in the South-eastern Part of Sweden: a Varve-chronological Time Scale for the Latest Part of the Late Weichselian. Department of Quaternary Research, Report 16. Stockholm University,

Stockholm, pp. 1–132.
Krog, H., Tauber, H., 1974. C-14 chronology of late- and post-glacial marine deposits in north Jutland. Danmarks Geol. Unders. Årb. 1973, 93–105.
Lagerbäck, R., 1988. The Veiki moraines in northern Sweden - widespread evidence of an early Weichselian deglaciation. Boreas 17, 469–486.
Lagerbäck, R., Robertsson, A.-M., 1988. Kettle holes - stratigraphical archives for Weichselian geology and palaeoenvironment in northernmost Sweden. Boreas 17, 439–468.
Lagerlund, E., Houmark-Nielsen, M., 1993. Timing and pattern of the last deglaciation in the Kattegat region, southwest Scandinavia. Boreas 22, 337–347.
Lambeck, K., 1999. Shoreline displacements in southern-central Sweden and the evolution of the Baltic Sea since the last maximum glaciation. J. Geol. Soc. Lond. 156, 465–486.
Lambeck, K., Smither, C., Johnston, P., 1998. Sea-level change, glacial rebound and mantle viscosity for northern Europe. Geophys. J. Int. 102–144.
Larsen, E., Lysa, A., Demidov, I., Funder, S., Houmark-Nielsen, M., Kjaer, K.H., Murray, A.S., 1999. Age and extent of the Scandinavian ice sheet in northwest Russia. Boreas 28, 115–132.
Larsen, E., Kjær, K.H., Demidov, I.N., Funder, S., Grøsfjeld, K., Houmark-Nielsen, M., Jensen, M., Linge, H., Lyså, A., 2006. Late Pleistocene glacial and lake history of northwestern Russia. Boreas 35, 394–424.
Larsen, N.K., Linge, H., Håkansson, L., Fabel, D., 2012. Investigating the last deglaciation of the Scandinavian Ice Sheet in southwest Sweden with ^{10}Be exposure dating. J. Quat. Sci. 27, 211–220.
Larsen, E., Fredin, O., Jensen, M., Kuznetsov, D., Lyså, A., Subetto, D., 2014. Subglacial sediment, proglacial lake-level and topographic controls on ice extent and lobe geometries during the Last Glacial Maximum in NW Russia. Quat. Sci. Rev. 92, 369–387.
Lasberg, K., Kalm, V., 2013. Chronology of Late Weichselian glaciation in the western part of the East European Plain. Boreas 42, 995–1007.
Lemdahl, G., Broström, A., Hedenäs, L., Arvidsson, K., Holmgren, S., Gaillard, M.-J., Möller, P., 2013. Eemian and Early Weichselian environments in southern Sweden: a multi-proxy study of till-covered organic deposits from the Småland peneplain. J. Quat. Sci. 28, 705–719.
Li, Y.K., Harbor, J., Stroeven, A.P., Fabel, D., Kleman, J., Fink, D., Caffee, M., Elmore, D., 2005. Ice Sheet erosion patterns in valley systems in northern Sweden investigated using cosmogenic nuclides. Earth Surf. Process. Landforms 30, 1039–1049.
Li, Y.K., Napieralski, J., Harbor, J., Hubbard, A., 2007. Identifying patterns of correspondence between modeled flow directions and field evidence: an automated flow direction analysis. Comput. Geosciences 33, 141–150.
Li, Y.K., Fabel, D., Stroeven, A.P., Harbor, J., 2008. Unraveling complex exposure-burial histories of bedrock surfaces under ice sheets by integrating cosmogenic nuclide concentrations with climate proxy records. Geomorphology 99, 139–149.
Lidén, R., 1938. Den senkvartära strandförskjutningens förlopp och kronologi i Ångermanland. Geol. Fören. Stockh. Förh. 60, 397–404.
Lifton, N., Sato, T., Dunai, T.J., 2014. Scaling *in situ* cosmogenic nuclide production rates using analytical approximations to atmospheric cosmic-ray fluxes. Earth Planet. Sci. Lett. 386, 149–160.
Liiva, A., Ilves, E., Punning, J.M., 1966. Tartu radiocarbon dates I. Radiocarbon 8, 430–441.
Lindeberg, G., 2002. The Swedish Varved Clays Revisited: Spectral- and Image Analysis of Different Types of Varve Series from the Baltic Basin. Thesis in Quaternary Geology, No. 1. Department of Physical Geography and Quaternary Geology. Stockholm University, Stockholm.
Lindén, M., Möller, P., Björck, S., Sandgren, P., 2006. Holocene shore displacement and deglaciation chronology in Norrbotten, Sweden. Boreas 35, 1–22.
Lindström, M., Lundqvist, J., Lundqvist, T., 2000. Sveriges geologi från urtid till nutid. Studentlitteratur, Lund.
Linge, H., Brook, E.J., Nesje, A., Raisbeck, G.M., Yiou, F., Clark, H., 2006a. In situ ^{10}Be exposure ages from southeastern Norway: Implications for the geometry of the Weichselian Scandinavian ice sheet. Quat. Sci. Rev. 25, 1097–1109.
Linge, H., Larsen, E., Kjær, K.H., Demidov, I.N., Brook, E.J., Raisbeck, G.M., Yiou, F., 2006b. Cosmogenic ^{10}Be exposure age dating across Early to Late Weichselian ice-marginal zones in northwestern Russia. Boreas 35, 576–586.
Linge, H., Olsen, L., Brook, E.J., Darter, J.R., Mickelson, D.M., Raisbeck, G.M., Yiou, F., 2007. Cosmogenic nuclide surface exposure ages from Nordland, northern Norway: implications for deglaciation in a coast to inland transect. Norw. J. Geol. 87, 269–280.
Linton, D.L., 1963. The forms of glacial erosion. Trans. Inst. Br. Geogr. 33, 1–28.
Livingstone, S.J., Piotrowski, J.A., Bateman, M.D., Ely, J.C., Clark, C.D., 2015. Discriminating between subglacial and proglacial lake sediments: an example from the Dänischer Wohld Peninsula, northern Germany. Quat. Sci. Rev. 112, 86–108.
Ljungner, E., 1943. Isdelarstudier vid polcirkeln. Geol. Fören. Stockh. Förh. 65, 198–210.
Lohne, Ø.S., Bondevik, S., Mangerud, J., Svendsen, J.I., 2007. Sea-level fluctuations imply that the Younger Dryas ice-sheet expansion in western Norway commenced during the Allerød. Quat. Sci. Rev. 26, 2128–2151.
Lohne, Ø.S., Mangerud, J., Birks, H.H., 2013. Precise 14C ages of the Vedde and Saksunarvatn ashes and the Younger Dryas boundaries from western Norway and their comparison with the Greenland Ice Core (GICC05) chronology. J. Quat. Sci. 28, 490–500.
Longva, O., Thoresen, M.K., 1991. Iceberg scours, iceberg gravity craters and current erosion marks from a gigantic Preboreal flood in southeastern Norway. Boreas 20, 47–62.
Lundqvist, G., 1921. Den baltiska issjöns tappning och strandlinjerna vid Billingens nordspets. Geol. Fören. Stockh. Förh. 43, 381–385.
Lundqvist, G., 1959. Description to accompany the map of the Quaternary deposits of Sweden. Sveriges Geol. Unders. Ba 17, 1–116.
Lundqvist, J., 1969. Beskrivning till jordartskarta över Jämtlands län. Sveriges Geol. Unders. Ca 45, 418.
Lundqvist, J., 1972. Ice-lake types and deglaciation pattern along the Scandinavian mountain range. Boreas 1, 27–54.
Lundqvist, J., 1973. Isavsmältningens förlopp i Jämtlands län. Sveriges Geol. Unders C 681, 1–187.
Lundqvist, J., 1979. Morphogenetic classification of glaciofluvialdeposits. Sveriges Geol. Unders. 767C, 1–71.
Lundqvist, J., 1986. Late Weichselian glaciation and deglaciation in Scandinavia. Quat. Sci. Rev. 5, 269–292.
Lundqvist, J., 1987. Beskrivning till jordartskarta over Västernorrlands län och förutvarande Fjällsjö k:n. Sveriges Geol. Unders Ca 55, 1–270.
Lundqvist, J., 1990. The Younger Dryas event in Scandinavia. Opas-Guide. In: Lundqvist, J., Saarnisto, M. (Eds.), Termination of the Pleistocene, vol. 31. Geological Survey of Finland, pp. 5–24.
Lundqvist, J., 1994. Inlandsisens avsmältning. In: Fredén, C. (Ed.), Berg och Jord. Sveriges Nationalatlas, pp. 124–136.
Lundqvist, J., 2004. Glacial history of Sweden. In: Ehlers, J., Gibbard, P.L. (Eds.), Quaternary Glaciations- Extent and Chronology. Elsevier, pp. 401–412.
Lundqvist, J., 2007. Surging ice and break-down of an ice dome - a deglaciation model for the Gulf of Bothnia. GFF 129, 329–336.
Lundqvist, J., Saarnisto, M., 1995. Summary of project IGCP-253. Quat. Int. 28, 9–18.
Lundqvist, J., Wohlfarth, B., 2001. Timing and east-west correlation of south Swedish ice marginal lines during the Late Weichselian. Quat. Sci. Rev. 20, 1127–1148.
Lüthgens, C., Böse, M., Preusser, F., 2011. Age of the Pomeranian ice marginal position in north-eastern Germany determined by Optically Stimulated Luminescence (OSL) dating of glaciofluvial sediments. Boreas 40, 598–615.
Lyså, A., Demidov, I., Houmark-Nielsen, M., Larsen, E., 2001. Late Pleistocene stratigraphy and sedimentary environment of the Arkhangelsk area, northwest Russia. Glob. Planet. Change 31, 179–199.
Lyså, A., Jensen, M.A., Larsen, E., Fredin, O., Demidov, I.N., 2011. Ice-distal landscape and sediment signatures evidencing damming and drainage of large pro-glacial lakes, northwest Russia. Boreas 40, 481–497.
Lyså, A., Larsen, E., Buylaert, J.-P., Fredin, O., Jensen, M.A., Kuznetsov, D., Murray, A.S., Subetto, D.A., van Welden, A., 2014. Late Pleistocene stratigraphy and sedimentary environments of the Severnaya Dvina-Vychegda region in northwestern Russia. Boreas 43, 759–779.
MacLeod, A., Brunnberg, L., Wastegård, S., Hang, T., Matthews, I.P., 2014. Lateglacial cryptotephra detected within clay varves in Östergötland, south-east Sweden. J. Quat. Sci. 29, 605–609.
Malmberg Persson, K., Persson, M., Lindén, A.G., 2007. Israndstråket Vimmerbymoränen mellan Knivshult och Vanstad i nordöstra Småland. SGU-rapport 2007:7. Geological Survey of Sweden (in Swedish).
Mangerud, J., 1977. Late Weichselian marine sediments containing shells, foraminifera, and pollen, at Ågotnes, western Norway. Nor. Geol. Tidsskr. 57, 23–54.
Mangerud, J., Gulliksen, S., 1975. Apparent radiocarbon ages of recent marine shells from Norway, Spitsbergen, and Arctic Canada. Quat. Res. 5, 263–273.
Mangerud, J., Gyllencreutz, R., Lohne, Ø.S., Svendsen, J.I., 2011. Glacial history of Norway. Dev. Quat. Sci. 15, 279–298.
Mangerud, J., Goehring, B.M., Lohne, Ø.S., Svendsen, J.I., Gyllencreutz, R., 2013. Collapse of marine-based outlet glaciers from the Scandinavian Ice Sheet. Quat. Sci. Rev. 67, 8–16.
Mannerfelt, C.M., 1945. Några glacialmorfologiska formelement och deras vittnesbörd om inlandsisens avsmältningsmekanik i svensk och norsk fjällterräng. Geogr. Ann. 27, 3–235.
Mannerfelt, C.M., 1949. Marginal drainage channels as indicators of the gradients of Quaternary ice caps. Geogr. Ann. 31, 194–199.
Margold, M., Jansson, K.N., Kleman, J., Stroeven, A.P., 2011. Glacial meltwater landforms of central British Columbia. J. Maps 2011, 486–506.
Margold, M., Jansson, K.N., Kleman, J., Stroeven, A.P., Clague, J.J., 2013. Retreat pattern of the Cordilleran Ice Sheet in central British Columbia at the end of the last glaciation reconstructed from glacial meltwater landforms. Boreas 42, 830–847.
Marks, L., 2012. Timing of the Late Vistulian (Weichselian) glacial phases in Poland. Quat. Sci. Rev. 44, 81–88.
Marshall, S.J., James, T.S., Clarke, G.K.C., 2002. North American ice sheet reconstructions at the last glacial maximum. Quat. Sci. Rev. 21, 175–192.
Marsiat, I., 1994. Simulation of the Northern Hemisphere continental ice sheets over the last glacial-interglacial cycle: experiments with a lititude-longitude vertically integrated ice sheet model coupled to a zonally averaged climate model. Palaeoclimates 1, 59–98.
Matthews, J.A., Shakesby, R.A., Schnabel, C., Freeman, S., 2008. Cosmogenic ^{10}Be and ^{26}Al ages of Holocene moraines in southern Norway I: testing the method and confirmation of the date of the Erdalen Event (c. 10 ka) at its type-site. Holocene 18, 1155–1164.
Melander, O., 1977. Torneträskområdets issjöstrandlinjer. Report STOU-NG 28. Department of Physical Geography, Stockholm University, Stockholm, pp. 1–71.
Milne, G.A., Gehrels, W.R., Hughes, C.W., Tamisiea, M.E., 2009. Identifying the causes

of sea-level change. Nat. Geosci. 2, 471–478.
Möller, P., 2010. Melt-out till and ribbed moraine formation, a case study from south Sweden. Sediment. Geol. 232, 161–180.
Möller, P., Östlund, O., Barnekow, L., Sandgren, P., Palmbo, F., Willerslev, E., 2013. Living at the margin of the retreating Fennoscandian Ice Sheet: the early Mesolithic sites at Aareavaara, northernmost Sweden. Holocene 23, 104–116.
Murray, A.S., Wintle, A.G., 2000. Luminescence dating of quartz using an improved single-aliquot regenerative-dose protocol. Radiat. Meas. 32, 57–73.
Muscheler, R., Kromer, B., Björck, S., Svensson, A., Friedrich, M., Kaiser, K.F., Southon, J., 2008. Tree rings and ice cores reveal ^{14}C calibration uncertainties during the Younger Dryas. Nat. Geosci. 1, 263–267.
Muscheler, R., Adolphi, F., Knudsen, M.F., 2014. Assessing the differences between the IntCal and Greenland ice-core time scales for the last 14,000 years via the common cosmogenic radionuclide variations. Quat. Sci. Rev. 106, 81–87.
Napieralski, J., Hubbard, A., Li, Y.K., Harbor, J., Stroeven, A.P., Kleman, J., Alm, G., Jansson, K.N., 2007. Towards a GIS assessment of numerical ice-sheet model performance using geomorphological data. J. Glaciol. 53, 71–83.
Nese, H., Lauritzen, S.-E., 1996. Quaternary stratigraphy of the Sorsteinhola cave system, Kjøpsvik, north Norway. Special Publication 2. In: Lauritzen, S.-E. (Ed.), Climate Change: the Karst Record. Karst Waters Institute, pp. 116–120.
Nesje, A., Rye, N., 1990. Radiocarbon dates from the mountain area northeast of Årdal, southern Norway: evidence for a Preboreal deglaciation. Norges Geol. Unders. Bull. 418, 1–7.
Nesje, A., Dahl, S.O., Linge, H., Ballantyne, C.K., McCarroll, D., Brook, E.J., Raisbeck, G.M., Yiou, F., 2007. The surface geometry of the Last Glacial Maximum ice sheet in the Andøya-Skånland region, northern Norway, constrained by surface exposure dating and clay mineralogy. Boreas 36, 227–239.
NGU, 2014. Løsmasser – Nasjonal løsmassedatabase. Norges Geologiske Undersøkelse. http://geo.ngu.no/kart/losmasse/ (accessed 15.09.14.).
Niemelä, J., Tynni, R., 1979. Interglacial and interstadial sediments in the Pohjanmaa region. Finl. Geol. Surv. Finl. Bull. 302, 1–48.
Niemelä, J., Ekman, I., Lukashov, A., 1993. Quaternary Deposits of Finland and Northwestern Part of Russian Federation and Their Resources: 1: 1 Mill. Geological Survey of Finland and Institute of Geology at the Karelian Science Centre of the Russian Academy of Sciences.
Nilsson, E., 1968. Södra Sveriges senkvartära historia. Geokronologi, issjöar och landhöjning. Kungliga Svenska Vetenskapsakademiens Handlingar. Fjärde Serien 12 (1), 1–117.
Nishiizumi, K., Imamura, M., Caffee, M.W., Southon, J.R., Finkel, R.C., McAninch, J., 2007. Absolute calibration of ^{10}Be AMS standards. Nucl. Instrum. Methods Phys. Res. Sect. B – Beam Interact. Mater. Atoms 258, 403–413.
Noe-Nygaard, N., Heiberg, E.O., 2001. Lake-level changes in the Late Weichselian Lake Tøvelde, Møn, Denmark: induced by changes in climate and base level. Palaeogeogr. Palaeoclimatol. Palaeoecol. 174, 351–382.
Noormets, R., Flodén, T., 2002. Glacial deposits and ice-sheet dynamics in the north-central Baltic Sea during the last deglaciation. Boreas 31, 362–377.
Nordkalott Project, 1986. Map of Quaternary Geology, Sheet 2: Glacial Geomorphology and Paleohydrography, Northern Fennoscandia, Scale 1:1 000 000. Geological Surveys of Finland, Norway and Sweden.
Nydal, R., Gulliksen, S., Lövseth, K., 1972. Trondheim natural radiocarbon measurements VI. Radiocarbon 14, 418–451.
Olsen, L., 1997. Rapid shifts in glacial extension characterise a new conceptual model for glacial variations during the mid and late Weichselian in Norway. Norges Geol. Unders. Bull. 433, 54–55.
Olsen, L., 2000. The Last Glaciation in Norway - Glaciation Curves along Nine Transects from Inland to Coast. internal report 2000.122. NGU, pp. 1–49.
Olsen, L., 2002. Mid and late Weichselian, ice-sheet fluctuations northwest of the Svartisen glacier, Nordland, northern Norway. Norges Geol. Unders. Bull. 440, 39–52.
Olsen, L., 2004. Norges Geologiske Undersøkelse (Unpublished Report).
Olsen, L., Mejdahl, V., Selvik, S.F., 1996. Middle and late Pleistocene stratigraphy, chronology and glacial history in Finnmark, North Norway. Nor. Geol. Unders. Bull. 429, 1–111.
Olsen, L., Van der Borg, K., Bergstrøm, B., Sveian, H., Lauritzen, S.-E., Hansen, G., 2001. AMS radiocarbon dating of glacigenic sediments with low organic carbon content - an important tool for reconstructing the history of glacial variations in Norway. Nor. Geogr. Tidsskr. 81, 59–92.
Olsen, L., Sveian, H., Bergstrøm, B., Ottesen, D., Rise, L., 2013a. Quaternary glaciations and their variations in Norway and on the Norwegian continental shelf. Special Publication. In: Olsen, L., Fredin, O., Olesen, O. (Eds.), Quaternary Geology of Norway, vol. 13. Geological Survey of Norway, pp. 27–78.
Olsen, L., Sveian, H., Ottesen, D., Rise, L., 2013b. Quaternary Glacial, Interglacial and Interstadial Deposits of Norway and Adjacent Onshore and Offshore Areas. Special Publication 13. Geological Survey of Norway, pp. 79–144.
Paasche, Ø., Strømsøe, J.R., Dahl, S.O., Linge, H., 2006. Weathering characteristics of arctic islands in northern Norway. Geomorphology 82, 430–452.
Payne, A.J., Sugden, D.E., Clapperton, C.M., 1989. Modeling the growth and decay of the Antarctic Peninsula Ice Sheet. Quat. Res. 31, 119–134.
Pitkäranta, R., Lunkka, J.-P., Eskola, K.O., 2014. Lithostratigraphy and optically stimulated luminescence age determinations of pre-Late Weichselian deposits in the Suupohja area, western Finland. Boreas 43, 193–207.
Portenga, E.W., Bierman, P.R., 2011. Understanding Earth's eroding surface with ^{10}Be. GSA Today 21, 4–10.
Punkari, M., 1982. Glacial geomorphology and dynamics in the eastern parts of the Baltic Shield interpreted using Landsat imagery. Photogramm. J. Finl. 9, 77–93.
Punkari, M., 1995. Function of the ice streams in the Scandinavian ice sheet: analyses of glacial geological data from southwestern Finland. Trans. R. Soc. Edinb. Earth Sci. 85, 283–302.
Putkinen, N., Lunkka, J.-P., 2008. Ice stream behaviour and deglaciation of the Scandinavian Ice Sheet in the Kuittijärvi area, Russian Karelia. Bull. Geol. Soc. Finl. 80, 19–37.
Putkinen, N., Lunkka, J.P., Ojala, A.E.K., Kosonen, E., 2011. Deglaciation history and age estimate of the Younger Dryas end moraines in the Kalevala region, NW Russia. Quat. Sci. Rev. 30, 3812–3822.
Rainio, H., 1993. The Heinola deglaciation and Salpausselkä readvance as recorded in the lithostratigraphy of the distal area of Salpausselkä I at Ihalainen, Lappeenranta, Finland. Special Paper 18. Geological Survey of Finland, pp. 53–62.
Rainio, H., Kejonen, A., Kielosto, S., Lahermo, P., 1986. Avancerade inlandsisen på nytt också till mellanfinska randformationen? Summary: Is the Central Finland ice-marginal formation terminal? Geologi 38, 95–109.
Rainio, H., Saarnisto, M., Ekman, I., 1995. Younger Dryas end moraines in Finland and NW Russia. Quat. Int. 28, 179–192.
Rasmussen, S.O., Bigler, M., Blockley, S.P., Blunier, T., Buchardt, S.L., Clausen, H.B., Cvijanovic, I., Dahl-Jensen, D., Johnsen, S.J., Fischer, H., Gkinis, V., Guillevic, M., Hoek, W.Z., Lowe, J.J., Pedro, J.B., Popp, T., Seierstad, I.K., Steffensen, J.P., Svensson, A.M., Vallelonga, P., Vinther, B.M., Walker, M.J.C., Wheatley, J.J., Winstrup, M., 2014. A stratigraphic framework for abrupt climatic changes during the Last Glacial period based on three synchronized Greenland ice-core records: refining and extending the INTIMATE event stratigraphy. Quat. Sci. Rev. 106, 14–28.
Rattas, M., 2007. Spatial Distribution and Morphological Aspects of Eskers and Bedrock Valleys in North Estonia: Implications for the Reconstruction of a Subglacial Drainage System under the Late Weichselian Baltic Ice Stream. Special Paper 46. Geological Survey of Finland, pp. 63–68.
Raukas, A., Stankowski, W.T.J., Zelčs, V., Šinkunas, P., 2010. Chronology of the last deglaciation in the southeastern Baltic region on the basis of recent OSL dates. Geochronometria 36, 47–54.
Reimer, P.J., Baillie, M.G.L., Bard, E., Bayliss, A., Beck, J.W., Blackwell, P.G., Ramsey, C.B., Buck, C.E., Burr, G.S., Edwards, R.L., Friedrich, M., Grootes, P.M., Guilderson, T.P., Hajdas, I., Heaton, T.J., Hogg, A.G., Hughen, K.A., Kaiser, K.F., Kromer, B., McCormac, F.G., Manning, S.W., Reimer, R.W., Richards, D.A., Southon, J.R., Talamo, S., Turney, C.S.M., van der Plicht, J., Weyhenmeyer, C.E., 2009. INTCAL09 and MARINE09 radiocarbon age calibration curves, 0-50,000 Years Cal BP. Radiocarbon 51, 1111–1150.
Reimer, P.J., Bard, E., Bayliss, A., Beck, J.W., Blackwell, P.G., Ramsey, C.B., Buck, C.E., Cheng, H., Edwards, R.L., Friedrich, M., Grootes, P.M., Guilderson, T.P., Haflidason, H., Hajdas, I., Hatté, C., Heaton, T.J., Hoffmann, D.L., Hogg, A.G., Hughen, K.A., Kaiser, K.F., Kromer, B., Manning, S.W., Niu, M., Reimer, R.W., Richards, D.A., Scott, E.M., Southon, J.R., Staff, R.A., Turney, C.S.M., van der Plicht, J., 2013. INTCAL13 AND MARINE13 radiocarbon age calibration curves 0-50,000 years cal BP. Radiocarbon 55, 1869–1887.
Repo, R., Tynni, R., 1967. Zur spät- und postglazialen Entwicklung im Ostteil des Ersten Salpausselkä. Comptes Rendus Soc. géol. Finl. 39, 133–159.
Repo, R., Tynni, R., 1969. Morphologisch-stratigraphische Grundzüge des östlichen Salpausselkä-Gebiets. Bull. Geol. Soc. Finl. 41, 203–229.
Repo, R., Tynni, R., 1971. Observations on the Quaternary geology of an area between the 2nd Salpausselkä and the ice-marginal formation of central Finland. Bull. Geol. Soc. Finl. 43, 185–202.
Rhodes, E.J., 2011. Optically Stimulated Luminescence dating of sediments over the Past 200,000 years. Annu. Rev. Earth Planet. Sci. 39, 461–488.
Richardt, N., 1996. Sedimentological Examination of the Late Weichselian Sea-level History Following Deglaciation of Northern Denmark. Special Publications 111. Geological Society, London, pp. 261–273.
Rignot, E., Mouginot, J., Morlighem, M., Seroussi, H., Scheuchl, B., 2014. Widespread, rapid grounding line retreat of Pine Island, Thwaites, Smith, and Kohler glaciers, West Antarctica, from 1992 to 2011. Geophys. Res. Lett. 41, 3502–3509.
Rinterknecht, V.R., Clark, P.U., Raisbeck, G.M., Yiou, F., Brook, E.J., Tschudi, S., Lunkka, J.P., 2004. Cosmogenic ^{10}Be dating of the Salpausselkä I Moraine in southwestern Finland. Quat. Sci. Rev. 23, 2283–2289.
Rinterknecht, V.R., Marks, L., Piotrowski, J.A., Raisbeck, G.M., Yiou, F., Brook, E.J., Clark, P.U., 2005. Cosmogenic ^{10}Be ages on the pomeranian moraine, Poland. Boreas 34, 186–191.
Rinterknecht, V.R., Clark, P.U., Raisbeck, G.M., Yiou, F., Bitinas, A., Brook, E.J., Marks, L., Zelcs, V., Lunkka, J.-P., Pavlovskaya, I.E., Piotrowski, J.A., Raukas, A., 2006. The last deglaciation of the southeastern sector of the Scandinavian Ice Sheet. Science 311, 1449–1452.
Rinterknecht, V., Braucher, R., Böse, M., Bourlès, D., Mercier, J.-L., 2012. Late Quaternary ice sheet extents in northeastern Germany inferred from surface exposure dating. Quat. Sci. Rev. 44, 89–95.
Rinterknecht, V., Börner, A., Bourlès, D., Braucher, R., 2014. Cosmogenic ^{10}Be dating of ice sheet marginal belts in Mecklenburg-Vorpommern, Western Pomerania (northeast Germany). Quat. Geochronol. 19, 42–51.
Rise, L., Bøe, R., Sveian, H., Lyså, A., Olsen, H.A., 2006. The deglaciation history of Trondheimsfjorden and Trondheimsleia, Central Norway. Norw. J. Geol. 86, 415–434.
Rosén, P., 2005. Total organic carbon (TOC) of lake water during the Holocene inferred from lake sediments and near-infrared spectroscopy (NIRS) in eight lakes from northern Sweden. Biogeochemistry 76, 503–516.
Rosén, P., Segerström, U., Eriksson, L., Renberg, I., Birks, H.J.B., 2001. Holocene climatic change reconstructed from diatoms, chironomids, pollen and near-

infrared spectroscopy at an alpine lake (Sjuodjijaure) in northern Sweden. Holocene 11, 551–562.
Rother, H., Fink, D., Shulmeister, J., Mifsud, C., Evans, M., Pugh, J., 2014. The early rise and late demise of New Zealand's last glacial maximum. Proc. Natl. Acad. Sci. 111, 11630–11635.
Rotnicki, K., Borówka, R.K., 1995. The last cold period in the Gardno-Łeba coastal Plain. J. Coast. Res. (Special Issue 22), 225–229.
Rubensdotter, L., 2006. Alpine lake Sediment Archives and Catchment Geomorphology: Causal Relationships and Implications for Paleoenvironmental Reconstructions. Department of Physical Geography and Quaternary Geology. Stockholm University, pp. 1–100.
Rye, N., Nesje, A., Lien, R., Blikra, L.H., Eikenaes, O., Hole, P.A., Torsnes, I., 1997. Glacial geology and deglaciation chronology of the area between inner Nordfjord and Jostedalsbreen- Strynefjellet, western Norway. Nor. Geol. Tidsskr. 77, 51–63.
Saarnisto, M., Saarinen, T., 2001. Deglaciation chronology of the scandinavian ice sheet from the Lake Onega Basin to the Salpausselkä End Moraines. Glob. Planet. Change 31, 387–405.
Saarse, L., Niinemets, E., Amon, L., Heinsalu, A., Veski, S., Sohar, K., 2009. Development of the late glacial Baltic basin and the succession of vegetation cover as revealed at Palaeolake Haljala, northern Estonia. Est. J. Earth Sci. 58, 317–333.
Saarse, L., Heinsalu, A., Veski, S., Amon, L., Gaidamavicius, A., 2012. On the deglaciation chronology of the Palivere ice-marginal zone, northern Estonia. Bull. Geol. Soc. Finl. 84, 21–31.
Salonen, V.-P., 1990. Salpausselkä III, Pertille. In: Lundqvist, J., Saarnisto, M. (Eds.), Termination of the Pleistocene, Geological Survey of Finland, Opas-Guide, vol. 31, pp. 63–64.
Salonen, V.-P., Kaakinen, A., Kultti, S., Miettinen, A., Eskola, K.O., Lunkka, J.P., 2008. Middle Weichselian glacial event in the central part of the Scandinavian Ice Sheet recorded in the Hitura pit, Ostrobothnia, Finland. Boreas 37, 38–54.
Sandegren, R., 1929. Om isrecessionen i Gefletrakten och den senkvartära geokronologien. Geol. Fören. Stockh. Förh. 51, 573–579.
Sandgren, P., Snowball, I.F., Hammarlund, D., Risberg, J., 1999. Stratigraphic evidence for a high marine shore-line during the Late Weichselian deglaciation on the Kullen Peninsula, southern Sweden. J. Quat. Sci. 14, 223–237.
Sauramo, M., 1918. Geochronologische Studien über die spätglaziale Zeit in Südfinnland. Fennia 41, 1–44.
Sauramo, M., 1923. Studies on the Quaternary varve sediments in southern Finland. Bull. Comm. géol. Finl. 60, 1–164.
Schomacker, A., Benediktsson, I.Ö., Ingólfsson, Ó., 2014. The Eyjabakkajökull glacial landsystem, Iceland: geomorphic impact of multiple surges. Geomorphology 218, 98–107.
Sefström, N.G., 1836. Undersökning af de räfflor, hvaraf Skandinaviens berg äro med bestämd riktning fårade, samt om deras sannolika uppkomst. Kongliga Vetenskaps Akademiens Handlingar, pp. 141–255.
Segerström, U., von Stedingk, H., 2003. Early-Holocene spruce, Picea abies (L.) Karst., in west central Sweden as revealed by pollen analysis. Holocene 13, 897–906.
Seguinot, J., Khroulev, C., Rogozhina, I., Stroeven, A.P., Zhang, Q., 2014. The effect of climate forcing on numerical simulations of the Cordilleran ice sheet at the last glacial maximum. Cryosphere 8, 1087–1103.
Seguinot, J., Rogozhina, I., Stroeven, A.P., Margold, M., Kleman, J., 2015. Numerical simulations of the Cordilleran ice sheet through the last glacial cycle. Cryosphere Discuss. 9, 4147–4203.
Seidenkrantz, M.-S., Knudsen, K.L., 1993. Middle Weichselian to Holocene palaeoecology in the eastern Kattegat, Scandinavia: foraminifera, ostracods and ^{14}C measurements. Boreas 22, 299–310.
Šeirienė, V., Stančikaitė, M., Kisielienė, D., Šinkūnas, P., 2006. Lateglacial environment inferred from palaeobotanical and ^{14}C data of sediment sequence from Lake Kašučiai, West Lithuania. Baltica 19, 80–90.
Seppä, H., Birks, H.J.B., 2002. Holocene climate reconstructions from the Fennoscandian tree-line area based on pollen data from Toskaljavri. Quat. Res. 57, 191–199.
Seppä, H., Weckström, J., 1999. Holocene vegetational and limnological changes in the Fennoscandian tree-line area as documented by pollen and diatom records from Lake Tsuolbmajavri, Finland. Ecoscience 6, 621–635.
Seppä, H., Hannon, G.E., Bradshaw, R.H.W., 2004. Holocene history of alpine vegetation and forestline on Pyhäkero Mountain, northern Finland. Arct. Antarct. Alp. Res. 36, 607–614.
Seppä, H., Tikkanen, M., Mäkiaho, J.-P., 2012. Tilting of Lake Pielinen, eastern Finland - an example of extreme transgressions and regressions caused by differential post-glacial isostatic uplift. Est. J. Earth Sci. 61, 149–161.
Shakesby, R.A., Matthews, J.A., Schnabel, C., 2008. Cosmogenic ^{10}Be and ^{26}Al ages of Holocene moraines in southern Norway II: evidence for individualistic responses of high-altitude glaciers to millennial-scale climatic fluctuations. Holocene 18, 1165–1177.
Shemesh, A., Rosqvist, G., Rietti-Shati, M., Rubensdotter, L., Bigler, C., Yam, R., Karlén, W., 2001. Holocene climatic change in Swedish Lapland inferred from an oxygen-isotope record of lacustrine biogenic silica. Holocene 11, 447–454.
Siegert, M.J., Dowdeswell, J.A., Hald, M., Svendsen, J.-I., 2001. Modelling the Eurasian Ice Sheet through a full (Weichselian) glacial cycle. Glob. Planet. Change 31, 367–385.
Slangen, A.B.A., Carson, M., Katsman, C.A., van de Wal, R.S.W., Köhl, A., Vermeersen, L.L.A., Stammer, D., 2014. Projecting twenty-first century regional sea-level changes. Clim. Change 124, 317–332.
Smith, M.J., Rose, J., Booth, S., 2006. Geomorphological mapping of glacial landforms from remotely sensed data: an evaluation of the principal data sources and an assessment of their quality. Geomorphology 76, 148–165.
Snyder, J.A., Miller, G.H., Werner, A., Jull, A.J.T., Stafford Jr., T.W., 1994. AMS-radiocarbon dating of organic-poor lake sediment, an example from Linnévatnet, Spitsbergen, Svalbard. Holocene 4, 413–421.
Snyder, J.A., Forman, S.L., Mode, W.N., Tarasov, G.A., 1997. Postglacial relative sea-level history: sediment and diatom records of emerged coastal lakes, north-central Kola Peninsula, Russia. Boreas 26, 329–346.
Snyder, J.A., Macdonald, G.M., Forman, S.L., Tarasov, G.A., Mode, W.N., 2000. Postglacial climate and vegetation history, north-central Kola Peninsula, Russia: pollen and diatom records from Lake Yarnyshnoe-3. Boreas 29, 261–271.
Sollid, J.L., Torp, B., 1984. Glacialgeologisk kart over Norge 1:1000000. Nasjonalatlas for Norge. Geografisk Institutt, Oslo Universitet.
Sollid, J.L., Andersen, S., Hamre, N., Kjeldsen, O., Salvigsen, O., Sturød, S., Tveitå, T., Wilhelmsen, A., 1973. Deglaciation of Finnmark, North Norway. Nor. Geogr. Tidsskr. 27, 233–325.
Sørensen, R., 1992. The physical environment of Late Weichselian deglaciation of the Oslofjord region, southeastern Norway. Sveriges Geol. Unders Ca 81, 339–346.
Stančikaitė, M., Šinkūnas, P., Šeirienė, V., Kisielienė, D., 2008. Patterns and chronology of the Lateglacial environmental development at Pamerkiai and Kašučiai, Lithuania. Quat. Sci. Rev. 27, 127–147.
Stankowska, A., Stankowski, W., 1988. Maximum extent of the Vistulian ice sheet in the vicinity of Konin, Poland: a geomorphological, sedimentological and radiometric evidence. Geogr. Pol. 55, 141–150.
Stephan, H.-J., 2001. The Young Baltic advance in the western Baltic depression. Geol. Q. 45, 359–363.
Stokes, C.R., Clark, C.D., 1999. Geomorphological criteria for identifying Pleistocene ice streams. Ann. Glaciol. 28, 67–74.
Stokes, C.R., Spagnolo, M., Clark, C.D., 2011. The composition and internal structure of drumlins: complexity, commonality, and implications for a unifying theory of their formation. Earth-Science Rev. 107, 398–422.
Stokes, C.R., Corner, G.D., Winsborrow, M.C.M., Husum, K., Andreassen, K., 2014. Asynchronous response of marine-terminating outlet glaciers during deglaciation of the Fennoscandian Ice Sheet. Geology 42, 455–458.
Stone, J.O., Balco, G.A., Sugden, D.E., Caffee, M.W., Sass III, L.C., Cowdery, S.G., Siddoway, C., 2003. Holocene deglaciation of Marie Byrd Land, west Antarctica. Science 299, 99–102.
Storrar, R.D., Stokes, C.R., Evans, D.J.A., 2014. Morphometry and pattern of a large sample (>20,000) of Canadian eskers and implications for subglacial drainage beneath ice sheets. Quat. Sci. Rev. 105, 1–25.
Strickertsson, K., Murray, A.S., 1999. Optically stimulated luminescence dates for Late Pleistocene and Holocene sediments from Nørre Lyngby, northern Jutland, Denmark. Quat. Geochronol. 18, 169–178.
Stroeven, A.P., Fabel, D., Harbor, J., Hättestrand, C., Kleman, J., 2002a. Quantifying the erosional impact of the Fennoscandian ice sheet in the Torneträsk-Narvik corridor, northern Sweden, based on cosmogenic radionuclide data. Geogr. Ann. 84A, 275–287.
Stroeven, A.P., Fabel, D., Hättestrand, C., Harbor, J., 2002b. A relict landscape in the centre of Fennoscandian glaciation: cosmogenic radionuclide evidence of tors preserved through multiple glacial cycles. Geomorphology 44, 145–154.
Stroeven, A.P., Harbor, J., Fabel, D., Kleman, J., Hättestrand, C., Elmore, D., Fink, D., Fredin, O., 2006. Slow, Patchy Landscape Evolution in Northern Sweden Despite Repeated Ice-sheet Glaciation. Special Paper 398. GSA, pp. 387–396.
Stroeven, A.P., Fabel, D., Harbor, J.M., Fink, D., Caffee, M.W., Dahlgren, T., 2011. Importance of sampling across an assemblage of glacial landforms for interpreting cosmogenic ages of deglaciation. Quat. Res. 76, 148–156.
Stroeven, A.P., Fabel, D., Margold, M., Clague, J.J., Xu, S., 2014. Investigating absolute chronologies of glacial advances in the NW sector of the Cordilleran Ice Sheet with terrestrial in situ cosmogenic nuclides. Quat. Sci. Rev. 92, 429–443.
Stroeven, A.P., Heyman, J., Fabel, D., Björck, S., Caffee, M.W., Fredin, O., Harbor, J.M., 2015. A new Scandinavian reference ^{10}Be production rate. Quat. Geochronol. 29, 104–115.
Strömberg, B., 1985a. New varve measurements in Västergötland. Swed. Boreas 14, 111–115.
Strömberg, B., 1985b. Revision of the lateglacial Swedish varve chronology. Boreas 14, 101–105.
Strömberg, B., 1989. Late Weichselian deglaciation and clay varve chronology in east-central Sweden. Sveriges Geol. Unders Ca 73, 1–70.
Strömberg, B., 1990. A connection between the clay varve chronologies in Sweden and Finland. Ann. Acad. Sci. Fenn. AIII 154, 1–32.
Strömberg, B., 1994. Younger Dryas deglaciation at Mt. Billingen, and clay varve dating of the Younger Dryas/Preboreal transition. Boreas 23, 177–193.
Strömberg, B., 2005. Clay varve chronology and deglaciation in SW Finland, Annales Academiae Scientiarum Fennicae. Helsinki Geogr. Geogr. 167, 1–49.
Svedhage, K., 1985. Shore Displacement during Late Weichselian and Early Holocene in the Risveden Area, SW Sweden, Geologiska Lnstitutionen. Chalmers Tekniska Hogskola/Göteborgs universitet, pp. 1–111. PhD Thesis.
Sveian, H., Aa, A.R., Kjærnes, P.A., 1979. Isbevegelser og isavsmeltning i den sentrale delen av Saltfjellet, Nordland, Nord-Norge. Norges Geol. Unders. 348, 1–104.
Svendsen, J.I., Alexanderson, H., Astakhov, V.I., Demidov, I., Dowdeswell, J.A., Funder, S., Gataullin, V., Henriksen, M., Hjort, C., Houmark-Nielsen, M., Hubberten, H.W., Ingólfsson, Ó., Jakobsson, M., Kjaer, K.H., Larsen, E., Lokrantz, H., Lunkka, J.P., Lyså, A., Mangerud, J., Matiouchkov, A., Murray, A., Möller, P., Niessen, F., Nikolskaya, O., Polyak, L., Saarnisto, M., Siegert, C.,

Siegert, M.J., Spielhagen, R.F., Stein, R., 2004. Late Quaternary ice sheet history of northern Eurasia. Quat. Sci. Rev. 23, 1229–1271.
Svendsen, J.I., Briner, J.P., Mangerud, J., Young, N.E., 2015. Early break-up of the norwegian channel ice stream during the last glacial maximum. Quat. Sci. Rev. 107, 231–242.
Svensson, N.-O., 1989. Late Weichselian and Early Holocene Shore Displacement in the Central Baltic, Based on Stratigraphical and Morphological Records from Eastern Småland and Gotland, Sweden. Lund University, pp. 1–195. PhD Thesis, Lundqua thesis 25.
Syverson, K.M., Mickelson, D.M., 2009. Origin and significance of lateral meltwater channels formed along a temperate glacier margin, Glacier Bay, Alaska. Boreas 38, 132–145.
Tolonen, K., Ruuhijärvi, R., 1976. Standard pollen diagrams from the Salpausselkä region of Southern Finland. Ann. Bot. Fenn. 13, 155–196.
Torell, O., 1872. Undersökningar öfver istiden, vol. 29. I. Öfversigt af Kongliga Vetenskaps Akademiens Förhandlingar, pp. 25–66.
Torell, O., 1873. Undersökningar öfver istiden, vol. 30. II. Öfversigt af Kongliga Vetenskaps Akademiens Förhandlingar, pp. 47–64.
Tschudi, S., Ivy-Ochs, S., Schlüchter, C., Kubik, P., Rainio, H., 2000. ^{10}Be dating of Younger Dryas Salpausselkä I formation in Finland. Boreas 29, 287–293.
Ulfstedt, A.-C., 1981. Isrecessionen i Västerbottens och södra Norrbottens fjälltrakter. Department of Physical Geography, Stockholm University, Stockholm, pp. 1–106. Report STOU-NG 43.
Ullman, D.J., Carlson, A.E., LeGrande, A.N., Anslow, F.S., Moore, A.K., Caffee, M., Syverson, K.M., Licciardi, J.M., 2015. Southern Laurentide ice-sheet retreat synchronous with rising boreal summer insolation. Geology 43, 23–26.
Valen, V., Mangerud, J., Larsen, E., Hufthammer, A.K., 1996. Sedimentology and stratigraphy in the cave Hamnsundhelleren, western Norway. J. Quat. Sci. 11, 185–201.
Vorren, K.-D., 1978. Late and middle Weichselian stratigraphy of Andøya, north Norway. Boreas 7, 19–38.
Vorren, K.-D., Alm, T., 1999. Late Weichselian and Holocene environments of lake Endletvatn, Andøya, northern Norway: as evidenced primarily by chemostratigraphical data. Boreas 28, 505–520.
Vorren, T.O., Vorren, K.-D., Alm, T., Gulliksen, S., Løvlie, R., 1988. The last deglaciation (20,000 to 11,000 B.P.) on Andøya, northern Norway. Boreas 17, 41–77.
Vorren, T.O., Vorren, K.-D., Aasheim, O., Dahlgren, K.I.T., Forwick, M., Hassel, K., 2013. Palaeoenvironment in northern Norway between 22.2 and 14.5 cal. ka BP. Boreas 42, 876–895.
Walker, M., Johnsen, S., Rasmussen, S.O., Popp, T., Steffensen, J.-P., Gibbard, P., Hoek, W., Lowe, J., Andrews, J., Björck, S., Cwynar, L.C., Hughen, K., Kershaw, P., Kromer, B., Litt, T., Lowe, D.J., Nakagawa, T., Newnham, R., Schwander, J., 2009. Formal definition and dating of the GSSP (Global Stratotype Section and Point) for the base of the Holocene using the Greenland NGRIP ice core, and selected auxiliary records. J. Quat. Sci. 24, 3–17.
Warrick, R., Oerlemans, J., 1990. Sea level rise. In: Houghton, J.T., Jenkins, G.J., Ephraums, J.J. (Eds.), Climate Change: the IPCC Scientific Assessment. Cambridge University Press, Cambridge, pp. 261–281.
Wohlfarth, B., 1996. The chronology of the last termination: a review of radiocarbon-dated, high-resolution terrestrial stratigraphies. Quat. Sci. Rev. 15, 267–284.
Wohlfarth, B., Björck, S., Possnert, G., Lemdahl, G., Brunnberg, L., Ising, J., Olsson, S., Svensson, N.-O., 1993. AMS dating Swedish varved clays of the last glacial/interglacial transition and the potential/difficulties of calibrating Late Weichselian ‘absolute’ chronologies. Boreas 22, 113–128.
Wohlfarth, B., Björck, S., Possnert, G., 1995. The Swedish Time Scale: a potential calibration tool for the radiocarbon time scale during the late Weichselian. Radiocarbon 37, 347–359.
Wohlfarth, B., Björck, S., Possnert, G., Holmquist, B., 1998. An 800-year long, radiocarbon-dated varve chronology from south-eastern Sweden. Boreas 27, 243–257.
Wohlfarth, B., Bennike, O., Brunnberg, L., Demidov, I., Possnert, G., Vyahirev, S., 1999. AMS ^{14}C measurements and macrofossil analyses of a varved sequence near Pudozh, eastern Karelia, NW Russia. Boreas 29, 575–586.
Zernitskaya, V., Makhnach, N., Kolkovskij, V., 2007. Stratigraphy of late glacial and Holocene deposits in Belarusian Poozerie. In: Guobytė, R., Stančikaitė, M. (Eds.), The Quaternary of Western Lithuania: from the Pleistocene Glaciations to the Evolution of the Baltic Sea. The INQUA Peribaltic Group Field Symposium, May 27-June 2. Lithuanian Geological Survey, pp. 106–107.